



University of Bradford eThesis

This thesis is hosted in [Bradford Scholars](#) – The University of Bradford Open Access repository. Visit the repository for full metadata or to contact the repository team



© University of Bradford. This work is licenced for reuse under a [Creative Commons Licence](#).

Developing a Computer System for the Generation of Unique Wrinkle Maps for Human Faces

Ali Mehdi

PhD

2011

Developing a Computer System for the Generation of Unique Wrinkle Maps for Human Faces

Generating 2D Wrinkle Maps using Various Image
Processing Techniques and the Design of 3D Facial Ageing
System using 3D Modelling Tools

Ali Mehdi

A thesis submitted for the degree of
Doctor of Philosophy

School of Computing, Informatics & Media
University of Bradford

2011

ABSTRACT

Facial Ageing (FA) is a very fundamental issue, as ageing in general, is part of our daily life process. FA is used in security, finding missing children and other applications. It is also a form of Facial Recognition (FR) that helps identifying suspects. FA affects several parts of the human face under the influence of different biological and environmental factors. One of the major facial feature changes that occur as a result of ageing is the appearance and development of wrinkles. Facial wrinkles are skin folds; their shapes and numbers differ from one person to another, therefore, an advantage can be taken over these characteristics if a system is implemented to extract the facial wrinkles in a form of maps.

This thesis is presenting a new technique for three-dimensional facial wrinkle pattern information that can also be utilised for biometric applications, which will back up the system for further increase of security. The procedural approaches adopted for investigating this new technique are the extraction of two-dimensional wrinkle maps of frontal human faces for digital images and the design of three-dimensional wrinkle pattern formation system that utilises the generated wrinkle maps.

The first approach is carried out using image processing tools so that for any given individual, two wrinkle maps are produced; the first map is in a binary form that shows the positions of the wrinkles on the face while the other map is a coloured version that indicates the different intensities of the wrinkles.

The second approach of the 3D system development involves the alignment of the binary wrinkle maps on the corresponding 3D face models, followed by the projection of 3D curves in order to acquire 3D representations of the wrinkles. With the aid of the coloured wrinkle maps as well as some ageing parameters, simulations and predictions for the 3D wrinkles are performed.

Acknowledgement

First of all, I thank ALLAH the most merciful and the most kind. Without His blessing, this thesis would not have progressed nor has seen the light.

I would like to express my sincere gratitude to my supervisors Dr Rami Qahwaji and Prof Hassan Ugail; their ideas and comments were most beneficial, where they showed a high standard of continuous support and guidance throughout my research.

I was offered a grant by Dr Rami Qahwaji (from the DTA Studentship) to carryout my research; the words to describe my gratefulness are not enough.

I would like to thank my examiners Prof Christos Grecos (head of School of Computing at the University of West of Scotland) and Dr Stan Ipson (University of Bradford) for their time and effort in reviewing the thesis and conducting the viva.

I would also like to extend my thanks to all my family, especially, my mother, father and my four brothers: Omar, Mohammad, Mahmood and Ibrahim for their endless love and support during all stages of my studies. Most dearly, I dedicate this thesis to my father Dr Abdullah Mehdi who was always there for me and consistently gave me valuable advise and directions.

Special thanks go to Dr Mumtaz Kamala who believed in me; his help to establish myself and continue with my academic career was beyond imagination.

A high appreciation goes to my fellow students and friends, those who assisted me directly or indirectly in my research and those with whom I had happy days during my hard times; among them are: Dr Mohammad Al-Khedher, Dr Sokyna Al-Qatawneh and Dr Moi Yap; as well as, Charles Stuart, Michael Von Pokrzywnicki, Farzana Khan, Stuart Leader, Kate Lee, Andy Liu, Christina Li, Husam Al-Osta, Kenan Al-Khoury and Jassim Al-Hamar.

I also appreciate the assistance I received from Miss Rona Wilson (our research administrator) and Mr Mark Tympalski (in the Technical Support team).

Finally, I would like to thank all the people who contributed in my experiments by allowing me to use their face images.

Table of Contents

ABSTRACT	i
Acknowledgement	ii
Table of Contents	iv
List of Figures.....	vii
List of Tables	xi
1 Introduction.....	1
1.1 Background	1
<i>1.1.1 The Mechanism of the Formation of Wrinkles.....</i>	<i>2</i>
<i>1.1.2 Factors that Affect Facial Ageing.....</i>	<i>3</i>
<i>1.1.3 Facial Ageing Wrinkles by Decades.....</i>	<i>5</i>
1.2 Motivation.....	7
1.3 Research Challenges	8
1.4 Aims & Objectives.....	10
1.5 Original Contributions	12
1.6 Thesis Structure	13
2 Review of Related-Type of Schemes.....	14
2.1 Introduction.....	14
2.2 Literature Survey	15
<i>2.2.1 Early Methods.....</i>	<i>15</i>
<i>2.2.2 Overview of Statistical Representation of Faces.....</i>	<i>16</i>
<i>2.2.3 Statistical Methods for Age Transformation.....</i>	<i>19</i>
<i>2.2.4 Age Estimation.....</i>	<i>27</i>
<i>2.2.5 Overview on the Facial Expressions with Wrinkles Appearance</i>	<i>32</i>
2.3 Conclusion	34

3	Predicting the Change in Length for Forehead Wrinkles.....	38
3.1	Introduction.....	38
3.2	Pre-Processing Stage.....	40
3.3	Methodology.....	42
3.3.1	<i>NURBS Curves Projection.....</i>	<i>42</i>
3.3.2	<i>Calculating Wrinkle Lengths using the Geodesic Distance Algorithm</i>	<i>47</i>
3.3.3	<i>Wrinkle Length Estimations and Predictions using Linear Interpolation and Linear Extrapolation Algorithms</i>	<i>50</i>
3.4	Results.....	53
3.5	Testing Method.....	55
3.6	Evaluation Method.....	60
3.7	Discussion and Conclusion.....	63
4	Employing Image Processing Techniques in the Generation of Unique 2D Wrinkle Maps for Human Faces from Expressions	65
4.1	Introduction.....	65
4.2	Data Collection	67
4.3	Pre-Processing Stage.....	69
4.4	Experimental Methods	70
4.4.1	<i>Face Detection.....</i>	<i>70</i>
4.4.2	<i>Region of Interest (ROI) Detection.....</i>	<i>78</i>
4.4.3	<i>Face Crop and Size Filter</i>	<i>79</i>
4.4.4	<i>Wrinkles Detection</i>	<i>81</i>
4.4.5	<i>Generating Two-Dimensional RGB Wrinkle Maps</i>	<i>87</i>
4.5	Results.....	89
4.6	Testing.....	93
4.7	Discussion and Conclusion.....	95

5	3D Modelling, Simulation and Prediction of Facial Wrinkles	99
5.1	Introduction.....	99
5.2	3D Face Creation	101
5.3	The 3D Face Mesh.....	103
5.4	Texture Mapping.....	107
5.5	Wrinkles Construction	110
5.6	Wrinkles Simulation and Prediction	111
5.6.1	<i>Linear Regression Algorithm.....</i>	<i>115</i>
5.7	Results.....	117
5.8	Performance Evaluation Strategy.....	128
5.9	Discussion and Conclusion	129
6	Conclusion and Future Work	131
6.1	Conclusion	131
6.1.1	<i>General Conclusion.....</i>	<i>131</i>
6.1.2	<i>Comprehensive Conclusion and Achievements</i>	<i>133</i>
6.1.3	<i>Original Contributions</i>	<i>137</i>
6.1.4	<i>Opportunity for Developments</i>	<i>138</i>
6.2	Suggestions for Future Work	139
	References	141
	Appendices	I
	Appendix A: List of Publications.....	I

List of Figures

Figure 1. 1: The different layers of the human skin.....	2
Figure 1. 2: Inside the dermis layer.....	3
Figure 1. 3: Medical terms for the facial wrinkles	5
Figure 1. 4: Work plan	11
Figure 3. 1: A sample of 2D images with their IDs and ages	40
Figure 3. 2: 3D forehead model	41
Figure 3. 3: Textured 3D foreheads	41
Figure 3. 4: Maya environment.....	41
Figure 3. 5: A 3D curve with its control vertices	42
Figure 3. 6: A 3D curve with its edit points.....	43
Figure 3. 7: A sample forehead with curves projected.....	44
Figure 3. 8: 3D forehead wrinkles of P1	45
Figure 3. 9: 3D forehead wrinkles of P2	45
Figure 3. 10: 3D forehead wrinkles of P3	46
Figure 3. 11: Calculating wrinkle lengths using geodesic distance	47
Figure 3. 12: W1P1 prediction at age 35.....	50
Figure 3. 13: W1P3 prediction at age 56.....	52
Figure 3. 14: Predicted wrinkle behaviours at age 35 for P1	53
Figure 3. 15: Predicted wrinkle behaviours at age 68 for P1	53
Figure 3. 16: Predicted wrinkle behaviours at age 24 for P2	54
Figure 3. 17: Predicted wrinkle behaviours at age 51 for P2.....	54
Figure 3. 18: Predicted wrinkle behaviours at age 72 for P2.....	54
Figure 3. 19: Predicted wrinkle behaviours at age 28 for P3.....	55
Figure 3. 20: Predicted wrinkle behaviours at age 60 for P3.....	55
Figure 3. 21: Test images for the linear interpolation algorithm	56
Figure 3. 22: Test images for the linear extrapolation algorithm.....	56
Figure 3. 23: Estimated values against actual values for T1	58
Figure 3. 24: Estimated values against actual values for T2.....	58
Figure 3. 25: Estimated values against actual values for T3.....	59
Figure 3. 26: Estimated values against actual values for T4.....	59

Figure 3. 27: Data sets for the evaluation method	61
Figure 4. 1: The process of generating 2D wrinkle maps	66
Figure 4. 2: The 19 subjects with reference letters and ages	68
Figure 4. 3: Facial expressions.....	68
Figure 4. 4: Pre-processing stage	70
Figure 4. 5: A 3D representation of the HSV colour space	73
Figure 4. 6: Threshold operation.....	74
Figure 4. 7: Face detection algorithm	77
Figure 4. 8: Face detection process	78
Figure 4. 9: ROI stage	79
Figure 4. 10: Face crop.....	80
Figure 4. 11: Size filter.....	81
Figure 4. 12: One-dimensional Gaussian curves	83
Figure 4. 13: Two-dimensional Gaussian curve	83
Figure 4. 14: Non-maximum suppression.....	85
Figure 4. 15: Binary gradient masks	87
Figure 4. 16: An ellipse.....	87
Figure 4. 17: An ellipse with its major and minor axes	88
Figure 4. 18: A coloured wrinkle map with a side bar.....	89
Figure 4. 19: Results for person A	90
Figure 4. 20: Results for person B	90
Figure 4. 21: Results for person C	91
Figure 4. 22: Results for person D	91
Figure 4. 23: Results for person E.....	92
Figure 4. 24: Results for person F.....	92
Figure 4. 25: Comparison between the original and the detected wrinkles	93
Figure 4. 26: Detecting multiple faces in images.....	98
Figure 5. 1: Experimental procedures	100
Figure 5. 2: The process of generating and exporting the 3D face model	102
Figure 5. 3: Marked 2D face image	102
Figure 5. 4: The 3D face model	103
Figure 5. 5: Exported items.....	103

Figure 5. 6: 3D face mesh	104
Figure 5. 7: Facial muscles flow	104
Figure 5. 8: Smoothing process.....	105
Figure 5. 9: The smoothed face in comparison with the original one.....	106
Figure 5. 10: Our generated normal map	107
Figure 5. 11: A 3D sphere with its UV map	108
Figure 5. 12: Our 3D face and its UV map	108
Figure 5. 13: Texturing operation in MAYA	109
Figure 5. 14: Textured 3D head model	109
Figure 5. 15: Final texture	109
Figure 5. 16: The binary wrinkle map is textured on the 3D face model	110
Figure 5. 17: ‘Live’ 3D object.....	110
Figure 5. 18: An enhanced 3D wrinkle map	111
Figure 5. 19: Wrinkle elements and categorisations for age progression	112
Figure 5. 20: A sample process for wrinkle categorisation.....	113
Figure 5. 21: The number of wrinkles that appear at every age group	113
Figure 5. 22: A sample graph presenting the change in facial wrinkles against age	114
Figure 5. 23: A ‘best fit’ line is drawn across the points	115
Figure 5. 24: A straight line with its variables	116
Figure 5. 25: Person A, 20-29	117
Figure 5. 26: Person A, 30-39	118
Figure 5. 27: Person A, 40-49	118
Figure 5. 28: Person A, 50-59	118
Figure 5. 29: Person A, 60-69	119
Figure 5. 30: Person D, 20-29	119
Figure 5. 31: Person D, 30-39	119
Figure 5. 32: Person D, 40-49	120
Figure 5. 33: Person D, 50-59	120
Figure 5. 34: Person D, 60-69	120
Figure 5. 35: Person P, 20-29.....	121
Figure 5. 36: Person P, 30-39.....	121
Figure 5. 37: Person P, 40-49.....	121
Figure 5. 38: Person P, 50-59.....	122
Figure 5. 39: Person P, 60-69.....	122

Figure 5. 40: Person R, 20-29	122
Figure 5. 41: Person R, 30-39	123
Figure 5. 42: Person R, 40-49	123
Figure 5. 43: Person R, 50-59	123
Figure 5. 44: Person R, 60-69	124
Figure 5. 45: Person S, 20-29.....	124
Figure 5. 46: Person S, 30-39.....	125
Figure 5. 47: Person S, 40-49.....	125
Figure 5. 48: Person S, 50-59.....	125
Figure 5. 49: Person S, 60-69.....	126
Figure 5. 50: Person A, 2D ageing simulation and prediction using age-me software	126
Figure 5. 51: Person D, 2D ageing simulation and prediction using age-me software	127
Figure 5. 52: Performance evaluation strategy	128
Figure 6. 1: A 3D plane is drawn behind a face.....	140

List of Tables

Table 1. 1: Facial ageing wrinkles by decades.....	6
Table 3. 1: Wrinkle lengths for P1	48
Table 3. 2: Wrinkle lengths for P2.....	49
Table 3. 3: Wrinkle lengths for P3	49
Table 3. 4: Predicted wrinkle lengths for P1	53
Table 3. 5: Predicted wrinkle lengths for P2.....	54
Table 3. 6: Predicted wrinkle lengths for P3.....	54
Table 3. 7: Wrinkle lengths for T1	57
Table 3. 8: Wrinkle lengths for T2.....	57
Table 3. 9: Wrinkle lengths for T3.....	57
Table 3. 10: Wrinkle lengths for T4.....	57
Table 3. 11: Estimated lengths against the actual for age 33,T1.....	57
Table 3. 12: Estimated lengths against the actual for age 33,T2.....	57
Table 3. 13: Estimated lengths against the actual for age 48,T3.....	58
Table 3. 14: Estimated lengths against the actual for age 69,T4.....	58
Table 3. 15: Percentage errors.....	60
Table 3. 16: Wrinkle lengths for M1	61
Table 3. 17: Wrinkle lengths for M2.....	61
Table 3. 18: Linear, quadratic and cubic interpolation results.....	62
Table 3. 19: The generated percentage errors	62
Table 4. 1: Error rates for all experimental subjects	94
Table 4. 2: WM strengths against other biometric applications.....	96

CHAPTER ONE

1 Introduction

1.1 Background

Ageing is a natural phenomenon and it is part of our daily life process; it affects the human body including the face. The human face is a vital part that is used in face-to-face communication and identification; therefore, the Facial Ageing (FA) process has been of a great interest to many researchers and companies due to the fact that the face appearance changes as people age resulting in difficulties identifying certain individuals.

FA research is a form of Facial Recognition (FR) and “the main reason for facial recognition is delivered from the forensic needs to identify victims or suspects”[1]. FR is a remarkable process; in fact, even children have the ability to recognise people at early stages. The human brain has the ability and capacity to quickly distinguish between known and unknown faces.

The biggest advantage of using the face (over other parts of the human body) in many applications is that wherever a person may be, the face is also there. Moreover, the face carries a significant number of features that identify individuals such as gender, emotional state, ethnic origin, age etc. and according to [2] “It is impossible to find two identical people; even twins have some differences”.

The research of FA is just as important as FR and it is involved in a wide range of applications that include security, help identifying missing children and other applications that are listed in [3], such as a web browser can decide by itself whether the user satisfies the age restrictions to view certain web pages; a vending machine

will not sell cigarettes or alcohol to underage people. It is also used for plastic surgeries and cosmetics.

One of the most important and pronounced changes that occur on the face as people age is the appearance of wrinkles (skin creases), which are the focus of this research.

Wrinkles can be divided into two types [4]: large-scale wrinkles, such as those on the forehead area and fine-scale wrinkles, such as those that form around the mouth area.

Generally, wrinkles start to appear in the upper part of the face before the lower.

On the other hand, plastic surgeons [5-7] often divide the skin creases into three categories: lines, wrinkles and folds based on their depth (Figure 1.1). However, in this document, any type of skin crease will be referred to as a wrinkle.

1.1.1 The Mechanism of the Formation of Wrinkles

The epidermis and the dermis (Figure 1.1) are two layers that form the human skin. The epidermis is the skin's defense layer against the surrounding environment while the dermis layer contains the connective tissues and provides a support to the skin; wrinkles occur within the dermal layer of the skin [7].

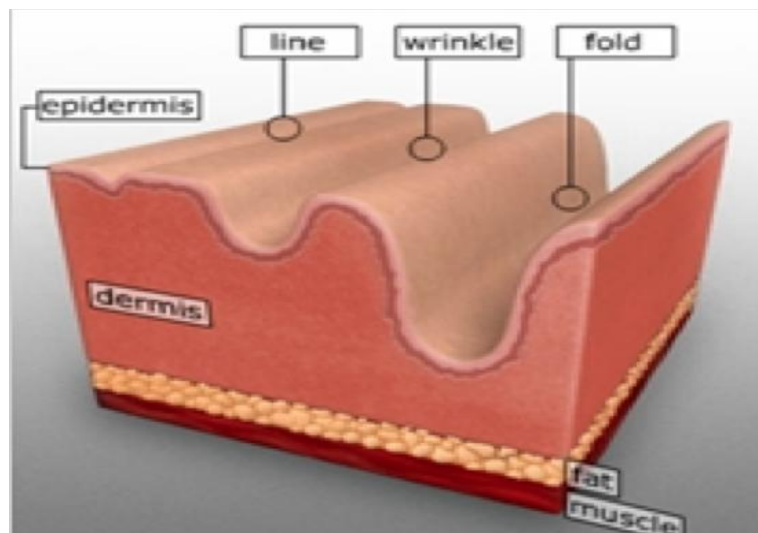


Figure 1. 1: The different layers of the human skin [7]

The connective tissues of the dermis layer contain collagen and elastin fibers that give the skin the support, structure and elasticity. They also contain fat cells and

other molecules, such as hyaluronic acid that helps to form volume underneath the facial skin. As time passes and with the effects of different factors (that are stated in section 1.1.2), this structure of collagen and elastin fibers breaks down and the hyaluronic acid molecules as well as fat cells that form the volume are reduced, resulting in the formation of wrinkles [7, 8]. Figure 1.2 shows the structure within the dermis layer.

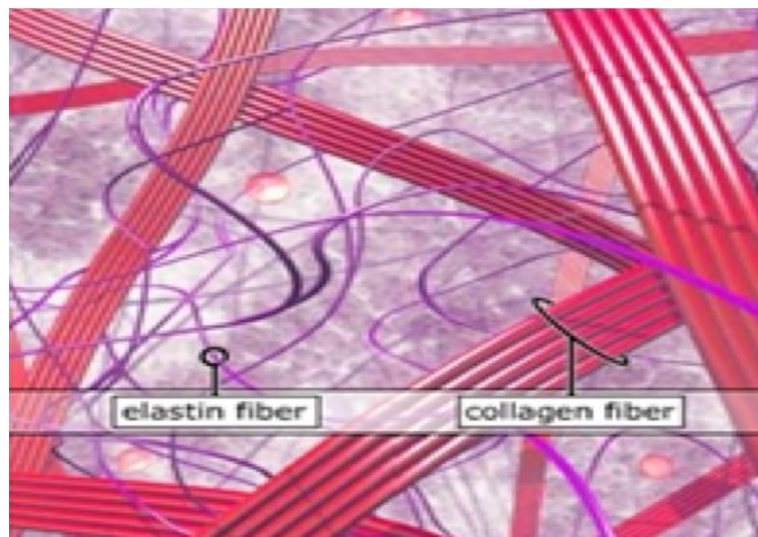


Figure 1. 2: Inside the dermis layer [7]

1.1.2 Factors that Affect Facial Ageing

The factors that influence FA can be divided into two causes: internal and external. The internal causes occur within the human body as a result of biological changes, while the external causes are related to the surrounding environment.

Some internal causes:

- A minor change in the shape of the skull occurs as people age and the jaw shrinks [9-11]. The size of the skull is very small for newly born babies, then it increases rapidly as people age until it reaches a steady stage. Any minor decrease in the skull's size affects the skin and could lead to the generation of wrinkles.

- The soft tissues change their shape due to degeneration causing the skin wrinkling and sagging [9].
- Illness, which causes slow but constant deterioration of organs and cells resulting in the production of wrinkles.

Some external causes:

- Photoaging [9, 12], which is the damage to the skin caused by the sun radiations or ultraviolet rays.
- Smoking, drugs & stress; Smoking removes vital vitamin C from the body (roughly 35mg for each cigarette) [13], this vitamin cannot be generated by the body. The body benefits from vitamin C as it protects the collagen in the skin.

Stress can weaken the overall health of the skin; it generates hormonal changes that might cause many skin problems such as spots, itching and the thinning of the skin. When a person is stressed, the body sends essential nutrients from the skin to the vital organs (heart, brain and lungs) causing the skin to weaken and therefore, wrinkles start to appear [14].

- Ethnic origin & lifestyle [9, 15, 16]; People from different races age in different ways. This might be related to the fact that the temperature differs from one place to another; furthermore, the wind force has its impact on facial ageing. Lifestyle might include the type of food or certain activities done by certain people etc.

Although there are different factors that affect the way people age, the major challenge is to find a pattern to predict where certain wrinkles start to appear first and which ones form later. The disparities in the formation of these ageing wrinkles are influenced by the gender and life history of the individuals. Even facial expressions

have their effects in the appearance of wrinkles, for instance, lifting the eyebrows frequently, constant eye squinting or skin furrowing [9].

1.1.3 Facial Ageing Wrinkles by Decades

This section gives a description of the facial wrinkles that generally appear on the face every 10 years. This is presented in Table 1.1 (on the next page), while Figure 1.3 illustrates the medical terms.

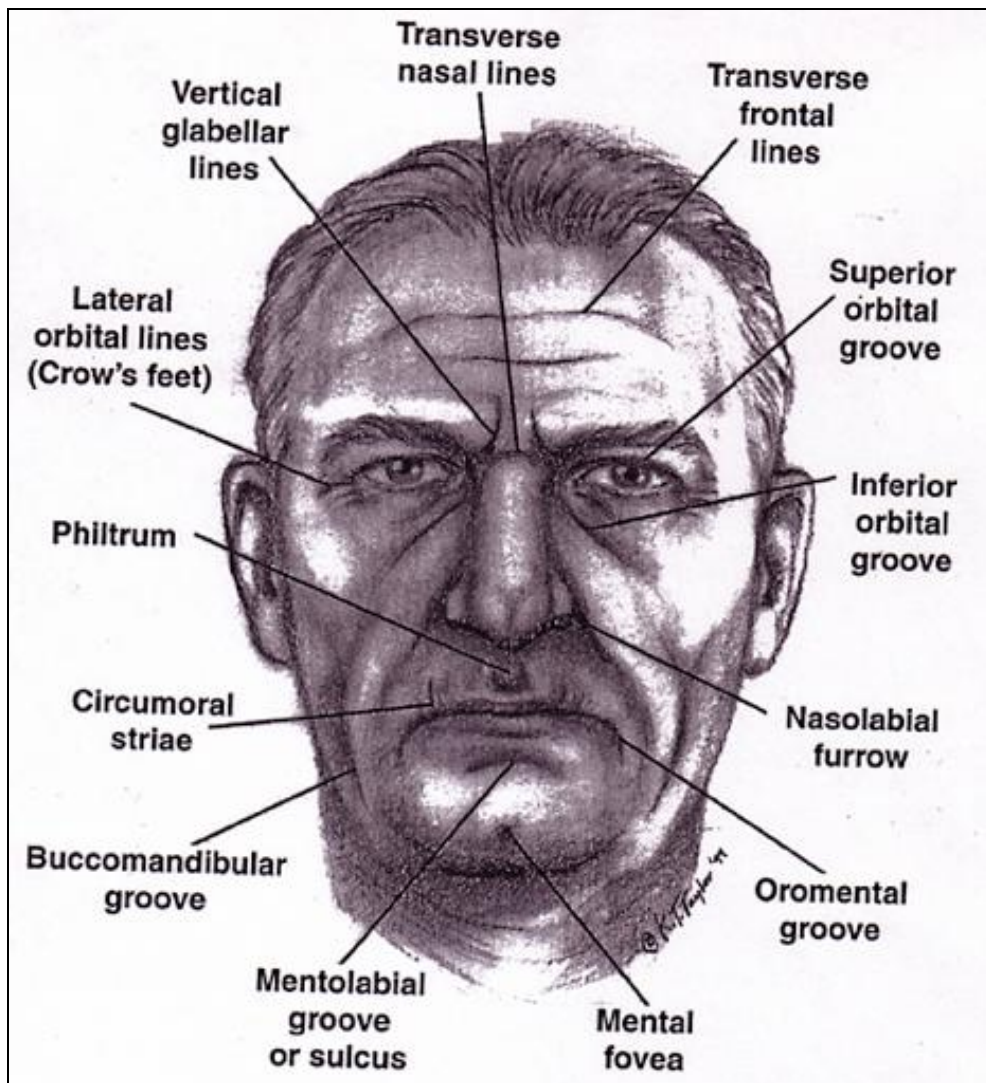


Figure 1. 3: Medical terms for the facial wrinkles [9]

Table 1. 1: Facial ageing wrinkles by decades [9]

<p>20s</p>	<ul style="list-style-type: none"> • Fine transverse frontal lines may appear across the forehead • Fine vertical glabellar lines appear in people who frown frequently • Fine lateral orbital lines or “crow’s feet” may appear in people who smile often or spend a lot of time in the sun
<p>30s</p>	<ul style="list-style-type: none"> • Transverse frontal lines deepen • Vertical glabellar lines deepen • Lateral orbital lines increase in number and deepen • Transverse nasal lines may form across the top of the nose • Nasolabial lines or furrows become noticeable
<p>40s</p>	<ul style="list-style-type: none"> • Inferior orbital groove may become apparent • The eyebrows may descend slightly • An excess of upper lid skin may develop and a portion of the superior orbital groove may be obscured at the lateral side • The jaw line becomes less firm • Circumoral striae become noticeable, especially in smokers • The lips may begin to thin • The oromental groove begin, depending on the facial structure • The mentolabial groove becomes more apparent, depending of facial structure
<p>50s</p>	<ul style="list-style-type: none"> • Inferior orbital groove may define a developing pouch under the eyes • Excess upper lid tissue may worsen, obscuring more of the superior orbital groove at the lateral side and creating more lateral orbital lines • The nasolabial furrow is more noticeable • The oromental groove deepens • The lips continue to thin, especially in people with thin lips in youth • Dental changes may become apparent, increasing lines accordingly • A buccomandibular groove may appear • The jaw line becomes much less firm • Jowls and a double chin may appear
<p>60s</p>	<ul style="list-style-type: none"> • All of the above-mentioned lines are exaggerated • The circumoral striae may cross over the vermilion border of the lips
<p>70s</p>	<ul style="list-style-type: none"> • All of the above-described lines become more defined, accompanied by marked loss of elasticity of the skin and sagging of tissues

1.2 Motivation

The essential need for the research into different human-machine interaction systems has endorsed the creation and increase of various face recognition systems, for example [17-20]. This increase of FR systems is a result of the constant growth to the global population in which a number of issues have arisen. The security issue is one of the main concerns, where governments, airports and many other firms [21-23] invest much time and funds in maintenance as well as improving their security systems. It is also reported by the News KF that some schools in the UK implement FR systems to monitor late or absent students [24].

FA is a derivative of FR and it actually forms a challenge for those who work in the FR field due to the change in the face appearance with respect to age [25], which could lead to failure in some face recognition systems. In comparison to other sources of variation in face images, the process of ageing results in significant changes to the facial appearance of individuals. For example, the ageing process is specific to a given individual; it happens slowly and is highly influenced by other factors as explained before. Changes in facial appearance due to ageing can even affect some facial features making it difficult for humans and machines to identify aged individuals.

FA has a high importance and involvement in many applications. According to [26] there are at least two areas where facial ageing could be used: in automated computer face recognition and in human use of hypothetically updated images in law enforcement applications. FR systems that incorporate FA elements in their original design can help recognising criminals or suspects years after committing an offence. It can also help identify missing children.

The applications of FA are not only limited to forensic sciences but it is extended to include medical research [27] as well as plastic surgery and cosmetics [28, 29].

FA is relatively a new field of research in comparison to FR and despite the huge amount of work that was and still is being conducted in different aspects of this significant topic, there are accuracy limitations especially in the task of FA predictions and 3D simulations.

Facial wrinkles are major features that occur as a result of the ageing process and they are unique for each individual. Being such a prominent facial feature, wrinkles have the potential to be utilised in different ways, particularly, if their maps are extracted. Wrinkle maps indicate the position of the wrinkles on the faces; therefore, they can be integrated in various facial ageing systems to provide more accurate simulation. Furthermore, due to the uniqueness of the wrinkle maps, they can be added to the biometrics i.e. finger prints, voice recognition, etc, as another security element (more information about the biometrics can be found in [30]).

1.3 Research Challenges

In addition to the challenges of predicting the change in facial wrinkle appearance (as ageing varies from one person to another), there are research limitations and issues that have to be taken into consideration.

In the field of 3D facial ageing, there is the lack of available data. Unlike FR, there is no 3D database available for FA research and if there is any plan to create a 3D database, it will not be practical due to the time factor; in other words, it will take decades to develop one.

With regards to the 2D facial ageing study, researchers usually rely on two databases: the FG-NET database [31] and the MORPH database [32]. The advantage

of the first one is the sufficient number of images covering different stages of the age period, unlike the MORPH database. Both databases share the same limitations of having a huge variation and inconsistency in the data. In other words, they contain a mixture of coloured, greyscale and blurred images, as well as variation in pose and head orientations, variation in lighting; some subjects are wearing hats or glasses, etc. All these variations and inconsistencies can create difficulties in the processing of the images.

Furthermore, FA challenges with regards to the state-of-the-art technologies can be highlighted as insufficient research has been carried out on the facial wrinkles development over the years. These limitations in the general research include:

- The prediction and observation of the change in the wrinkle lengths and numbers as age progresses. This will help future understanding of the general behaviour of the wrinkles.
- The detection and extraction of the prime locations of the wrinkles on the individual faces (i.e. wrinkle maps). By doing so, more accurate simulations of the facial wrinkles can be performed in the facial ageing systems, hence, increase security.
- Categorising facial wrinkles (for every individual) according to their intensities. This can lead to a new research onto what affect the intensity of the wrinkles.
- The available 2D and 3D facial ageing systems lack in accuracy as no real wrinkles information are integrated into these systems.
- Calculating the 3D wrinkles depth is also a challenge. Finding a method to perform such task will certainly add further accuracy to the 3D facial ageing systems.

All these challenges and limitations indeed form obstacles that affect FA research.

1.4 Aims & Objectives

This research aims to tackle the following FA challenges:

- Predict the length of the wrinkles on the forehead area of face images at any given age.
- Extract the facial wrinkles for any individual in a form of a unique map that reveals the locations of these wrinkles, this is referred to as a wrinkle map. As well as categorising the extracted wrinkles into groups based on their intensities.
- Integrate the extracted wrinkles in order to perform a 3D simulation and prediction system for facial wrinkle pattern formation.

The objectives of this research are summarised below:

- The initial stage of the work aims to create techniques to predict the length of wrinkles on the forehead area of 2D face images. For any given individual at a certain age, the method will be implemented by projecting Non-Uniform Rational B-Spline (NURBS) curves on the wrinkles to form a 3D representation, then employing mathematical and statistical algorithms to study the behaviour of those curves (wrinkles).
- The work will then be taken to a more advanced level to include the whole face by creating a fully automated system that generates 2D binary wrinkle maps based on facial expressions using image processing techniques. However, those binary wrinkle maps will indicate the location of the wrinkles but not the order of their likely appearance, such information will

assist with the design of the wrinkle formation system. Therefore, RGB wrinkle maps will also be generated. The colours will represent the depth of the wrinkles.

- Finally, the above two types of wrinkle maps will be generated for any given individual and transferred onto a corresponding 3D face model to develop a 3D wrinkle formation system. The system will predict the change in the appearance of the wrinkles in the range from 20 to 79 years.

The block diagram below shows the three stages of the work:

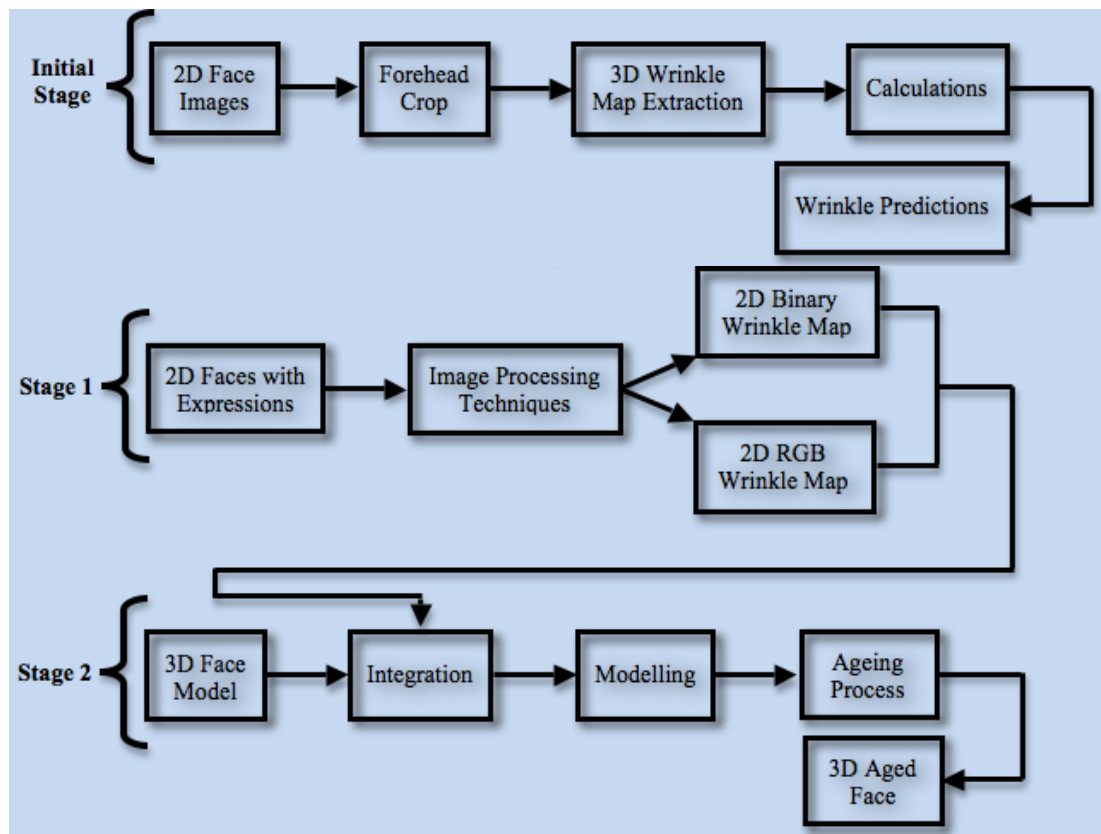


Figure 1. 4: Work plan

1.5 Original Contributions

This research holds four original contributions that are summarised below. The contributions will be discussed in more depth later in this thesis.

- Developing new techniques to predict the shape of the wrinkles on the forehead area for 2D images of human faces in ageing sequences. This technique was tested on facial ageing databases.
- Creating a fully automated and robust method to detect facial wrinkles for digital images of frontal human faces. The method generates unique 2D binary wrinkle maps from facial expressions using various image processing techniques. These maps are used to display the location of the wrinkles.
- New tools are developed to generate 2D coloured wrinkle maps. The colours represent the depth of the wrinkles and can be used to determine the order in which wrinkles appear on the human face.
- A novel system was developed to generate 3D facial wrinkles from the wrinkle maps and predicts the change in wrinkle appearance over time based on qualitative analysis. The performance of the system was compared to existing facial ageing systems.

1.6 Thesis Structure

Chapter one gave an introduction to the facial ageing research along with the factors that it is influenced by. The mechanism of the formation of wrinkles was also presented. The chapter then moved on to explain the nature of the research that is carried out in this thesis, starting by addressing the reasons behind conducting this work and the existing challenges. The aims and objectives of this research are also highlighted giving brief descriptions of the methodologies and the outcome results. The research contributions are listed in the ‘Original Contributions’ section. Finally the outlines of this thesis are being discussed in this section.

Chapter two discusses a range of literature and provides comparisons between different methods and results.

Chapters three, four and five are the core chapters of this thesis as they provide a detailed explanation of the different experimental methodologies and techniques that are used in this research. Results are also presented in these three chapters along with comparisons to other available research.

In Chapter three, the idea of generating wrinkle maps is introduced and a method to predict the wrinkle lengths in the forehead area for missing images in an ageing sequence is implemented.

Chapter four explains in detail, the image processing techniques that are used in generating the two-dimensional wrinkle maps. Moreover, it will reveal the mathematical algorithm that is used to generate the coloured wrinkle maps.

Chapter five shows the development stages of the three-dimensional wrinkle formation system.

Finally, chapter six concludes the thesis and presents suggestions for future work with implementation proposals.

CHAPTER TWO

2 Review of Related-Type of Schemes

2.1 Introduction

This chapter describes the current state-of-the-art in the visual ageing of human face images and provides a historical overview of its development. Some Facial Expressions (FE) research in connection with wrinkle appearance will also be considered.

Previous research into ageing of face images has concentrated on transforming a two-dimensional image into another image in order to produce the appearance of ageing and this transform should maintain the identity of the person. At their core, these methods work by applying shape and colour changes to the input images, often based on a statistical model. Early methods such as cardioidal strain were non-statistical and relied on the similarity between mathematical functions and large-scale biological changes [33-36]. More recent researchers have used statistical modelling methods to derive a model from a set of training images [37, 38]. The primary variations in these methods have been the functions and methods used to train the models.

Previous research can be broken down into two major categories that are: age simulation and age estimation. Age simulation is the process of synthesising a face image such that it resembles an input face aged a specified number of years. Age estimation is the reverse of age simulation that uses computer models to estimate the age of a person based on their physical appearance. Some methods of automated age estimation have also been used to perform ageing simulation, where image parameters are altered in order to match the recognised age to the desired one [37].

Although this research concentrates on ageing simulation many of the ideas and principles behind age-estimation are still relevant.

2.2 Literature Survey

2.2.1 Early Methods

One of the earliest recorded techniques for face synthesis was invented by Galton in 1878 [39]. His method involved using multiple exposures of a single photographic plate to produce a composite image of a group of individuals. Alignment of individuals in the photographs proved difficult, as faces come in a variety of different proportions. The resulting photographs were blurred but common features throughout the group could be perceived. Thompson [40] suggested the use of coordinate transforms for altering the shape of biological organisms. Notably, he showed that linear and non-linear transforms could be used to alter the profile of one species such that it approximated the profile of a different but related species.

Cardioidal strain has been used by a number of researchers [33-36]; Cardioidal strain approximates shape changes caused by bone growth, elongating the chin and raising the position of the nose and eyes. Pittenger and Shaw [33] discovered how humans perceived the age of an outline of the face. Similarly, Mark and Todd [35] found that applying cardioidal strain to a three-dimensional model of 15 year old female heads also positively affected perceived age. However, as reported by Bruce et al. [36], many of the observers did not see the faces transformed to be younger for younger individuals. Cardioidal strain has proved effectiveness at simulating the large-scale shape changes caused by ageing, but is less suited to modelling smaller local changes, which did affect how ageing is perceived by a viewer [41]. Ramanathan et al. [42] used a modified version of the cardioidal strain, whereby the parameters of

the modified cardioidal strain were adjusted such that the shape changes produced corresponded to the changes in a ratio of a number of anthropometric measurements taken at key feature points on the face. These measurements were taken at a number of different age ranges and prototypes generated at 2, 5, 8, 12, 15 and 18 years. The cardioidal strain model was fitted to this set of prototypes. They evaluated the results using a recognition experiment based on eigenfaces [43] and found that correct identification rates improved with their method with 58% accuracy as opposed to 44% without, using 109 test images. Although this method can be adopted for individualised shape transforms, it is not applicable to colour transforms.

2.2.2 Overview of Statistical Representation of Faces

Kirby and Sirovich [44], as well as Turk and Pentland [43], modelled the space of human faces using the Karhunen-Loeve theorem to build a set of basis vectors on a set of face images. The set of faces were centred by subtracting the average from each face image and a set of eigenvectors, known as eigenfaces, computed from the matrix of covariants. The face images could be approximately reconstructed from a weighted linear combination of a lower dimensional subset of eigenfaces and these coefficients are then used for identification. The representation suffered from blurring effects, as the features of the face were not in full alignment, meaning that the edges of the same feature (e.g. edge of the face) were not likely to be in the same sample area in multiple images. The result was a low frequency approximation.

The algorithm was based on the intensity of the image samples only and so shape, view and illumination changes were only implicitly modelled and could not be separated from colour-based variances. A more meaningful statistical face model can be constructed by bringing the faces into correspondence so that each pixel sample in the model corresponds to the same position on each face.

In order to bring the face images into correspondence, numerous authors have defined landmarks on the image e.g. [45, 46] to bring the images into a coarse correspondence. These methods relied on manual placement of these points. Craw and Cameron [45] were the first to align a set of face images using a point model. They warped the face images to match a common reference set of points in order to find a dense correspondence between faces in the set. Principal Component Analysis (PCA) was then performed on the set of aligned faces to build a parameterised face model [45]. By applying PCA to the set of landmark points, Cootes et al. produced a Point Distribution Model. A series of similar PCA based face descriptors, for example, Active Blobs (Scharloff et al. [47]) and the Active Appearance Models (AAMs) (Cootes et al. [48]) described the face using both shape and colour, as two separate components of the model. The shape is defined as a non-rigid two-dimensional triangle mesh, the space of face shapes was found using Principal Components Analysis. To model the colours of human faces, the faces were warped to average face shape and PCA was performed with the features of the face mostly falling in corresponding samples. Like before, a new face was constructed as a linear combination of shape and colour bases plus the mean. In order to find the parameters of an unseen face, an iterative method was used that minimised the squared pixel difference between the target image and the AAM.

The three-dimensional morphable model [49] introduced by Blanz and Vetter was an extension of the idea of using PCA to model variations in face shape and colour from two-dimensional face images to three-dimensional models. As two-dimensional images are representations of three-dimensional objects, they suffered from problems associated with pose and illumination. The projection of a simple rotation onto a two-dimensional image plane resulted in a warp that was neither linear nor injective.

Linearity is a precondition for effective modelling with a linear basis such as PCA. The mappings were not injective (one-to-one) because points in three-dimensional space could appear and disappear as they became occluded and un-occluded. Illumination also possessed a problem, although it has been shown empirically [50] that variations in lighting (including shadowing) could be modelled using a low-dimensional linear basis. This assumed no variation in the shape of the object and it also excluded shadowing. When either pose or shape was altered, the relationship between illumination and image intensity became non-linear. Using a three-dimensional model, these effects could be modelled physically. Like previous methods, the morphable model described the shape and colour of the face separately as a weighted linear combination of basis vectors constructed from PCA plus the mean. Their implementation differed from AAMs in a number of respects; the shape is a mesh of three-dimensional points instead of two-dimensional points, the mesh contained many more vertices than an AAM and thus provided a dense representation of the face shape, the colour components were only defined on the vertex points and linearly interpolated between them. This was justified on the basis of the dense representation of the shape.

2.2.3 Statistical Methods for Age Transformation

Rather than developing a model for ageing independently, many researchers have used a set of training-data usually in the form of images, although some researchers have used three-dimensional scanning equipment [51] and Morphable Models [52, 53].

Benson and Perrett [54] used image blending along with a warping function to create an average face image. Their method involved delineating 208 key features (eyes, ears, chin etc.) on a set of standardised photographs by hand. A shape average could then be computed by averaging the positions of the feature points. The face was coloured using a per pixel average of pixels at corresponding positions on the face. The correspondences were calculated by warping the face image into the average position using a triangulated linear warp, with the warp offsets defined as the shift between a feature point position on the face and the feature point's position in the average. Rowland and Perrett [46] extended the method to perform facial transforms. The shape and colour differences between the averages of 20 young faces (males between 25 and 29) and 20 other faces (also males between 3 and 54 years) were used to create a simple transform (relied on manual placement of points on individual face features for each face and made no attempt to automate the delineation process). The differences were added to a target face using image warping to produce the appearance of ageing. They noted that both shape and colour changes, separately produced an increase in perceived age, although the age difference produced by the combined shape and colour transform was significantly less than the 25-year age gap. They postulated that this was caused by the algorithm blurring out textural detail such as wrinkles. Importantly, they showed that the transform maintained the identity

of the person, thus the resulting image not only looked older but looked like the same person in an older form.

Burt and Perrett further investigated the process of ageing using these facial composites and transform algorithms [41]. They collected face images of 147 Caucasian males between 20 and 62 and divided the images into 7 sets, each spanning 5 years. An average for each group was calculated along with a population average made by combining the groups. They found that the perceived age of the composite average of each group was consistent with the average perceived age of the individuals that made up the group but noted that raters tended to underestimate the age of the composite images. This underestimation was greater in the older age groups than in the younger age groups. They concluded that the warping and blending process retained most of the age related information and suggested that the underestimation was due to a loss of textural details in the blending process. In the same work, they described two different ageing transforms, one was based on colour caricatures and the other was based on the vector difference between the oldest and the youngest groups. Colour caricatures were created by doubling the colour difference (in RGB space) between the average of the 3-54 age group and the population average. In the second transform they calculated the difference, in the shape and colour, between the oldest and the youngest age group. The shape and colour differences were then superimposed onto a target image. Experimental evaluation showed that both techniques produced a significant increase in the perceived age, although significantly less than the age difference between the original groups used to train the transform.

Many methods in modern ageing research stems from the work of Lanitis et al. [37]. Ageing functions were generated by fitting polynomial curves through a set of faces parameterised using PCA. Their technique involved parameterising a set of two-dimensional face images using PCA, in a similar manner to AAMs [52], and then calculating the ageing paths through the parameterised space. They delineated key features (eyes, ears, chin etc.) on a set of photographs. A shape average could then be computed by averaging the positions of the feature points. Intensity information was also sampled from within the facial region. The feature points were concatenated into a single shape-vector. The intensity information of the shape-normalised faces was also concatenated into a single colour-vector.

Principal Component Analysis performed on the covariance matrix of the shape-vector deviations was used to find the main axis of variations from the mean, leading to a compact parametric description of the shape of each face. PCA was also performed on the colour-vectors. This method gave them a set of low-dimensional parameters that can be used to both describe a set of faces and also by manipulating the parameters to describe new faces. Given a set of parameterised faces of a set of individuals at various age points they were able to generate a series of age functions through the PCA face space that describe ageing. Using a genetic algorithm, they were able to find polynomial curves, of degree 1, 2 and 3, that related the parameters of the face model to the age of the face. They called this, a global ageing function, as it assumed that all faces age in the same manner. These functions were used to estimate the ages of face images. They compared the accuracy of the age estimation produced by the polynomials to the known age of the individual. They found that both the quadratic and cubic polynomials offered a significant improvement over the linear, degree one, age functions. However the improvement offered by the cubic

polynomial over the quadratic was slight, and so they chose the quadratic polynomial, as it was the simpler of the two.

In general, individuals age differently so therefore, this global ageing function is inappropriate. A key insight of their paper was that people of similar appearance age in a similar manner. As such, examining the relationship between the parameters of facial appearance and the parameters of the ageing path for a particular person could generate ageing functions tailored to an unseen individual. An ageing path for a specific individual was generated by fitting a quadric polynomial curve to the facial parameters from face images of the same person at different age points in that person's life. They found that the facial appearance parameters and ageing function parameters had a correlation coefficient of 0.55 suggesting that faces with similar facial appearance age in a similar manner. Using this, they were able to generate 15 individualised ageing functions for an unseen individual as a weighted sum of the ageing functions for similar individuals in the dataset. The similarity between two faces was estimated using the probability distribution generated from the construction of the PCA model. They also gathered lifestyle information about the individuals in the dataset, information such as gender, socio-economic factors, weather exposure etc, by asking those volunteering facial images to fill in questionnaires. The lifestyle information was vectorised and scaled such that the total variance in lifestyle information equaled the total variance of the facial parameters. In this way, a new ageing function could be generated by weighting the ageing functions in the dataset by the combined appearance-lifestyle probabilities. This produced a higher correlation co-efficient of 0.72 suggesting that lifestyle has a significant impact on the visual effects of ageing, thus, they were able to confirm known results from (biology, medicine references). By comparing the estimated ages

of the face images to the known ages using a leave-one-out method, they were able to show that individualised age models produced a more accurate estimation than global ageing functions. This was the case for both appearance based weighting and combined lifestyle appearance weighting. However, this method relied on the existence of similar faces in the training set, otherwise, the age function tended towards the global age function, as Lanitis et al. showed by attempting to estimate the ages of faces from a different ethnic group than that used to train the age model. Their work also covered the area of synthesising facial ageing, generating the aged face images using the inverse of the polynomial functions used in age estimation. The results of the age synthesis were evaluated both quantitatively and perceptually. The parameters of the aged faces were compared to the parameters of a face image of the same individual at the target age using the Mahalanobis distance. The rendered face image was also shown to a set of human raters, who were asked to judge whether the synthesised image looked older than the original un-aged image and whether the rendered image was more similar to the target individual than the original. They concluded from both the quantitative and perceptual results that both global and individual ageing functions produced suitably aged individuals but that the individualised method was the superior method.

Scandrett et al. [38] investigated ageing functions using combinations of ageing trajectories. Like Lanitis et al. [37], they used a face model parameterised using PCA, and aged the model through this PCA space. In order to eliminate variations caused by pose and expression, the horizontal and vertical rotations were weighted subjectively by human observers and then defined in the face space as the sum of score weighted face parameters. Weighted multiples of these vectors were then used to alter the pose and expression so that they became uniform. This method

approximated the rotation of a three-dimensional object on a two-dimensional plane by a linear method; this was a reasonable approximation providing that the angles between the face pose and the normalised pose were small. In the event that the angle was large, this approximation became less accurate.

Even in small rotations, parts of the face that were occluded became visible, their textures were unknown and must be approximated. Scandrett et al. achieved this by reflecting the normalised image about its vertical axis. Like other 2D ageing methodologies, Scandrett found that lighting variations reduced clustering of face parameters of around the same age and thus the quality of aged textures. This effect was particularly pronounced with trajectories derived from an individual's history using fewer face samples resulting in less smoothing of errors.

Each of the trajectories were designed to extract different factors that affect ageing, such as personal history, sex, how parents aged etc. The trajectories were defined as the sum of the face parameters centred on the group mean weighted by the mean shifted age of each face. Face images were aged by altering their parameters in the direction of one or more combined ageing trajectories until the target age was reached.

As males and females are known to age in different ways, separate ageing trajectories were produced for male and female in each group. An input face was then compared to these ageing trajectories to determine the comparative influence of the male and female trajectories using a ratio of distances from the face to each trajectory.

It is often the case that multiple images of an individual that are available covering a range of ages, all of which pre-date the 'start' age of an ageing function. The 'start' age being the age of the most recent image and therefore, the closest to the target

age. Scandrett et al. used these images to construct what they called a ‘historical’ ageing trajectory, using the age weighted average of the images in the same manner as they had for other groups of images. This historical trajectory could then be combined with the ageing trajectory for the age group of the starting image from the training set to produce an aged face image. They weighted the trajectories according to a maximum-likelihood metric driving it to be a typical member of the set of trajectories between the source and target age groups, and driving the target of the ageing trajectory to be a typical member of the set of faces at the target age.

The results were analysed using the root-mean-squared error, both on the shape vertices and per pixel, between the resulting face image and a known ground truth image of the individual at the target age. All faces were converted to greyscale and normalised to have a mean intensity of zero and standard deviation of one in order to remove some of the effects of lighting. They found that in general, the root-mean squared shape and texture errors were lower when compared to a the ground truth image than with other images in the target age set, and concluded that the ageing methods both aged the individuals appropriately and retained identity through the transform. They found that the most accurate method of ageing varied between individuals and so could not conclude which method had the best performance.

Scherbaum et al. [52] fitted a three-dimensional morphable model to a database of laser scanned cylindrical depth-maps. They used a database of 200 adult images and 238 teenagers. The later group ranged in age from 96 months to 191 months. In order to improve the resolution of the face texture map, they reconstructed the textures from three photographs taken at three separate angles. They used the parameters of the model and the age of the subject to train a Support Vector Regression (SVR) model. The SVR formed a mapping from the high dimensional parameter space of

the model to the space of the subject's age. This was used to estimate the age of the subject once the parameters of the morphable model have been found. A new face model could be synthesised from a given set of parameters by 'stepping' through the curved SVR space using a fourth order Runge-Kutta algorithm, using the parameters and an estimated age as the starting point. They didn't use multiple time-space images of the same individual in building the model, their claim to individualisation is the observation that is based on the mean angles between the support vector gradients; the SVR produced different ageing trajectories for different individuals and could therefore be said to be individualised. While this was true, the variation was derived from a large number of single 'snapshots,' i.e. it described the variations within a population. It might not necessarily capture the variations due to ageing in a particular individual. An alternative direction based on dynamic Markov models was developed by Suo et al. [55]; they used a Grammatical Model [56] to describe a set of faces as a hierarchical set of face components, (eyes, nose, skin patches etc.), with an individual face defined as a particular choice of components from the set. An input face was aged in a probabilistic manner using a dynamic Markov chain to select the most likely set of face components at a target age given the current set.

Park et al. [53] performed a similar experiment; fitting a three-dimensional Morphable Model to a set of delineated faces using point data. Ageing was performed by calculating a set of weights between an input face and exemplar faces in the same age group. These weights are then used to build an aged face as a weighted sum of the corresponding faces at the target age. The results were compared using Cumulative Match Characteristic curves to other ageing methods and reported similar results to other methods. They observed that shape modelling in

three-dimensions gave improved performance in pose and lighting compensation. Their method only fit to the delineated point data.

2.2.4 Age Estimation

Age estimation is the conceptual opposite of ageing synthesis. The age of the face is estimated from an image rather than synthesising a change resulting from age. Kwon et al. [57] used the ratio between facial features, the nose, eyes and mouth, as well as wrinkle analysis. If wrinkles were found and ratios indicated an adult face, the image was marked as a senior adult. An image with no wrinkles and a baby-like ratio between features was marked as a baby; otherwise, the image was marked as an adult. This idea was expanded upon by Horng et al [58], who used a three phase method; feature location, extraction and classification. Two geometric features; the ratio distances between eyes and nose and between nose and mouth were detected using a Sobel edge detector; and three wrinkle regions were detected. A Sobel edge detector was used to classify wrinkle density that was defined as edges area. The age was classified to one of four age groups using back propagation Neural Networks. Kalamani and Balasubramanie [59] used a fuzzy Neural Network to account for uncertainty in the classification model. Images were classified according to a degree of inclusion that indicated the degree of truth of the lattice [59]. A fuzzy lattice is a lattice that fuzzifies the conventionally binary valued lattice-inclusion relation, which was applicable to any pair of lattice elements. A complete lattice is a lattice with a minimum and a maximum element denoted by 0 and 1 respectively. The training by Fuzzy Lattice Neural (FLN) required two inputs, these were, a set S , which included all wrinkle features to be used for training as well as the vigilance parameter, which was the real number between 0 and 1. The output of training algorithm was a set of clusters, these were age groups which have been learned during training [59].

Lanitis et al. [60] compared four classifiers for age estimation; quadratic ageing curve, Mahalanobis distance (i.e. probability that the input face belongs to a particular group), back propagation Neural Network (using multilayer perceptions), and Kohonen self organising maps. They also introduced three new types of classifiers based on the training method. Firstly, a classifier they called age-specific, in which the faces were grouped into strata according to age prior to training, where the classifier was only expected to place the input face into the relevant strata. Secondly, a classifier that they called appearance-specific, which grouped images according to observation [37] of the relationship between appearance and ageing patterns, divided the individuals into groups of faces that appeared similar or aged in a similar manner. Thirdly, a combination of the two classifiers was also introduced. The methods were evaluated and compared using two-fold cross validation with the mean average error in years between the classification result and the known ground truth. The new classifiers improved accuracy and offered greater improvements when combined. They used perceptual evaluation of the training images with 20 human raters to gauge the accuracy of human age perception. The raters were shown the whole image, including details such as hairlines. This was known to affect how humans rate an individual's age. Human raters out performed the computers albeit on a much reduced number of test images.

A number of authors have used Support Vector Regression (SVR) [61] for age estimation [62] and synthesis in three-dimensions [52]. Gandhi [62] used SVR, which is a modification of SVMs, to perform age estimation using a training set of normalised face images. The images were first compensated for illumination using the Retinex algorithm [63] to perform dynamic range compression and a histogram equalisation algorithm to bring the images to the same intensity range. The images

were delineated and compensated for pose using an affine transform. Images, where the face did not have a neutral expression, were rejected as this would affect the formation of wrinkles. A Support Vector Regression machine was trained on the pixel intensities of 818 images ranging from 15 to 99, using a variety of different bases, polynomial, radial, and sigmoid. They found that a polynomial basis of degree 3 produced the most accurate age estimation for an unseen image producing an average of 9.31 years absolute error and a squared correlation coefficient of 0.69 when validated using 4-fold cross-validation. Lanitis [60] used Support Vector Machines to derive a non-Gaussian similarity and age metric, with a hyper plane separating faces in an age or identity group from other faces in the set, and a scalar between 0 and 1 indicating the degree of dissimilarity between an input face and the set. An ageing trajectory was found that maximised the similarity metrics between the target age group and the groups of individuals using a sequential quadratic programming method. The identity of an unseen individual was maintained throughout the process by maximising the sum of differences between the similarity metrics before and after age progression.

Many of the statistical methods that were used lost textural detail such as wrinkles; few researchers developed methods that attempted to create appropriate textural detail in aged images. Tiddeman et al. [64] used a wavelet transform and Markov Models [65], Hussein [66] used Bidirectional Reflectance Distribution Functions and Gandhi [62] used Gaussian filters. These methods worked by attempting to replace or adjust the high-frequency components of the image to match the high frequency components of a prototype at the target age. Hussein [66] synthesised wrinkles by attempting to align the surface normal of two faces, an older and a younger, using the relationship between pixel intensity and surface orientation. Under the assumption

that the two surfaces shown in the image were under the same lighting conditions, surface details such as wrinkles would become the primary changes in intensity. They used the ratio of the two images smoothed with a Gaussian filter multiplied with one of the images so that the fine detail of the other was applied to it.

Their methods suffered from two main drawbacks; firstly, they could not be used under varying lighting effects; and secondly, the age was defined from only one image and thus would not in general produce a convincing ageing result for an arbitrary individual. Gandhi [62] used an Image Based Surface Detail Transfer [67] procedure to map the high frequency information from an older prototype to a younger, and vice-versa using a Gaussian convolution as a low pass filter. The idea here was to take the high-frequency details of the input image and replace them with the targets. The Gaussian convolution produced two images, one was the smoothed original image containing the low-frequency large-scale detail and the other was the result of applying a standard boost filter containing the high-frequency fine-scale detail. An aged image was synthesised by combining the high-frequency of a prototype with the low-frequency of the image. Varying the width of the kernel would vary the size of details captured and thus the perceived age of the person. The prototypes at each age were created by averaging all the images in an age group. Smoothing problems were avoided by combining the high-frequency parts of the training images with the combined average to retain fine details.

Tiddeman et al. [64] used a Gabor wavelet function to detect edges in the image and decomposed it into a pyramid of images containing edge information at varying scales. The edge magnitudes were then smoothed with a B-spline filter to give a measure of edge strength about a particular point in each sub-band. Prototypes at each age were generated using the technique of Burt and Perrett and the wavelets

then were amplified locally to match the mean of the set. The values of the input wavelet images were modified to more closely match those of the target prototype. These were tested perceptually and found to reduce the gap between the perceived age of the image and the intended age. They extended their method using Markov Random Fields (MRF) [58]; an individual was aged using the prototyping method of Burt and Perrett described above [41]. Detail was added to the resulting face by decomposing the image into a wavelet pyramid and scanning across the sub-bands using the MRF Model to choose wavelet coefficients that match the cumulative probability of the input values. They concluded that the resulting image was matched to the target age of the older group by human raters in a more precise manner than either the Wavelet method or the prototyping method [65].

However, the comparison between different facial ageing estimation techniques is very challenging for a number of reasons. Firstly, there are very few standardised 2D facial ageing databases which are used for benchmarking purposes. Thus, the size and the type of the datasets vary across different publications. Secondly, there are differences in the experimental setups and in the metrics used to evaluate the performance of the facial ageing estimation techniques.

2.2.5 Overview on the Facial Expressions with Wrinkles Appearance

In addition to the fact that facial wrinkle appearance is a vital sign of ageing, it also plays an important feature in presenting FE; therefore, it became the focus of a number of FE researches.

Yin and Basu [68] presented a partial texture updating method for facial expression synthesis with facial wrinkles. They started by estimating fiducial points on the face using a colour-based deformable template matching method. Then, a dynamic mesh-matching algorithm was developed for face tracking. Textures of Interest (TOI) in the potential expressive wrinkles and mouth–eye texture areas were captured by the detected fiducial points. Among the TOI, the expressive textures were extracted by exploring temporal correlation information. Finally, the entire facial texture was synthesised using the active texture. They extended their work in [69] to use facial wrinkle textures for recognising facial expressions. Based on the observation of the wrinkle appearance and the change along with performed expressions, they extracted the partial texture information in both the facial organ areas; for example, eyes and mouth, and the facial wrinkle areas. They used the texture dissimilarity between the neutral expression and the active expression to extract the active texture for the expression representation.

In the muscle-driven modelling of wrinkles for 3D facial expressions, Zhang [70] presented a geometric wrinkle model that was defined according to facial muscle anatomy for simulation of dynamic wrinkles within expressions. His method was applied to an anatomy-based face model with a multi-layer structure of skin, muscles, and skull. The location and orientation of the wrinkles were automatically determined based on muscle contraction and its influence on the skin. Corresponding to two types of facial muscles, the geometric wrinkle model governed the

development of wrinkle amplitude in the local deformed face regions. It provided intuitive parameters for easy control over wrinkle characteristics by considering the properties of real wrinkles.

Similar to [68], the work in [71] used facial wrinkles in synthesising and analysing FE. They, [71], developed a system to analyse subtle changes in facial expressions based on both permanent (e.g. mouth, eye, and brow) and transient (e.g. furrows and wrinkles) facial features in a nearly frontal image sequence. Multi-state facial component models were proposed for tracking and modelling different facial features. Based on these multi-state models, they detected facial features including mouth, eyes, brow, cheeks, and their related wrinkles and facial furrows.

For expressive facial animations, Li et al. [72] developed a method for modelling dynamic facial wrinkle. They started with structured facial mesh, then divided the face region into wrinkle sub-regions, and created some wrinkle lines with their algorithm in these sub-regions. Some key nodes were labeled on the facial mesh; these key nodes affect wrinkle lines if wrinkle lines located the sub-regions that abut on the key nodes. With the algorithm, motion of wrinkle lines was produced by movement of the key nodes. Consequently, wrinkle lines derived facial mesh to model expressive wrinkles.

From expressions on a 3D face model, Antini et al. [73] proposed a framework for three-dimensional face representation and matching for identification purposes. Basic traits of a face were encoded by extracting curves (wrinkles) of salient ridges and ravines from the surface of a dense mesh. A compact graph representation was then extracted from these curves through a modelling technique that was capable to quantitatively measure spatial relationships between curves in a three-dimensional

space. Therefore, face recognition was obtained by matching 3D graph representations of faces.

2.3 Conclusion

From previous research, it can be seen that a number of studies have been conducted in the tasks of age estimation and simulation. All of this research was carried out for different purposes using various techniques and using different datasets. The common aim for these studies can be described as an attempt to increase accuracy as the ageing process itself differs from one person to another for a myriad of reasons, which makes the accuracy of the estimation and prediction rather difficult.

It can also be noted that previous work did not concentrate on the visual representation of wrinkles. It is known that wrinkles form major ageing feature and can change the texture appearance on individuals; omitting their significance could lead to uncertain results, as seen in the work of Rowland and Perrett [46], where the wrinkles happened to be blurred in the process, thus, affecting the accuracy of the estimated results.

In addition to this, many of the statistical methods used in the field of age estimation lost textural detail (wrinkles). Few researchers have developed methods that attempt to create suitable textural detail in aged images, such as the work found in [62] and [66]. This is because it is important to reduce the gap between the perceived age of the image and the intended age.

Nevertheless, some work in the facial expressions area extracted wrinkles in different face regions, like the work in [69] and [74], but no work has combined those regional wrinkles to one unique wrinkle map that can identify individuals.

The vast majority of the previous and current research, in both facial ageing estimation and facial ageing simulation, adopt two-dimensional approaches; perhaps owing to the limitation of 3D data resources. 3D facial ageing has the potential to achieve better accuracy than its 2D counterpart by measuring the geometry of rigid features on the face. This avoids such pitfalls of 2D facial ageing as a change in lighting, the use of low quality images, etc. The following is a further explanation on the advantages of 3D data over the 2D data:

Two-dimensional face models, by definition, store no information about the shape of the face in the depth plane, i.e. along an imaginary axis that points into the image. This results in a number of shortcomings in using these models for face analysis. The models are highly vulnerable to changes caused by rotations, perspective effects, or changes in the lighting conditions around the face being studied. As these effects are not related to ageing it is important to eliminate them before attempting to train an ageing model, to avoid any spurious correlations. As an example, if most or all of the images of individuals in one age range were taken from a frontal view and most of the images of another age range were at an angle, the naive method would consider the changes in the image related to rotation to be the strongest correlation to ageing. Previous researchers have attempted to deal with the problem of pose in two-dimensions either by using a standardised image sets, or by using a two-dimensional linear transform to ‘de-rotate’ images. Standardised image sets, where the pose and lighting of the subject can be controlled, are not always available and even small rotations can affect the results, so a method that eliminates the effects of rotations is preferable.

Lighting effects cause similar problems, although lighting can be described in a linear fashion in two-dimensions, either as a low frequency approximation [75] or as

a point light source in image template alignment [47], these methods both rely on the absence of rotations and shadowing. Image normalisation can remove the effects of ambient lighting but are still prone to the effects of more directional lighting effects, such as diffuse lighting specular highlights and even area lighting. As a result, lighting effects have been found by some authors [76] to creep into ageing functions even when the images have been normalised.

A two-dimensional model can capture the shading changes related to three-dimensional shape change, provided the lighting is constant. However, the lighting sources in our dataset are not constant and exhibit changes in lighting angle, composition and spread. Using a three-dimensional model to describe the face can deal with these problems by synthesis.

The effects of rotation, perspective changes, and lighting transfer can be described using physical modelling. As a result, these effects can be used as independent parameters in the description of the fitted face model and normalised in the age-model to remove their effects. Another shortcoming of two-dimensional images is the loss of information in the parts of the image occluded, either by rotations causing self-occlusions in the face or by other objects.

Although, the utilisation of 3D facial data in general research has shown to be more robust with respect to handling poses and lighting variations, 3D facial ageing is still facing several challenges such as the lack of the availability of real information regarding the change in facial appearance in accordance to ageing.

In conclusion, it is believed that generating wrinkle maps will solve many of the issues discussed and will boost accuracy to a higher level. Moreover, they can be utilised in many different applications, for example, in ageing simulation; they can be used to create a wrinkle pattern formation system. This system may even be

developed further to be integrated with facial ageing simulation systems to increase the level of accuracy.

This research will tackle the knowledge gaps in the current state-of-the-art by developing methods to predict the length of the wrinkles on the forehead area of face images at any given age. Then full facial wrinkle maps will be extracted from faces with expressions, thus, giving an indication on the locations of the facial wrinkles for any individual. Every extracted wrinkle map will undergo a further process in order to calculate the intensity of the wrinkles and categorise them into colour groups. Finally, both wrinkle maps will be employed in the development of a 3D system that simulates and predicts facial wrinkles.

In the next chapter, the idea of generating wrinkle maps will be applied on the forehead area of 2D images. Using mathematical algorithms, wrinkle lengths will be predicted for other images of the same ageing sequence of a given individual.

CHAPTER THREE

3 Predicting the Change in Length for Forehead Wrinkles

3.1 Introduction

From the findings of chapter two, it was noted that there is a lack in the facial wrinkles study; therefore, facial wrinkles will be the focus of this research starting by experimenting with the wrinkles on the forehead area. This involves the development of methods to predict the length of the wrinkles on the forehead area of face images at any given age, starting at the age of 19.

The forehead area forms the major wrinkles on the face; its wrinkles are categorised in the large-scale wrinkle group (as mentioned in section 1.1). In this chapter, mathematical and statistical methods are devoted to predict the characteristics of the forehead wrinkles, in terms of lengths, of 2D images by the means of novel techniques. The purpose of this work is to establish a new approach in dealing with facial wrinkles in connection with the ageing process.

This work will be conducted and tested on real 2D images of people taken from facial ageing databases. The FG-NET database and the MORPH database are used for this purpose. The FG-NET database contains 1002 face images of 82 individuals, whereas the MORPH database consists of two albums; the first album contains scanned photographs of 515 subjects with 1690 images, while the second one contains digital photographs with 55606 images. Both databases are widely used to carryout experiments, such as the works in [3, 15, 37, 77-79].

The low quality images of the two databases were the reason to concentrate on the forehead area in this chapter. Nevertheless, this work will demonstrate new

techniques in the process of predicting wrinkle changes across time and will prove validity and innovation by means of the method testing and comparisons.

The work starts by cropping the forehead area on every image and texture those cropped images onto a 3D forehead that is extracted from a constructed 3D face model [80]. NURBS curves [81, 82] are then projected on the wrinkles to form a 3D representation of those wrinkles.

A Geodesic Distance algorithm [83] will be used to calculate the length of each 3D curve (wrinkle) and will compare the outcome to the same curve of different ages to obtain a pattern, hence enabling the estimation and prediction of the length of wrinkles in the missing images. This is done by using Linear Interpolation [84] and Linear Extrapolation [85] methods.

The validity of the experimental methods will be tested using known data. The testing will be carried out by calculating the error rates that result from comparing the generated values to the actual data. Then the linear interpolation method will be compared to the quadratic and cubic interpolation methods.

The rest of this chapter is organised in the following manner: section 3.2 explains the pre-processing stage, in which a dataset for the experiment is produced. Section 3.3 discusses the methodology used and all the experimental stages that are tackled. The results are presented in section 3.4, while the experimental testing is performed in section 3.5. Section 3.6 will include comparisons between the linear, quadratic and cubic interpolation techniques. Finally, in section 3.7, a conclusion is drawn based on the findings of this chapter.

3.2 Pre-Processing Stage

For the pre-processing stage, 236 images of 50 people were selected from the two databases (Figure 3.1). Each person was given an ID as a unique reference. Through the use of MATLAB commands, the forehead areas are cropped to remove unwanted parts of the images and create a new image from a part of the original image. This procedure was done using ‘Crop Image Tool’ and the forehead area of each image was defined manually by the rectangular crop region that was generated by MATLAB.

The cropped foreheads are then textured on the 3D forehead model using Maya. Figure 3.2 shows the extracted 3D forehead model while Figure 3.3 presents foreheads that are textured on the 3D forehead model.

Maya is a very powerful 3D modelling tool that can interpret many file formats and can also convert between supported formats. It has been developed by Autodesk [86] and is used in the game and movie industries; for example, it was used as one of the tools in the creation of the science-fiction movie Avatar [87]. Figure 3.4 shows a screenshot of the Maya environment.

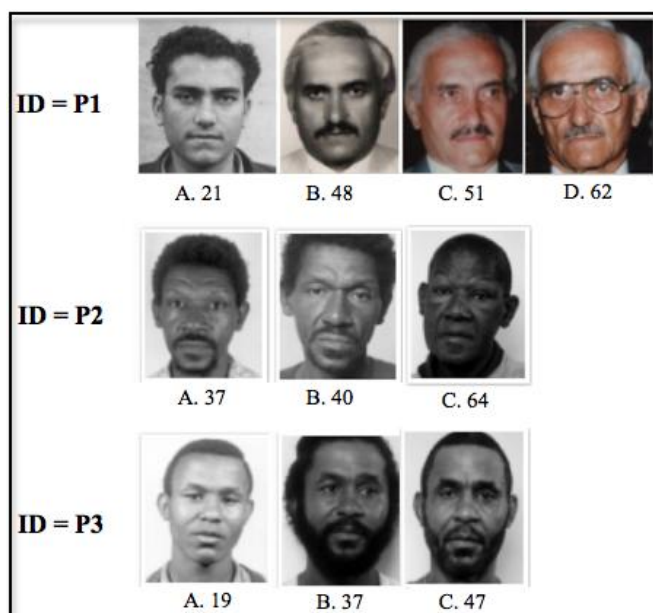


Figure 3. 1: A sample of 2D images with their IDs and ages



Figure 3. 2: 3D forehead model

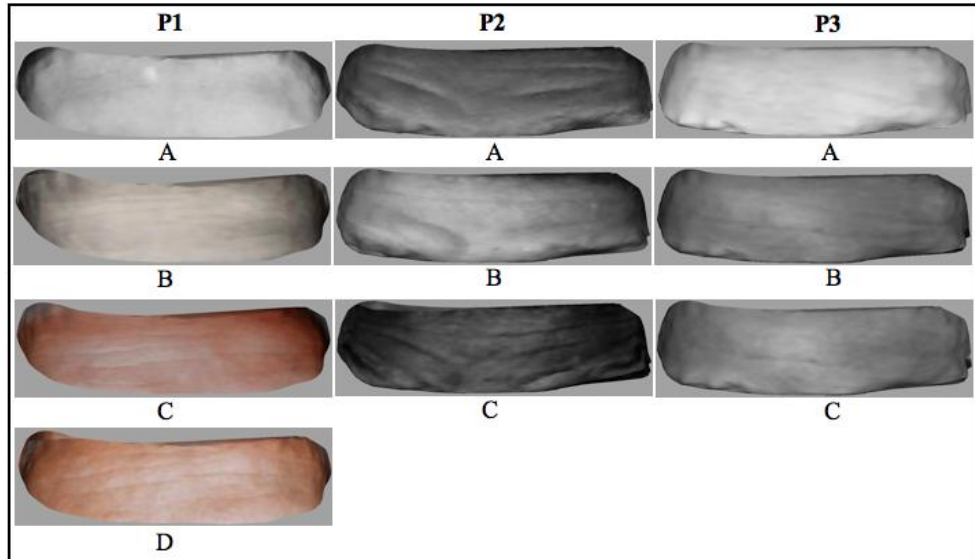


Figure 3. 3: Textured 3D foreheads

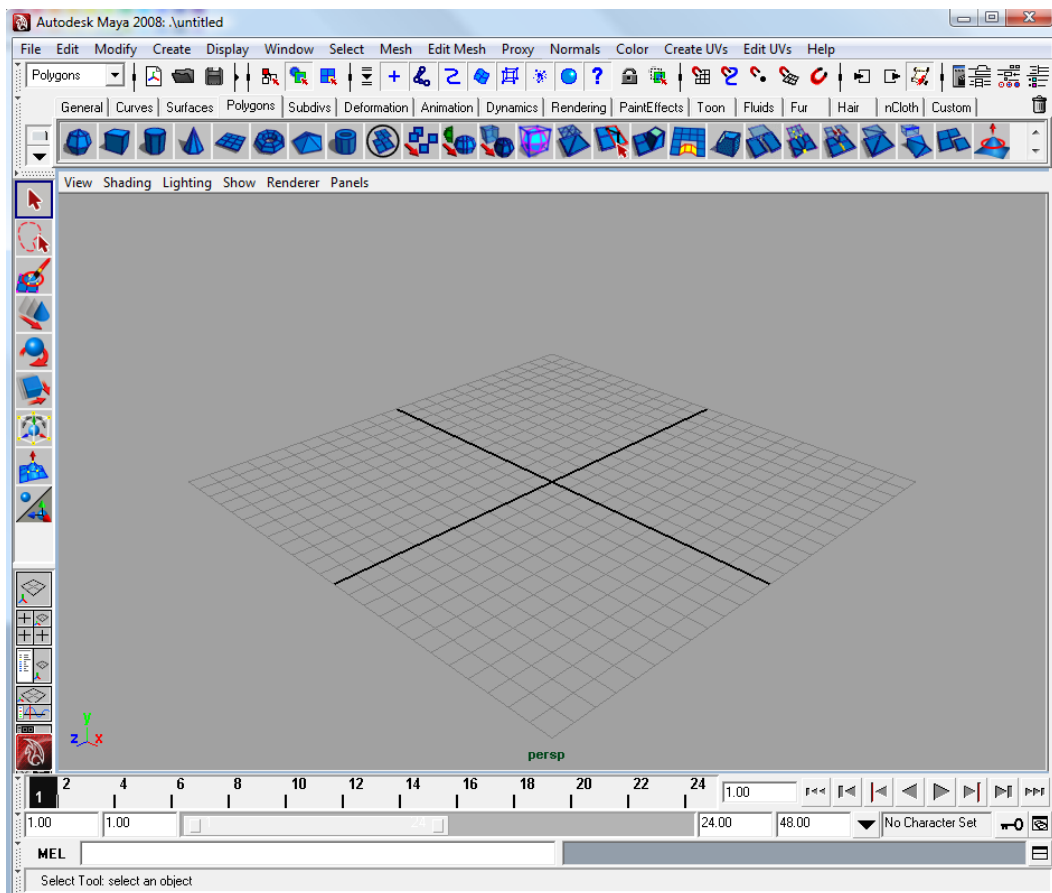


Figure 3. 4: Maya environment

3.3 Methodology

3.3.1 NURBS Curves Projection

There are many types of curves [81], such as the Bezier, Hermite, uniform B-splines and non-uniform B-splines. The variation between these curves can be distinguished by how the control points (vertices) are weighted. Each curve is defined by a set of points and in this aspect, a curve can be called interpolate or approximate. The curve is called interpolate if it passes through the control points and is called approximate if it goes close to them. The curve can also be interpolate and approximate at the same time if some parts of the curve go through the control points and the other parts get close to them. Figure 3.5 illustrates a 3D curve with its control points (vertices).

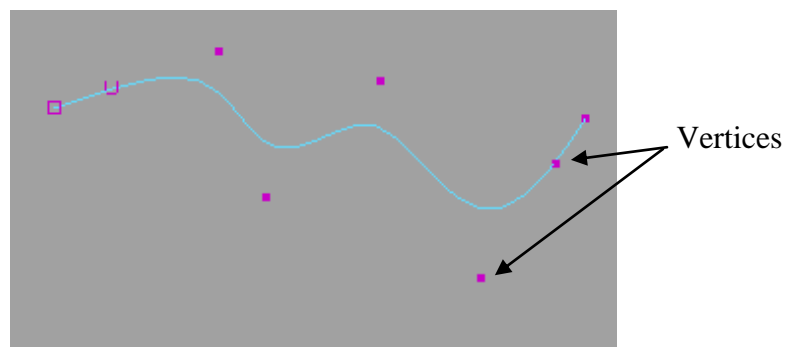


Figure 3. 5: A 3D curve with its control vertices

The control points act as weights that affect the shape and movement of the curve. The closer the point to the curve, the higher the weight therefore, the more influence that the control point has on the curve.

One type of curve is called NURBS, which stands for Non-Uniform Rational B-Spline [81, 82]. Non-Uniform references the behaviour that some control vertices affect a larger region of the curve than others [88]. Rational is pointing out that the NURBS curves are based on a ratio of a sum of polynomials, which allocate each control point to a weight [81]. B-Spline is Basis Spline and the word 'Basis' is taken

from an equation that is called the ‘Basis Function’. The basis function equation works out the weight of a given control point.

Some characteristics of the NURBS curves can be concluded in:

- The NURBS curve passes through the first and last points but only gets close to the other control points [81].
- They can represent virtual shapes [88].
- By using their edit points (Figure 3.6), shape of the curves can be controlled.
- They can represent complicated shapes with only a small number of control points.
- They are smooth, i.e. no sharp corners or rapid change in the direction can be observed.

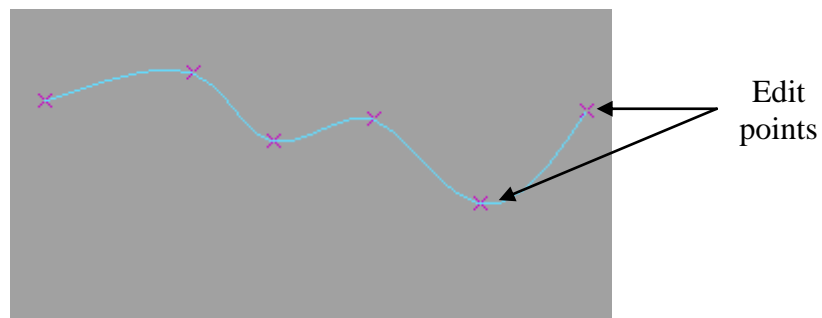


Figure 3. 6: A 3D curve with its edit points

The edit points separate the spans, which are smaller curves (segments) that construct the NURBS curve. When manipulating a curve, it is ideal to use its edit points as they lie on the curve. It is therefore easier to observe the way a particular part of the curve changes; bearing in mind that when altering an edit point, it is not the edit point that is changing the curve but it is the control vertices.

To find how much influence the control vertices have on a point (p) on the curve, a location is selected on the curve and the basis function ($N_{i,k}(p)$) is applied on each vertex to determine its weight. To calculate the location $L(p)$, the weights are

multiplied by the control points so a series of points (C_i) is obtained, which are then added together to generate the final position $L(p)$. The following equation is formed as a result:

$$L(p) = \sum_{i=0} C_i N_{i,k}(p) \quad (3.1)$$

Where k is the order of the basis function, which is calculated by the degree of the curve plus 1.

The above is a general explanation of the NURBS curves, which is necessary as all the 3D curves that are used in this thesis are of this type.

The end points of the forehead wrinkles are marked and NURBS curves are projected to form 3D wrinkle maps. Figure 3.7 shows a sample forehead with curves projected.



Figure 3. 7: A sample forehead with curves projected

Once the projection process is completed, the forehead is then hidden to allow a clear observation of the generated 3D wrinkles. Figures 3.8 – 3.10 present the results of the obtained 3D wrinkles for P1, P2 and P3 respectively with referencing numbers.

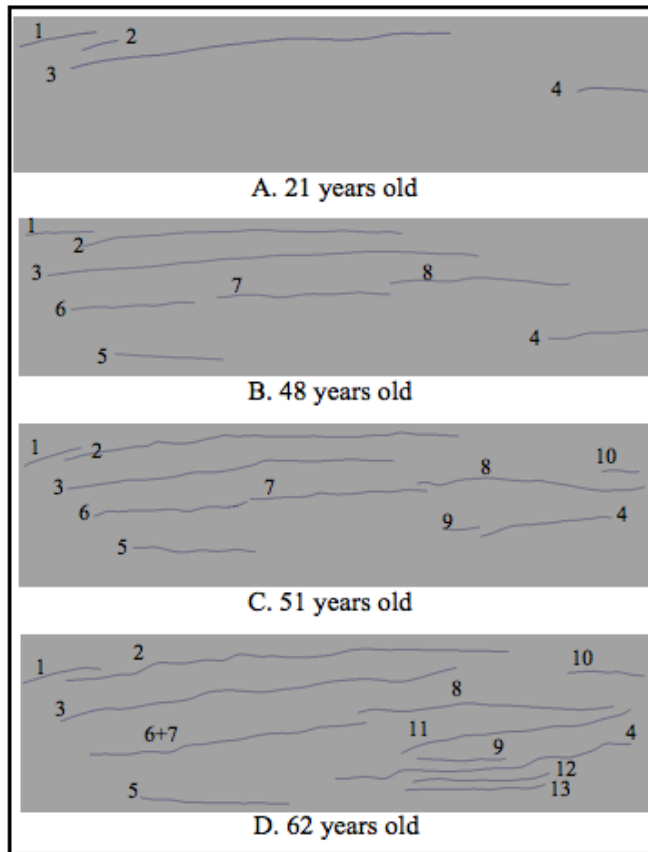


Figure 3. 8: 3D forehead wrinkles of P1

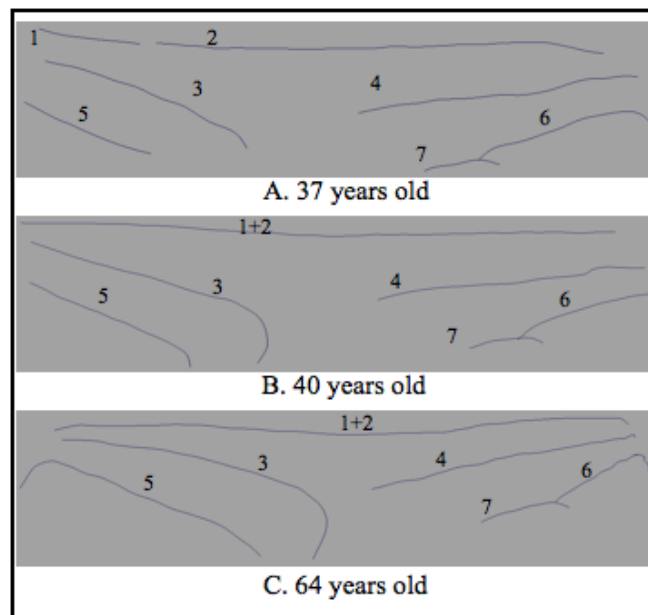


Figure 3. 9: 3D forehead wrinkles of P2

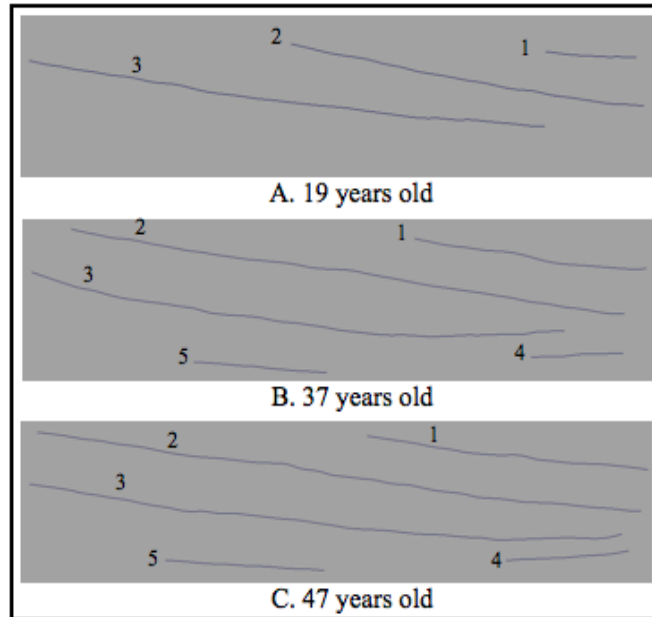


Figure 3. 10: 3D forehead wrinkles of P3

From Figure 3.8, a notable increase in the number of wrinkles can be seen as the person ages. A substantial increase in the length of wrinkle 2 (W2) can be observed; also W6 and W7 can be seen to join up at a later age.

According to Figure 3.9, a steady number of wrinkles from age 37 to age 64 can be noticed with a joint between W1 and W2 at a later age and a minor increase in the forehead wrinkles is displayed as age progresses, as shown in Figure 3.10.

From the observation of the 50 individuals, it is concluded that the degree of changes is subjective and depends on the life style of each individual, where the number and the length of the wrinkles increase as age progresses. The orientation and the appearance of new wrinkles vary from one person to another.

3.3.2 Calculating Wrinkle Lengths using the Geodesic Distance Algorithm

MATLAB codes are generated for this specific purpose. The following pseudocode represent the algorithm used for calculating the length of each curve:

```
Find the length of the wrinkle  
  
  Read the number of points on the curve  
  
  Read the first point  
  
  Read the second point  
  
  Read the last point  
  
  While the second point  $\diamond$  the last point  
  
    Calculate the distance between the first point and the second point  
  
    First point = second point  
  
    Second point = second point + 1  
  
  Calculate the geodesic distance of the curve  
  
End
```

Figure 3. 11: Calculating wrinkle lengths using geodesic distance

The calculation between any two points on the curve was performed using the *Euclidean Distance* (d) algorithm [89, 90]:

$$d = \sqrt{(x_2 - x_1)^2 + (y_2 - y_1)^2} \quad (3.2)$$

Since the curves are in three-dimensional space, a z-dimension is added to the equation so that the distance between the points (x_i, y_i, z_i) and $(x_{i+1}, y_{i+1}, z_{i+1})$ is:

$$d = \sqrt{(x_2 - x_1)^2 + (y_2 - y_1)^2 + (z_2 - z_1)^2} \quad (3.3)$$

Once all the distances between the points are calculated, *Geodesic Distance* (l) is applied to find the total length of the curve by adding all the neighbouring distances dN . Suppose that $D = \{d_1, d_2, \dots, d_n\}$ is a path in a connected domain between

points d_1 and d_n , i.e. d_i and d_{i+1} are connected neighbours for $i \in \{1, 2, \dots, n - 1\}$ and d_i belong to the domain for all i . The Geodesic Distance equation is:

$$l(D) = \sum_{i=1}^{n-1} dN(d_i, d_{i+1}) \quad (3.4)$$

The results are presented in Table 3.1 – 3.3. The values in the tables are rounded up to the nearest decimal point.

Table 3. 1: Wrinkle lengths for P1

W \ Age	21	48	51	62
1	11.2	15.8	16.7	17.4
2	4.7	38.2	57.8	62.1
3	43.2	49.2	46.9	53.8
4	11.0	13.2	20.9	41.7
5		12.9	16.5	18.3
6		13.6	21.9	36.8
7		15.9	20.0	
8		17.2	33.2	35.2
9			4.6	10.6
10			8.8	14.0
11				34.2
12				16.8
13				16.9

In the above table, a general increase in the length of wrinkles is noticed. The amount of the increase varies from one wrinkle to another depending on the deterioration of cells in the underlying surface of the skin.

Errors occurred in the two values that are highlighted in red. For W3-Age51, a decrease in the length of the wrinkle has been identified due to some lighting effects on the original 2D image. The same may apply on W6+7-Age62; when the two wrinkles are joined up, the total value is less than the values of W6-Age51 + W7-Age51.

Table 3. 2: Wrinkle lengths for P2

W \ Age	37	40	64
1	22.5	90.4	119.1
2	65.8		
3	38.9	45.5	75.2
4	49.5	46.6	60.1
5	26.7	28.8	63.2
6	36.7	30.0	51.6
7	14.5	16.1	18.8

A general increase in the lengths can be noticed in Table 3.2 with error occurrence in W4-Age40 and W6-Age40. It is also noticed that there is a minor increase in the lengths from age 37 to age 40, as there is only a 3-year gap between the two ages. On the other hand there is a considerable increase in the lengths from age 40 to age 64 due to the time separation between the two original 2D images.

Table 3. 3: Wrinkle lengths for P3

W \ Age	19	37	47
1	17.8	47.0	54.1
2	47.7	89.6	100.6
3	68.2	85.2	86.9
4		17.0	19.2
5		15.5	20.1

Again, an increase in the lengths is spotted with greater values from age 19 to age 37 than age 37 to age 47 due to the difference in the ages.

Based on the findings of this section, a common conclusion is drawn: the results suggest that the increase in the wrinkle lengths is proportional to the age progression and the amount of change is not known yet as wrinkles develop in different manners. This work aims to estimate predictions for these lengths at different ages, so linear functions will be implemented. It is suggested that linear functions will be valid in these particular experiments, as the estimations will be carried out using known information for pattern analysis; in other words, the estimated values are dependant

on the actual data. However, the linear function methods will be tested to prove their suitability.

Now, all the lengths are available, the next step is to perform the length predictions for some missing wrinkles.

3.3.3 Wrinkle Length Estimations and Predictions using Linear Interpolation and Linear Extrapolation Algorithms

Linear interpolation is used to estimate values in a set of data, given that two end values of the data are known. It is often used in numerical analysis (mathematics) and computer graphics. In this work, this technique is used to predict the change in the wrinkle lengths at a given age within the known data boundaries.

So for example, if the lengths are to be estimated at age 35 for P1, a graph is drawn for each wrinkle with the age is being the x-axis and the length is being the y-axis, then a straight line is drawn between the data to represent the linear interpolation. A sample graph is presented in Figure 3.12 for the change in W1.

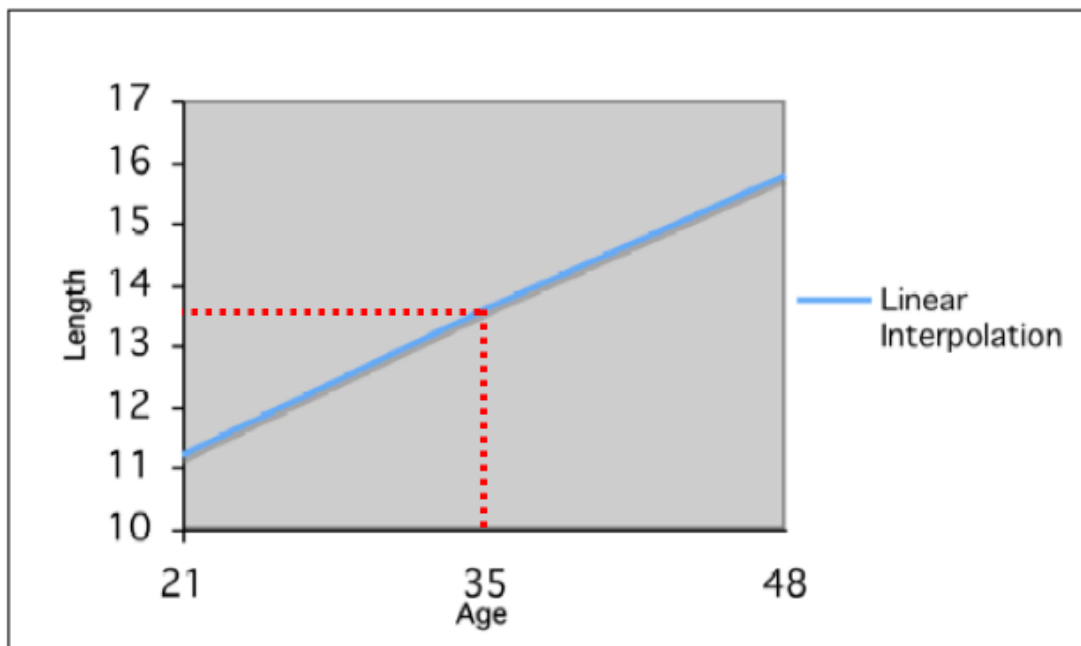


Figure 3. 12: W1P1 prediction at age 35

If the two known points at age 21 and 48 are given by the coordinates (x_1, y_1) and (x_2, y_2) respectively, the value of y along the straight line when $x = 35$ can be found by the following equation:

$$\frac{y - y_1}{x - x_1} = \frac{y_2 - y_1}{x_2 - x_1} \quad (3.5)$$

Solving the equation for the unknown value y at x gives:

$$y = y_1 + (x - x_1) \frac{y_2 - y_1}{x_2 - x_1} \quad (3.6)$$

Therefore:

$$y = \frac{(x - x_1)y_2 + (x_2 - x)y_1}{x_2 - x_1} \quad (3.7)$$

From the equation above, the length of the wrinkle at age 35 is estimated to be **13.6** to the nearest decimal point.

But on the other hand, the above method will not work when predicting future change, as the value of y_2 will not be known. To tackle this issue in order to predict future length change, linear extrapolation method is used as explained below.

Age 47 for WIP3 has the highest value of available data (Table 3.3), so for instance, to predict the length at age 56; the straight line of the graph (Figure 3.13) is extended to include the new data as shown below:

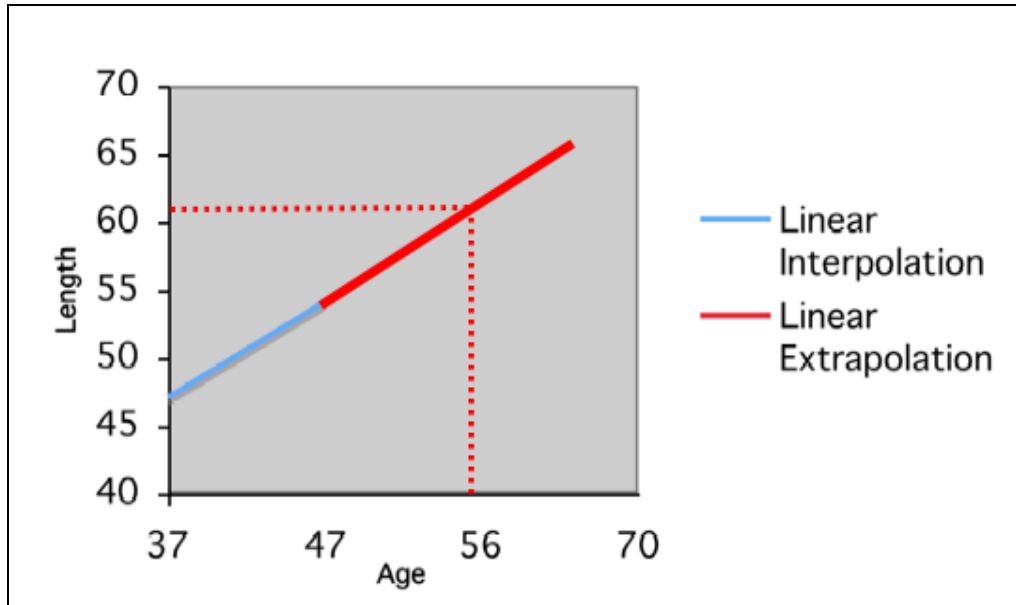


Figure 3. 13: WIP3 prediction at age 56

Suppose that the point (x_1, y_1) represents the coordinates at age 37, (x, y) represents the coordinates at age 47 and (x_2, y_2) is the point at age 56 i.e. y_2 is the unknown length; so from Eq. (3.5), y_2 can be found to be **60.5** to the nearest decimal point. Similarly, to estimate the length for a previous age, then y_1 will be the unknown variable.

The rest of the results along with the new predicted wrinkle behaviours are presented in the next section.

3.4 Results

In this section, the results of the predicted lengths for some selected ages are presented in the tables below while the predicted behaviours are illustrated in the images. The results in the tables are presented in blue.

Table 3. 4: Predicted wrinkle lengths for P1

Age W	21	35	48	51	62	68
1	11.2	13.6	15.8	16.7	17.4	17.8
2	4.7	22.1	38.2	57.8	62.1	64.5
3	43.2	46.3	49.2	46.9	53.8	53.8
4	11.0	12.1	13.2	20.9	41.7	53.0
5			12.9	16.5	18.3	19.3
6			13.6	21.9	36.8	36.8
7			15.9	20.0		
8			17.2	33.2	35.2	36.3
9				4.6	10.6	13.9
10				8.8	14.0	16.8
11					34.2	34.2
12					16.8	16.8
13					16.9	16.9

The highlighted values in the above table indicate anomalies due to either errors in the original values or lack of sufficient information available to perform the predictions. Figures 3.13 and 3.14 present the predicted wrinkle behaviours for age 35 and 68 respectively.



Figure 3. 14: Predicted wrinkle behaviours at age 35 for P1



Figure 3. 15: Predicted wrinkle behaviours at age 68 for P1

Table 3. 5: Predicted wrinkle lengths for P2

W \ Age	24	37	40	51	64	72
1	20.3	22.5	90.4	103.6	119.1	128.7
2	58.9	65.8		59.1	75.2	85.1
3	10.3	38.9	45.5	59.1	60.1	60.1
4	49.5	49.5	46.6	49.5	63.2	74.7
5	17.6	26.7	28.8	44.6	51.6	51.6
6	36.7	36.7	30.0	36.7	18.8	19.7
7	7.6	14.5	16.1	17.3		



Figure 3. 16: Predicted wrinkle behaviours at age 24 for P2



Figure 3. 17: Predicted wrinkle behaviours at age 51 for P2

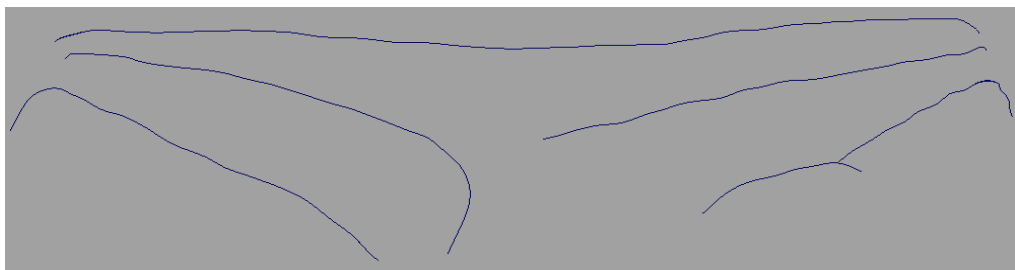


Figure 3. 18: Predicted wrinkle behaviours at age 72 for P2

Table 3. 6: Predicted wrinkle lengths for P3

W \ Age	19	28	37	47	60
1	17.8	32.4	47.0	54.1	63.3
2	47.7	68.7	89.6	100.6	114.9
3	68.2	76.7	85.2	86.9	89.1
4			17.0	19.2	22.1
5			15.5	20.1	26.1

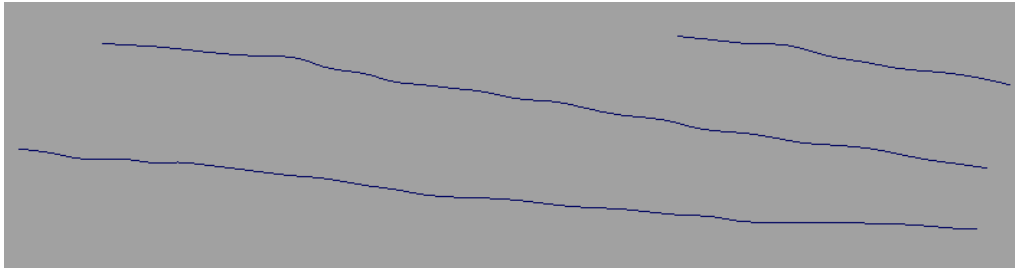


Figure 3. 19: Predicted wrinkle behaviours at age 28 for P3

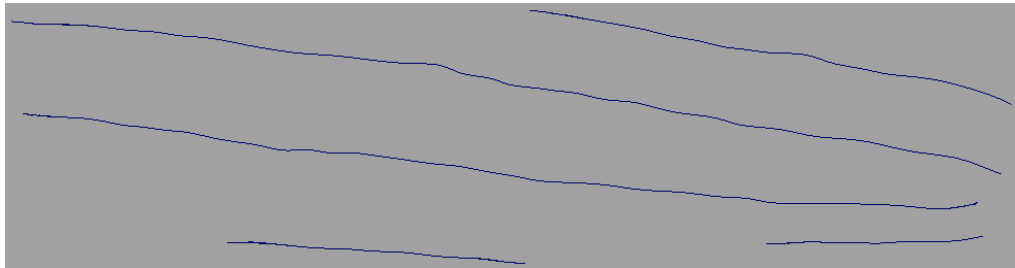


Figure 3. 20: Predicted wrinkle behaviours at age 60 for P3

3.5 Testing Method

The two algorithms (linear interpolation and linear extrapolation) that are used in this work give estimates based on the available data.

In this section, a method is harnessed to test the validity of the two algorithms by applying them on 30 different test subjects with the total of 85 wrinkles for each algorithm.

For every test subject, already known wrinkle lengths will be estimated then compared with the actual length values. The percentage error will then be calculated for evaluation.

Figures 3.20 and 3.21 show sample test images with their information for both linear interpolation and linear extrapolation.

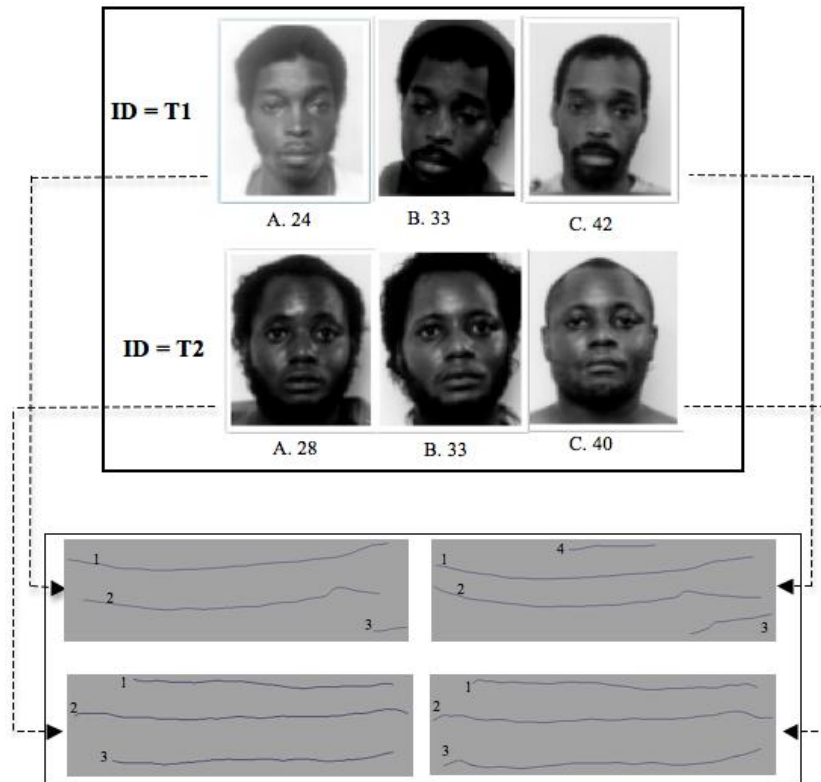


Figure 3. 21: Test images for the linear interpolation algorithm

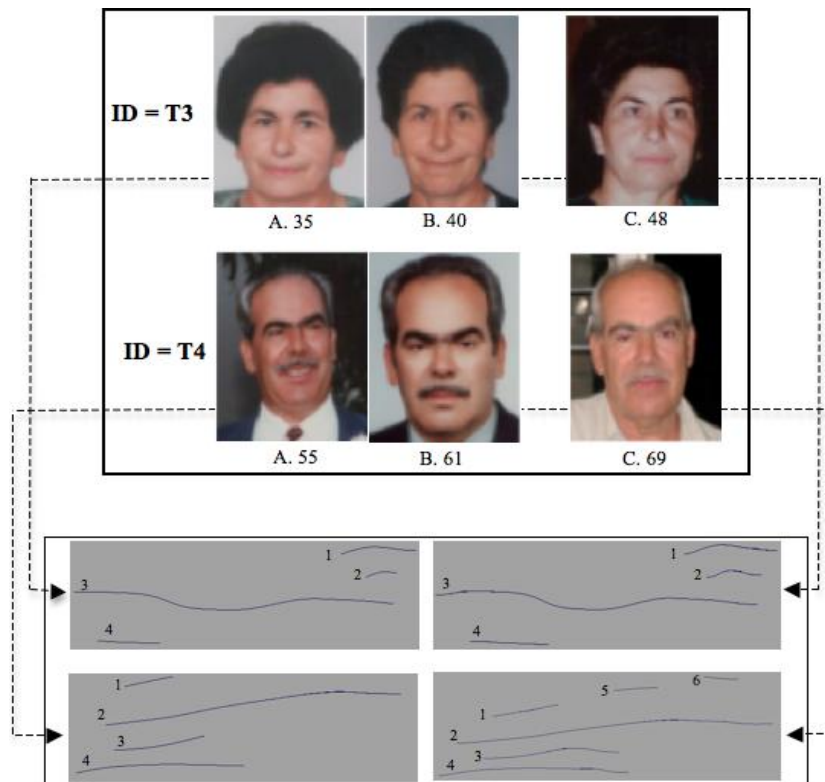


Figure 3. 22: Test images for the linear extrapolation algorithm

The lengths are calculated using geodesic distance as shown previously and the results are presented in the tables below. Any extra wrinkle that is developed at a later age is ignored as not enough information is given to perform the testing.

Table 3. 7: Wrinkle lengths for T1

W \ Age	24	42
1	76.0	93.6
2	69.0	91.0
3	10.7	24.5

Table 3. 8: Wrinkle lengths for T2

W \ Age	28	40
1	54.9	60.5
2	71.5	76.5
3	54.0	69.9

Table 3. 9: Wrinkle lengths for T3

W \ Age	35	40
1	19.8	25.2
2	8.4	16.1
3	65.2	70.2
4	11.7	15.0

Table 3. 10: Wrinkle lengths for T4

W \ Age	55	61
1	12.9	15.9
2	58.7	69.2
3	23.5	33.8
4	39.6	44.4

The tables below present the estimated values against the actual values.

Table 3. 11: Estimated lengths against the actual for age 33,T1

Wrinkle No.	Estimated Length	Actual Length
1	84.8	84.8
2	80.0	86.1
3	17.6	18.4

Table 3. 12: Estimated lengths against the actual for age 33,T2

Wrinkle No.	Estimated Length	Actual Length
1	57.2	56.1
2	73.6	73.7
3	60.6	63.4

Table 3. 13: Estimated lengths against the actual for age 48,T3

Wrinkle No.	Estimated Length	Actual Length
1	33.9	33.1
2	28.4	30.2
3	78.2	79.9
4	20.3	22.7

Table 3. 14: Estimated lengths against the actual for age 69,T4

Wrinkle No.	Estimated Length	Actual Length
1	19.9	22.4
2	83.2	83.6
3	47.5	49.8
4	50.8	52.0

The test results are also illustrated in the following charts:

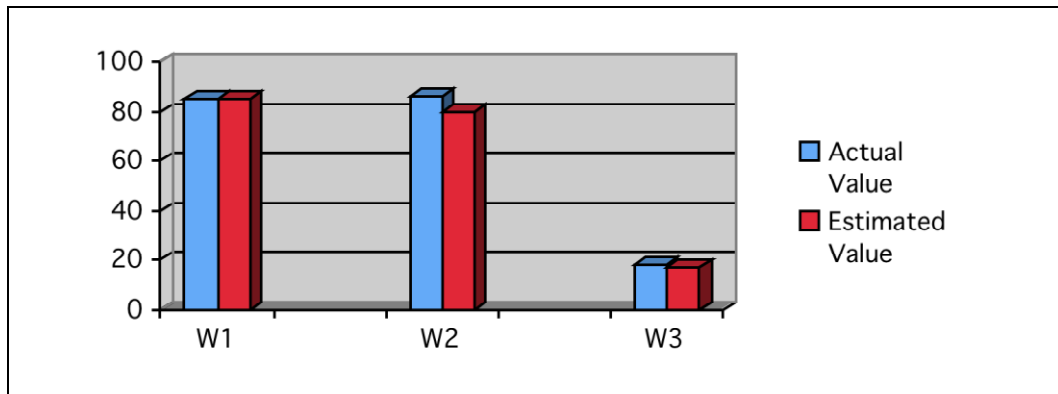


Figure 3. 23: Estimated values against actual values for T1

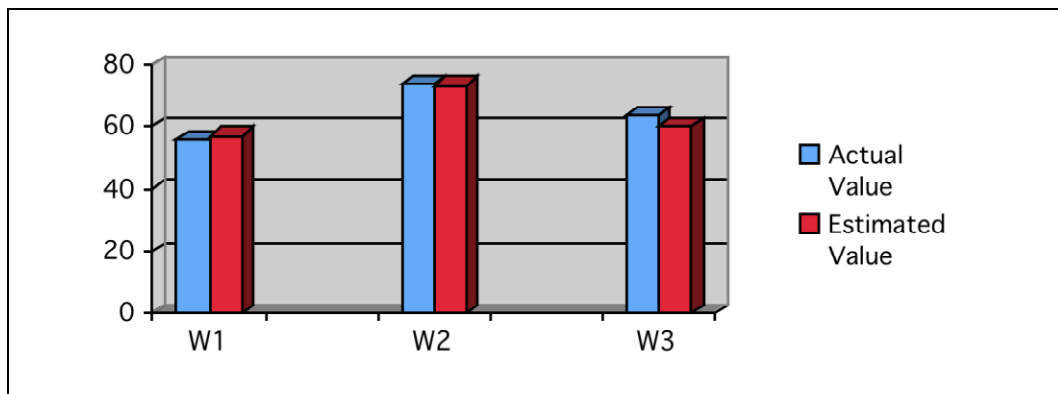


Figure 3. 24: Estimated values against actual values for T2

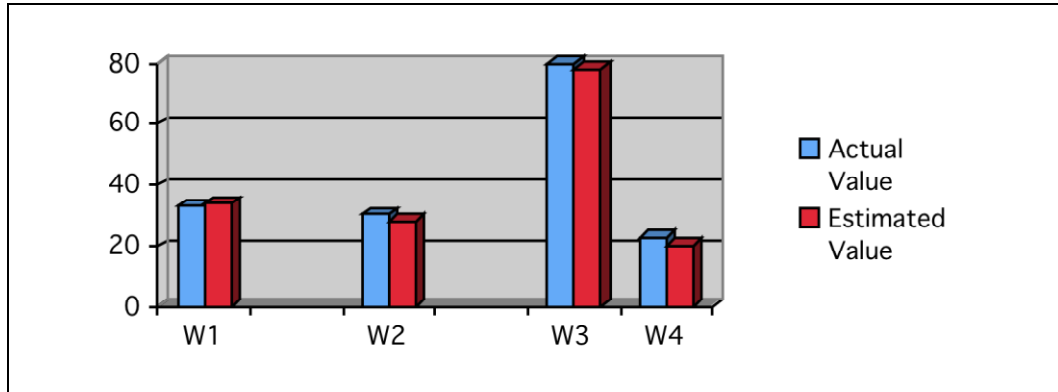


Figure 3. 25: Estimated values against actual values for T3

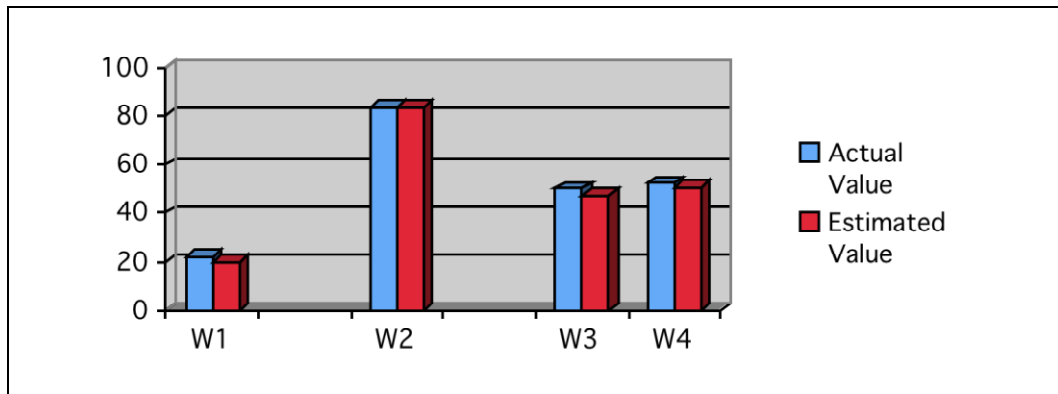


Figure 3. 26: Estimated values against actual values for T4

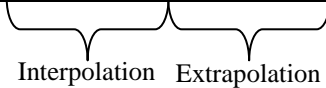
To calculate the percentage error (%E) for each wrinkle, the percentage error formula [91, 92] is used. The %E is calculated by taking the difference between the estimated value (Ev) and the actual value (Av) then divide it by the actual value. The quotient is then multiplied by a 100 and the result should be in absolute value. So the %E formula is:

$$|\%E| = \left(\frac{Ev - Av}{Av} \right) \times 100 \quad (3.8)$$

The percentage error for each wrinkle (to the nearest decimal point) is presented in the following table:

Table 3. 15: Percentage errors

W \ ID	T1	T2	T3	T4
1	0.0	2.0	2.4	11.2
2	7.1	0.1	6.0	0.5
3	4.3	4.4	2.1	4.6
4			10.6	2.3



From Table 3.15 and for the linear interpolation test results, a small percentage error is shown for each wrinkle. The highest error is 7.1% at T1W2 and the lowest is 0% at T1W1, which indicates an exact length estimation. On the other hand, for the linear extrapolation test results, the percentage error is slightly higher in general as the later method is known for giving less accurate estimations.

From the test data, the highest error rate came to 13.1% (for the linear interpolation) and 18.7% (for the linear extrapolation), thus, it is concluded that the length estimation and prediction methods work at small percentage errors, and therefore, efficiency is proved.

3.6 Evaluation Method

In this section, a comparison will be performed between the linear, quadratic and cubic interpolation techniques in order to evaluate which one out of the three gives the best results.

Similar procedure to the testing methodology used before will be implemented, that is, the lengths of some wrinkles will be estimated for a particular age then the estimated results will be compared to the actual data (known data) by calculating the error rate.

Figure 3.27 shows two sets of individuals in which the evaluation procedure will be implemented on.

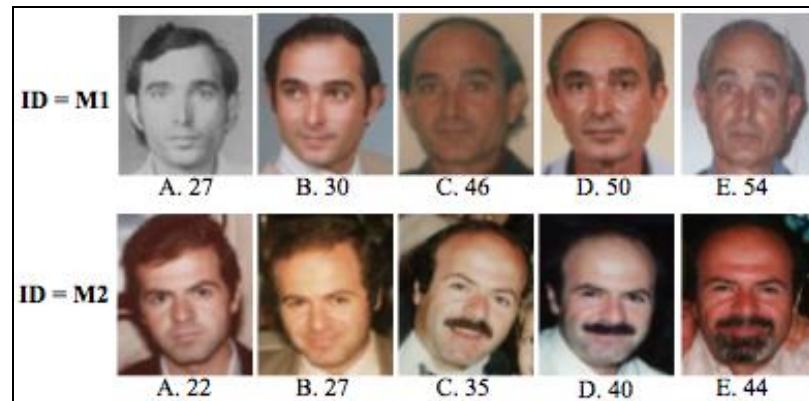


Figure 3. 27: Data sets for the evaluation method

The wrinkle lengths are presented in the following tables for M1 and M2 respectively:

Table 3. 16: Wrinkle lengths for M1

Age \ W	27	30	46	50	54
1	43.2	49.1	89.9	106.4	111.2
2	43.8	50.1	81.5	97.0	105.9
3	45.3	53.0	82.6	93.1	104.3

Table 3. 17: Wrinkle lengths for M2

Age \ W	22	27	35	40	44
1	23.4	25.8	53.0	59.1	65.1
2	26.7	31.9	55.7	62.6	70.3
3	43.6	50.7	64.5	72.4	78.0

The values of M1 (Age 46) and M2 (Age 35) will be omitted then the lengths will be estimated using:

- Linear interpolation, which can be calculated using *Eq. 3.7*.
- Quadratic interpolation, which can be calculated using

$$y = ax^2 + bx + c \quad (3.9)$$

- Cubic interpolation, which can be calculated using

$$y = ax^3 + bx^2 + cx + d \quad (3.10)$$

Where the lengths and the ages are represented by y and x respectively. a, b, c and d are variables.

The results for the 3 methods are presented in Table 3.18 below:

Table 3. 18: Linear, quadratic and cubic interpolation results

	Linear	Quadratic	Cubic	Actual
M1W1	94.9	92.4	79.3	89.9
M1W2	87.6	86.7	84.3	81.5
M1W3	85.1	86.6	85.9	82.6
M2W1	46.3	39.4	45.4	53.0
M2W2	50.8	47.9	53.2	55.7
M2W3	64.1	63.5	66.5	64.5

Table 3.19 presents the generated percentage errors for the three methods:

Table 3. 19: The generated percentage errors

	Linear	Quadratic	Cubic
M1W1	5.6	2.7	11.8
M1W2	7.5	6.4	3.4
M1W3	3.0	4.8	4.0
M2W1	12.6	25.6	14.3
M2W2	8.8	14.0	4.5
M2W3	0.6	1.6	3.1

From Table 3.19, the quadratic interpolation technique has the lowest error rate at M1W1, while the cubic interpolation technique has the lowest error rates at M1W2 and M2W2. There is no consistency in the advantage of one method over the others, but generally, the linear interpolation technique has the least percentage error rates.

3.7 Discussion and Conclusion

In this chapter, new efficient methods to estimate and predict the change in the length of forehead wrinkles for different ages were presented. The novelty of the work lies in the technical approaches that were used to perform the estimation and prediction processes with minimal percentage errors. The methods were carried out and tested on two-dimensional ageing databases; nevertheless, the methods are not limited to those databases. The purpose of the work was to introduce a new approach in dealing with wrinkles to establish a better understanding as wrinkles represent a major ageing feature. This will then help in developing future research. The results indicate that the increase in the wrinkle lengths is proportional to the increase in age. The methods can be developed further to include the entire human face and can be integrated, for instance, with life history survey of individuals to discover a real pattern in the change of wrinkle lengths across time, hence, produce quantitative analysis. For example, if the wrinkle length estimation and prediction techniques that were adopted in this chapter are linked to the parameters that affect facial ageing such as sun light, smoking, stress, alcohol, air pollution, diet etc, then a relationship can be established and therefore, quantitative information can be extracted.

Although ageing is a nonlinear process, linear functions were used in this work to estimate and predict the length of the wrinkles at certain ages. From the test results, it was noted that the linear methods were valid and effective. This is because the performed estimations and predictions were dependant on the behaviour of the given wrinkles that was based on the known data. The gaps between the known data were relatively small, which helped achieving small error rates, the highest was 13.1% for the linear interpolation technique while the highest was 18.7% for the linear extrapolation technique.

Moreover, some experiments were also conducted using quadratic and cubic interpolation techniques and compared to the linear interpolation method, the later proved to have the lowest error rates in most cases. Another advantage of the linear interpolation method over the quadratic and cubic methods is that the linear interpolation is the simplest method.

The work in this chapter is also distinctive among other similar type of research; for example, the work in [55] generates forehead wrinkles in groups of 10 years minimum, but wrinkles are in constant change i.e. wrinkles at the age of 43 in a person are likely to differ from those of age 49. In our work, wrinkle changes are estimated and predicted based on any given age (from 19 years and above); this feature indeed gives better results.

In many other research, such as [3, 15, 16, 78, 93-95], methods were implemented to estimate facial ageing overlooking the change in wrinkle formation. The work in this chapter has the advantage over other researches as it sets the initial stages in attempts to cover this important feature of ageing. Also in their works, only facial ageing estimations were considered but no predictions. Their systems look at the change in the facial texture and shape, then categorise the images into age groups. In our methods, wrinkle lengths were estimated and/or predicted for any specific age, providing that enough information were available to perform the operations.

Furthermore, the data sample that was used in this chapter covered a variety of races, which has given this work the advantage over the work in [55] as their research was limited to Asian faces only.

In the next chapter, the work will be extended to include the entire human face, that is, by generating wrinkle maps from facial expressions.

CHAPTER FOUR

4 Employing Image Processing Techniques in the Generation of Unique 2D Wrinkle Maps for Human Faces from Expressions

4.1 Introduction

Image processing [96] in computer science, is a type of signal processing for which the input is an image, such as a photograph, and the output can be either an image or some characteristics or parameters related to the image.

In this chapter, various image processing techniques are utilised to create a novel computer system that detects facial wrinkles for digital images of frontal human faces and generates two types of 2D wrinkle maps. The two types of wrinkle maps are binary maps that outline the location of the wrinkles and coloured (RGB) maps that define the intensity of the wrinkles.

Facial wrinkles are common signs of ageing and they are unique for every person, these two important characteristics are the reasons behind conducting the experiments in this chapter. The wrinkle maps can be used to predict the change in the wrinkle appearance of individuals when integrated in ageing systems; moreover, due to their uniqueness, they can be utilised as another biometric application for further increase to the security measures.

Facial Expressions (FE) are considered in conducting the experiments due to the fact that when performing FE, the wrinkles will become apparent and they are the likely future wrinkles. FE is a huge research topic; its value was derived from the importance of facial recognition and facial animation. A lot of work has been carried

out in this area for various purposes and it is a subset of Facial Action Codings (FACs) [70-72, 97].

The adopted techniques in this work involve taking 2D face images of 19 subjects of different ages, ethnics and genders. For every subject, six images are taken that include one neutral face and five faces with expressions to cover all potential wrinkles.

The five images with expressions will be entered to a computer system (designed in MATLAB) to go through a series of processes, illustrated in Figure 4.1, to detect and extract the wrinkles in order to generate the maps that are then saved into image files.

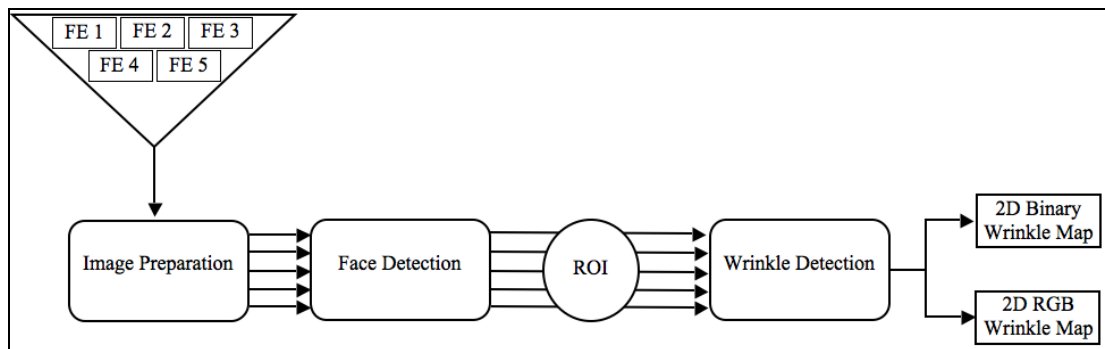


Figure 4. 1: The process of generating 2D wrinkle maps

The processes of the five faces will start by preparing each image in so-called pre-processing stage. In the pre-processing stage, the images will be converted to greyscale then filtered to reduce the noise. The conversion to greyscale is a vital step in order to simplify the intensity of the images as greyscale images only vary from black to white, where black has the weakest value at (0) and white has the strongest value at (255).

The prepared images will go through the ‘Face Detection’ block, which itself holds a process that will result in the detection of the face in every image to eliminate all the unwanted regions in that image.

The Region of Interest (ROI), which is the wrinkled regions in our case, on the detected faces will be identified. The images will move on to another phase of the process in which wrinkles will be detected and their intensities will be calculated.

The whole process will result in the generation of two outputs that are binary and coloured wrinkle maps.

The rest of this chapter is organised as follows: the collected experimental data set will be shown on the next section. Prior to the experiment, the preparation of the images will be described in the pre-processing stage of section 4.3. The experimental methods will be explained in section 4.4 along with all the stages of its process. The results will be presented in section 4.5 and tested in section 4.6. Finally the discussion and the conclusion are drawn in section 4.7.

4.2 Data Collection

A face dataset is collected to perform the experiment. The dataset contains 19 subjects, which include 16 males and 3 females at an age range of 19 to 43 years old (Figure 4.2). The subjects were asked to remove any spectacles or hats that could disturb the observation of wrinkles and some were asked to lift their hair back.

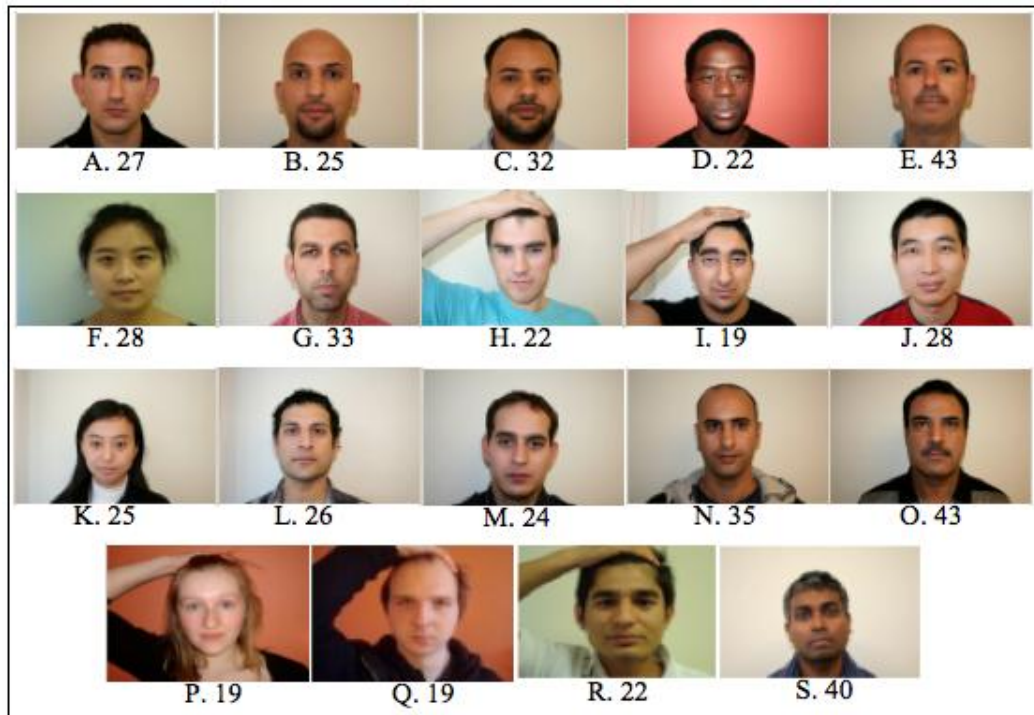


Figure 4. 2: The 19 subjects with reference letters and ages

For each of the 19 individuals, 6 close shots of their faces were taken: Neutral Face (NF), Eye-Brows Lifted (EL), Angry Face (AF), partially Closed Eyes with cheeks' muscles lifted (CE), Sad Face (SF) and Happy Face (HF) as illustrated on a sample subject in Figure 4.3.

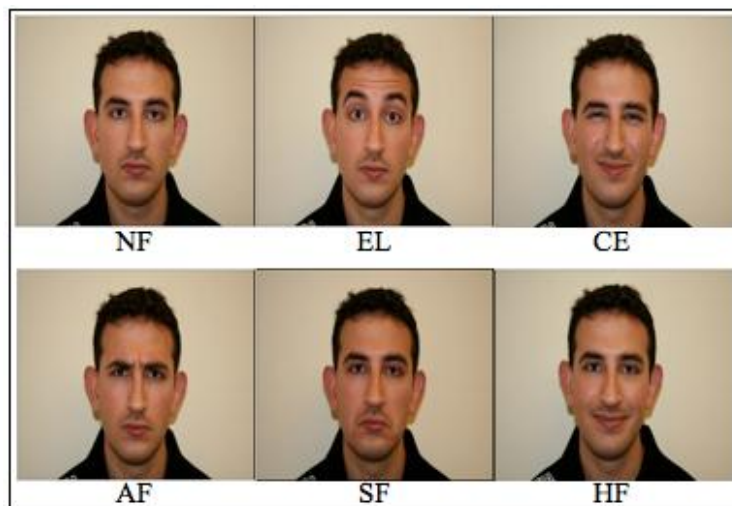


Figure 4. 3: Facial expressions

4.3 Pre-Processing Stage

Prior to the experiment, the images go through the following process:

- Converting RGB to greyscale: The conversion from the R'B'G' colour space to intensity is defined by the following equation:

$$\text{intensity} = [0.299 \quad 0.587 \quad 0.114] \begin{bmatrix} R' \\ G' \\ B' \end{bmatrix} \quad (4.1)$$

Where R', G' and B' are the pixel values.

- Adjusting image intensity: by mapping the values in image to new values such that intensities between low_in and high_in map to values between low_out and high_out.
- Noise filtration: using Wiener Filter.

A Wiener de-noise filter [98] is widely used in image processing to remove the blurriness in images due to linear motion or unfocussed optics. Its main advantage is the short computational time it takes to find a solution. The filter estimates the local mean and variance in the region of each pixel. The mean (μ) and the variance (σ) can be calculated from the following equations:

$$\mu = \frac{1}{NM} \sum_{n_1, n_2 \in \eta} I(n_1, n_2) \quad (4.2)$$

$$\sigma^2 = \frac{1}{NM} \sum_{n_1, n_2 \in \eta} I^2(n_1, n_2) - \mu^2 \quad (4.3)$$

Where η is the N-by-M neighbourhood of each pixel in the image (I); n_1 and n_2 are pixel values. To produce the filtered image (O), the Wiener filter is applied for each pixel using:

$$O(n_1, n_2) = \mu + \frac{\sigma^2 - v^2}{\sigma^2} (I(n_1, n_2) - \mu) \quad (4.4)$$

Where v^2 is the unknown noise variance, which is estimated from the difference between the filtered image and the original.

Sample products resulted from the pre-processing stage are illustrated in the figure below:

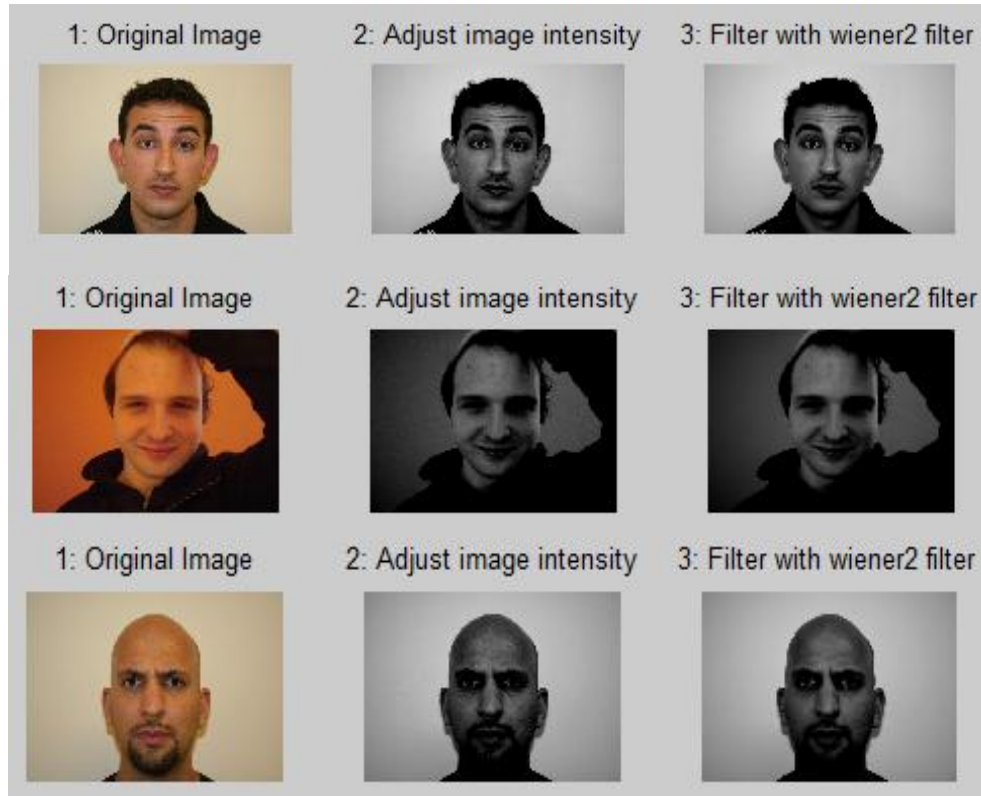


Figure 4. 4: Pre-processing stage

4.4 Experimental Methods

The experiment is tackled through various methods that are divided into stages and sub-stages.

4.4.1 Face Detection

This task is performed to detect the face in every image, thus, omitting backgrounds and any other part of the human body. It is divided into four steps; the first step is to perform the conversion between colour maps to distinguish skin colour. The second step is to detect the edges of the image to reduce the data. Then an automated

threshold for the image will be set to separate the skin region from the background or any other object. Finally, a method will be implemented to detect the face skin rather than any other type of skin (this may especially apply for those subjects who have their hands on the heads when pulling the hair back).

- ***Colour Conversion:***

There are different colour spaces used in the task of skin detection such as YCbCr and HSV. The existence of various colour spaces, in general, is due to the fact that they present colour information in ways that make certain calculations more convenient or because they provide a way to identify colours that is more spontaneous. For example, the RGB colour space defines a colour as the percentages of red, green, and blue hues mixed together, therefore, the relationship between the constituent amounts of red, green, and blue light and the resulting colour is unintuitive. Other colour models describe colours by their hue (blue), saturation (dark blue), and luminance, or intensity.

YCbCr is a practical approximation to colour, where the primary colours that are related roughly to red, green and blue are processed into perceptual information. In other words, the operations of image processing can be carried out in a more meaningful manner.

$$\begin{bmatrix} Y' \\ Cb \\ Cr \end{bmatrix} = \begin{bmatrix} 16 \\ 128 \\ 128 \end{bmatrix} + A \times \begin{bmatrix} R' \\ G' \\ B' \end{bmatrix} \quad (4.5)$$

$$\text{Where } A = \begin{bmatrix} 0.25678824 & 0.50412941 & 0.09790588 \\ -0.1482229 & -0.29099279 & 0.43921569 \\ 0.43921569 & -0.36778831 & -0.07142737 \end{bmatrix}$$

Y' is the luma component and Cb and Cr are the blue-difference and red-difference chroma components.

On the other hand, a commonly used colour space that corresponds more naturally to the human perception is the HSV colour space, which will be employed in this work. H stands for hue component, which describes the shade of the colour; S stands for saturation component, which describes the purity of the hue; V stands for value component, which describes the brightness.

The R'G'B' to HSV conversion is defined by the equations below. In these equations, MAX and MIN represent the maximum and minimum values of each R'G'B' triplet respectively. S and V vary from 0 to 1, where 1 represents the greatest saturation and value. H varies from 0 to 1 on a circular scale i.e. the colours represented by $H=0$ and $H=1$ are the same.

There is no consensus in the literature which is the best colour space to use so I chose HSV, preferred by some authors like Zarit et al. [99].

$$H = \begin{cases} \left(\frac{G' - B'}{MAX - MIN} \right) / 6 \\ \left(2 + \frac{B' - R'}{MAX - MIN} \right) / 6 \\ \left(4 + \frac{R' - G'}{MAX - MIN} \right) / 6 \end{cases} \quad (4.6)$$

$$S = \frac{MAX - MIN}{MAX} \quad (4.7)$$

$$V = MAX \quad (4.8)$$

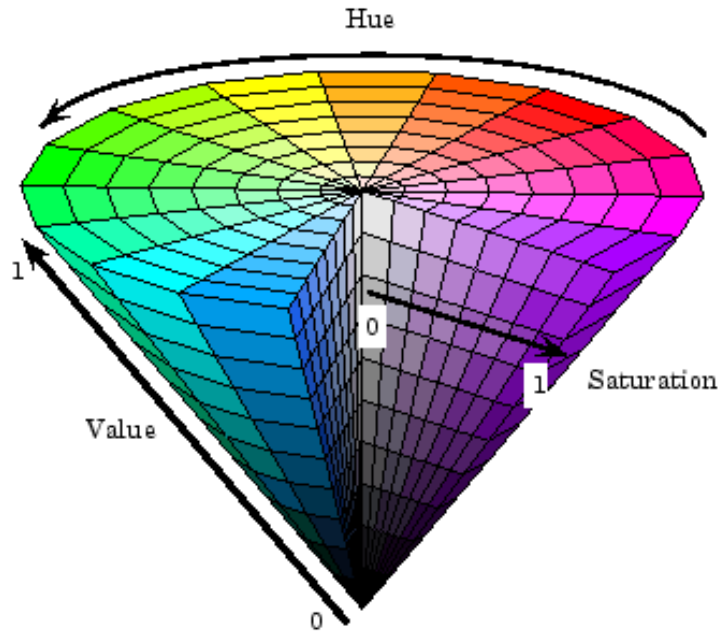


Figure 4. 5: A 3D representation of the HSV colour space [100]

- ***Edge Detection using Sobel Edge Operator:***

The purpose of edge detection, in general, is to radically reduce the amount of data in an image, while preserving the structural properties to be used for further image processing.

There are many ways to perform edge detection; however, most are categorised into two groups, gradient and Laplacian. The gradient method detects the edges by looking for the maximum and minimum in the first derivative of the image. The Laplacian method searches for zero crossings in the second derivative of the image to find edges. Sobel, Canny, Roberts Cross and Prewitt operators come under gradient method while Marrs-Hildreth is a Laplacian method [101].

In this task, the Sobel edge detector was used for the reason that it has a fast processing time, detects edges at finest scales and has smoothing along the edge direction, which improves noisy edges.

The Sobel edge detector calculates the gradient of the image intensity at each point, which results in providing the magnitude of the largest possible

increase from light to dark and the amount of change in that magnitude in the horizontal and vertical directions. As a result, a presentation of how abruptly or smoothly the image changes at that point is given; therefore, there is a possibility of that part of the image to represent an edge.

The Sobel edge detector uses two 3×3 kernels to calculate the derivatives, one for the horizontal changes and the other for the vertical. If G_x and G_y contain the horizontal and vertical derivative respectively, the computation is carried out as follows:

$$G_x = \begin{bmatrix} -1 & 0 & +1 \\ -2 & 0 & +2 \\ -1 & 0 & +1 \end{bmatrix} \text{ and } G_y = \begin{bmatrix} -1 & -2 & -1 \\ 0 & 0 & 0 \\ +1 & +2 & +1 \end{bmatrix}$$

Therefore, the gradient magnitude G can be calculated using:

$$|G| = \sqrt{g_x^2 + g_y^2} = |g_x| + |g_y| \quad (4.9)$$

Where g_x and g_y are the results of convolving the image with G_x and G_y respectively.

- **Skin Threshold:**

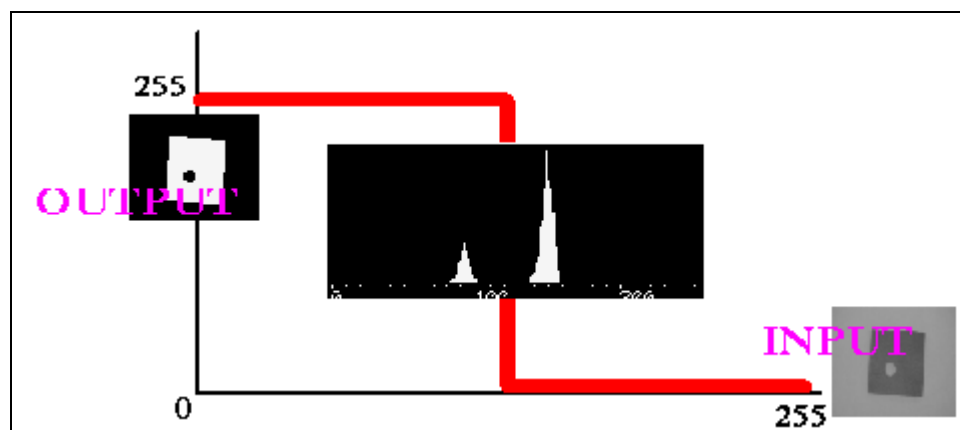


Figure 4. 6: Threshold operation

For various images, it is practical to be able to separate out the regions of the image corresponding to objects of interest from the regions of the image that correspond to background. Thresholding is commonly used to perform this

segmentation on the basis of different intensities or colours in the foreground and background regions in the image.

To detect the skin region in the images, we used the well-known thresholding technique that is called Otsu's method [102], which recognises that the image to be thresholded contains two classes of pixels, i.e. foreground and background. The algorithm then calculates the best possible threshold separating those two classes so that their intra-class variance of the skin and no-skin pixels is minimal.

The thorough search for the threshold that minimises the intra-class variance, which is defined as a weighted sum of variances of the two classes, can be found by the following [102]:

$$\sigma_w^2(t) = w_1(t)\sigma_1^2(t) + w_2(t)\sigma_2^2(t) \quad (4.10)$$

Where, w_i are the weights that are the probabilities of the two classes separated by a threshold t and variances of these classes.

- ***Connectivity Analysis:***

Up to this stage, binary images with 1's representing skin pixels and 0's representing non-skin pixels are obtained but it is not known whether a pixel belongs to a face or not. Also, when the thresholding is performed, it breaks up dark regions into many smaller regions so a clean up operation is needed.

In order to clean up the images (adjusting the skin area), we need to categorise the skin pixels into different groups so that meaningful representations of these pixels are acquired; for example: face, hand, etc. To perform this operation, pixels that are connected to each other geometrically are grouped. This is done based on a 8-connected neighbourhood, i.e. if a skin pixel has another skin pixel in any of its 8 neighbouring places, then both

pixels belong to the same region [101]. This *Morphological operation* is widely used in face detection, such as the works in [103, 104].

Finally, to classify whether any skin pixel is a face pixel or not, four elements are considered: the percentage of skin in the rectangular area defined by the 8-connected neighbourhood, the centroid of the rectangular area and the region's height and width.

The centroid is found by the average of the coordinates of all the pixels in the region. The height is found by first, subtracting the y-coordinates of the centroid from the y-coordinates of all pixels in the region. Then finding the average of all the positive and negative y-coordinates separately. Finally, the absolute values of both averages are added up and multiplied by 2. This gives the average height of the region. The width is found similarly by using the x-coordinates.

Because the height to width ratio of human faces falls within a small range on the real axis, using this parameter along with percentage of skin in a region, the algorithm should be able to exclude most of the non-face skin regions [101, 105]. So if the height to width ratio falls within the range of a specific face aspect ratio then that region is considered as a face region.

In this work, the face aspect ratio (f) is set empirically to be between 1 and 1.75, which can be found by the following equation:

$$f = \frac{f(h)}{f(w)} \quad (4.11)$$

Where $f(h)$ and $f(w)$ are the face height and width respectively.

The diagram below summarises the face detection process:

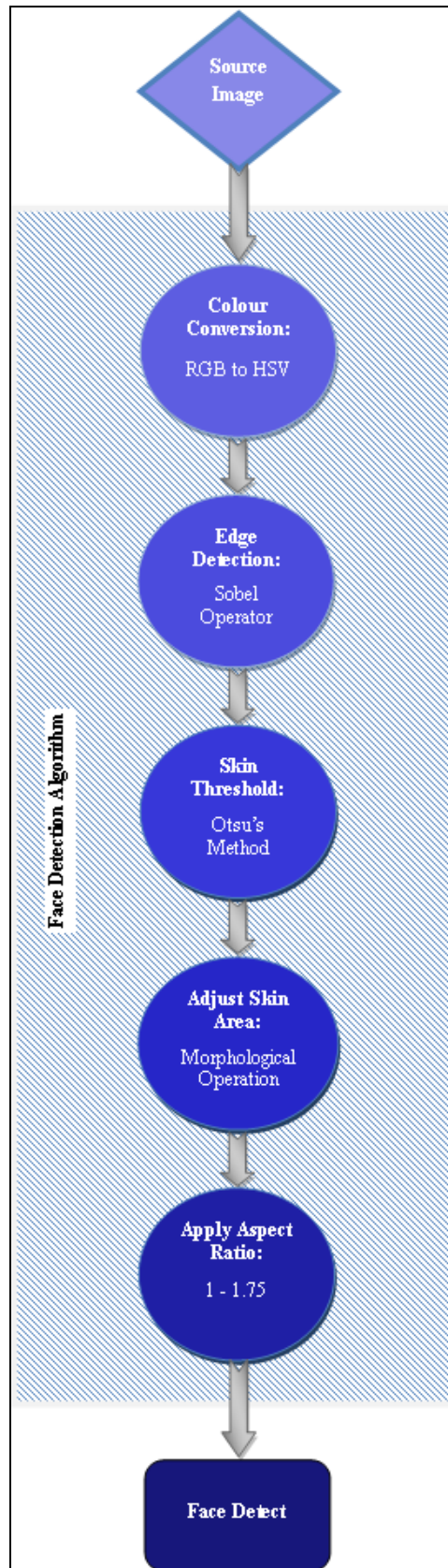


Figure 4. 7: Face detection algorithm

Sample results that are obtained by the above process are presented in the figure below:

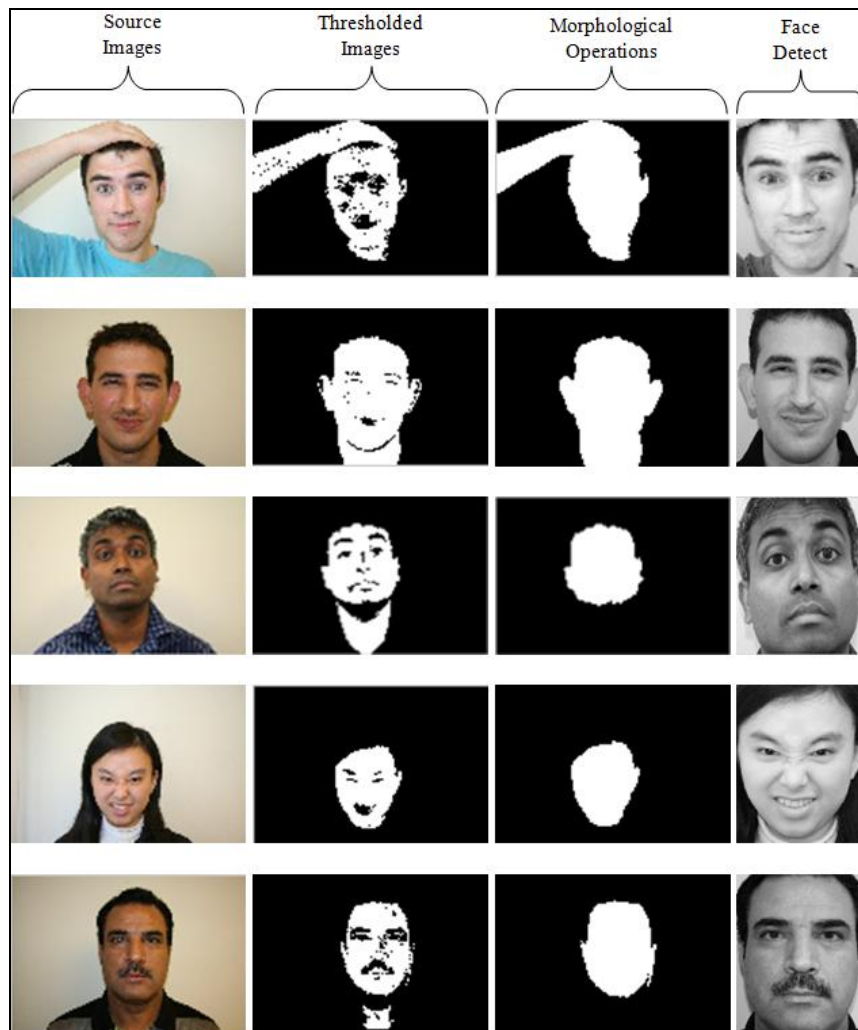


Figure 4. 8: Face detection process

4.4.2 Region of Interest (ROI) Detection

Having the face detected at this point, it is useful to highlight the ROI of the face. This will prevent the pronounced wrinkles such as the nasolabial furrow from overlapping when processing multiple images at the same time. The other advantage of having the ROI stage is to enable the user to choose whether a full wrinkle map is needed or just a map of a certain region on the face, for instance, forehead or crow's feet, etc. This may be beneficial, especially for medical research or plastic surgeries when observing a specific set of wrinkles on the face.

Some screenshots of the ROI stage are presented in the figure below.

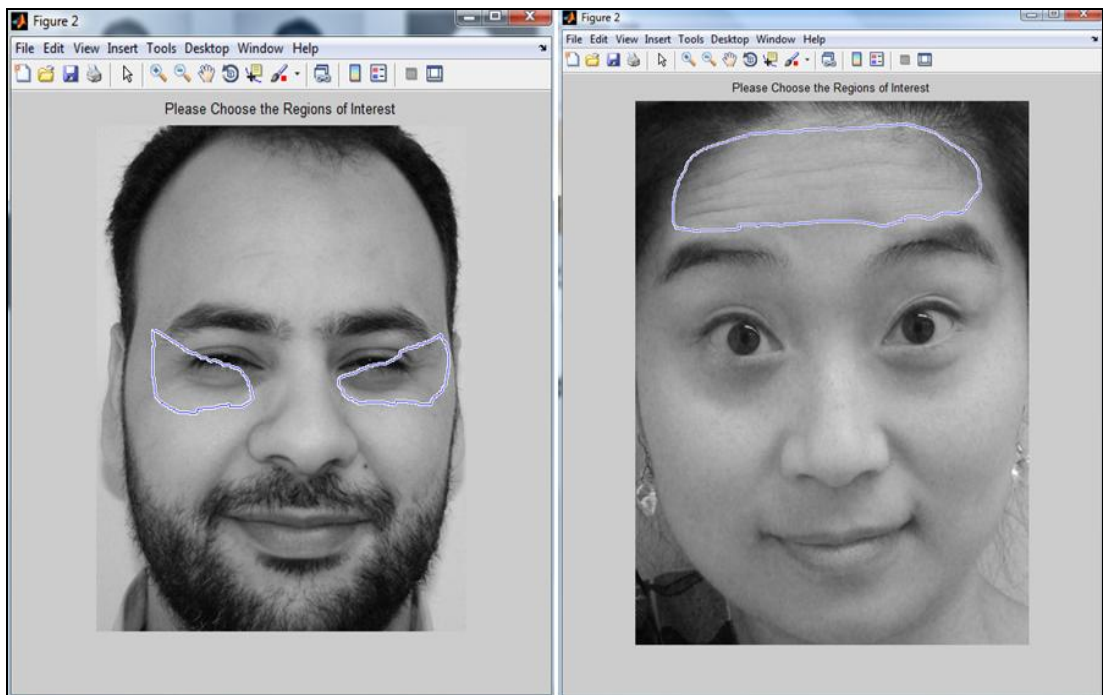


Figure 4. 9: ROI stage

4.4.3 Face Crop and Size Filter

- **Face Crop:**

Upon selecting the region of interest, the faces will undergo further processes starting by cropping the faces so that any selected area outside the face region will not be taken into consideration. Similar procedures that were used for the face detection are applied for the face crop.

- **Size Filter:**

After excluding any possible selected area outside the face boundary, unwanted regions within the face boundary will also need to be excluded, for example eyes, eye brows and any area that has no potential for appearance of wrinkles.

Another reason to perform the size filter is because sometimes due to threshold there will be objects (collection of pixels) in the image, which will be identified as skin, this usually happens with bad lighting.

These objects are always smaller in area (summation of number of pixels) than face skin, so with a size filter these objects can be eliminated.

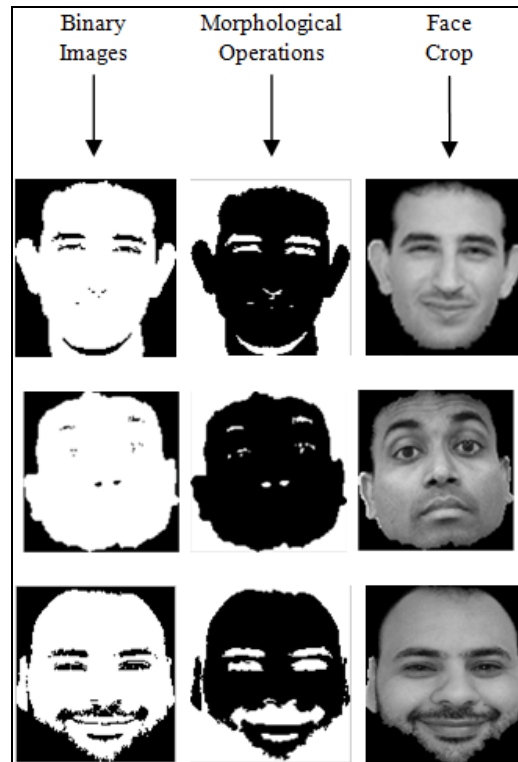


Figure 4. 10: Face crop

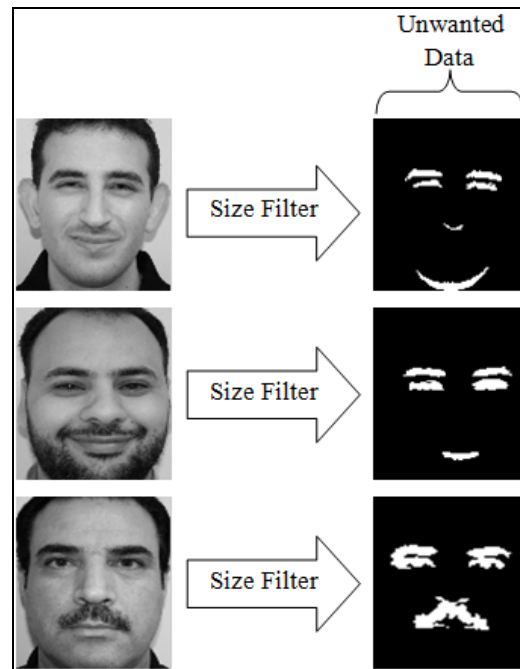


Figure 4. 11: Size filter

4.4.4 Wrinkles Detection

This task will be tackled using a gradient-base edge detector. A general problem with edge detection, especially in detecting thin lines such as wrinkles, is its sensitivity to noise. The reason being that calculating the derivative in the spatial domain corresponds to accentuating high frequencies and hence magnifying noise.

This problem was addressed by John Canny [106]; his method starts by convolving the image with *Gaussian* smoothing operator before calculating the derivative.

Canny edge detector is adopted for the implementation in this section to detect wrinkles by calculating the gradient in pixel values, in other words, it searches for any sudden change in the gradient, if this is present, it means that an edge of a wrinkle is detected.

In more details, the canny edge detection algorithm is processed in five stages [107]:

- Smoothing: Blurring of the image to reduce noise.

- Finding gradients: The edges should be marked where the gradients of the image have large magnitudes.
- Non-maximum suppression: Only local maxima should be marked as edges.
- Thresholding: Potential edges are determined by thresholding.
- Edge tracking: Final edges are determined by suppressing all edges that are not connected to a very strong edge.

Below, further explanation for each stage is discussed. (4.12)

- ***Smoothing:***

It is expected that all images taken from a camera will contain a certain amount of noise. This noise can be mistaken for edges, therefore, must be reduced. Gaussian filter is used, which produces a slightly blurred version of the original image that is not affected by a single noisy pixel to any significant degree. It is simply multiplying and summing all pixels within $N \times N$ window by Gaussian distribution function, which eliminates any abnormality in the pixel values with the $N \times N$ window.

A one-dimensional Gaussian distribution graph is presented in Figure 4.12, whose function is defined by:

$$g(x) = e^{-\frac{x^2}{2\sigma^2}}$$

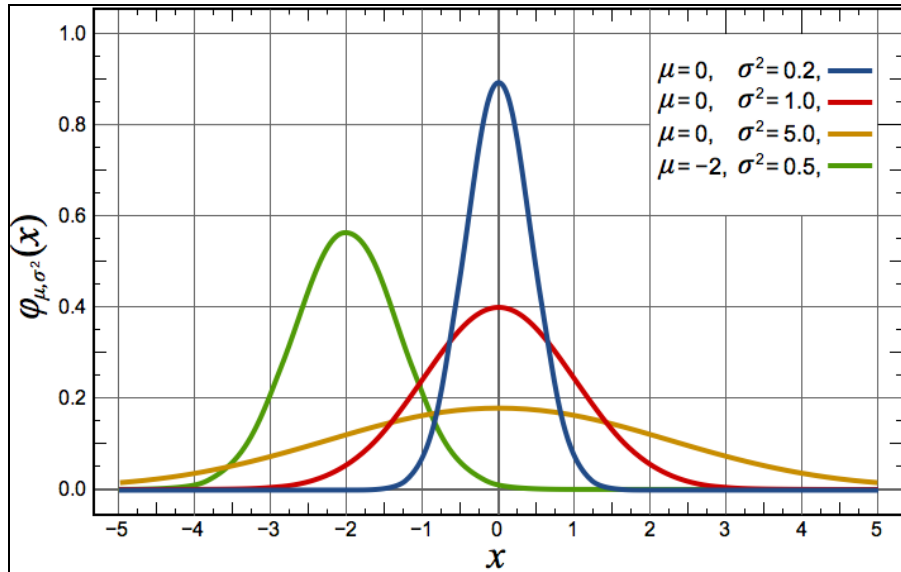
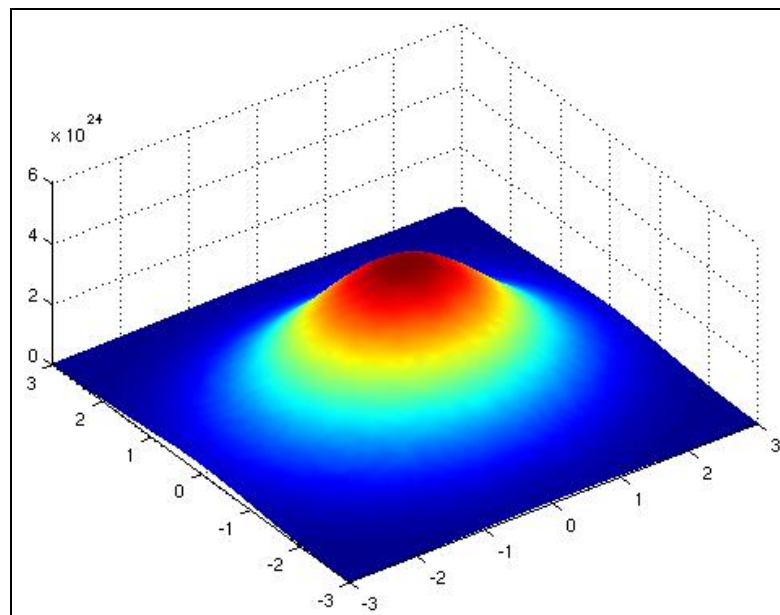


Figure 4. 12: One-dimensional Gaussian curves

In MATLAB, the command `{h=fspecial('gaussian')}` is used, which produces a discrete version of two-dimensional Gaussian function (Figure 4.13) using:

$$g(x,y) = e^{-\frac{x^2+y^2}{2\sigma^2}}$$

$$h(x,y) = \frac{g(x,y)}{\sum_x \sum_y g(x,y)}$$



(4.13)

(4.14)

Figure 4. 13: Two-dimensional Gaussian curve

Gaussian filters (with small σ) are usually used in detecting fine objects, for example, Geusebroek et al. [108] used Gaussian filter to detect worms in a soil sample and also to detect a line in a pattern.

- ***Finding Gradients:***

The Canny algorithm uses four filters to detect horizontal, vertical and diagonal edges in the blurred image; this is done using Sobel operator as described before. The edge gradient can be determined using Eq. (4.9), however, the edges are typically broad and thus do not indicate exactly where the edges are, this could create a problem when detecting the edges of the wrinkles. To make the determination possible, the direction of the edges must be calculated and stored as shown in the following equation:

$$\theta = \arctan\left(\frac{G_y}{G_x}\right)$$

The edge direction angle is rounded to one of four angles representing horizontal, vertical and the two diagonals (0, 45, 90 and 135 degrees for example).

- ***Non-Maximum Suppression:***

The purpose of this step is to convert the blurred edges in the image of the gradient magnitudes to sharp edges. This is done by maintaining all local maxima in the gradient image and deleting everything else. The algorithm for each pixel in the gradient image is described below:

(4.15)

- When the rounded angle is 0° , then the point will be considered to be on the edge if its intensity is greater than the intensities in the westward and eastward directions.

- When the rounded angle is 45° , the point will be considered to be on the edge if its intensity is greater than the intensities in the northeast and southwest directions.
- When the rounded angle is 90° , the point will be considered to be on the edge if its intensity is greater than the intensities in the northward and southward directions.
- When the rounded angle is 135° , the point will be considered to be on the edge if its intensity is greater than the intensities in the northwest and southeast directions.

A simple example of non-maximum suppression is shown in the figure below, where the edge strengths are indicated as colours and numbers, while the gradient directions are indicated as arrows. The resulting edge pixels are marked with white borders.

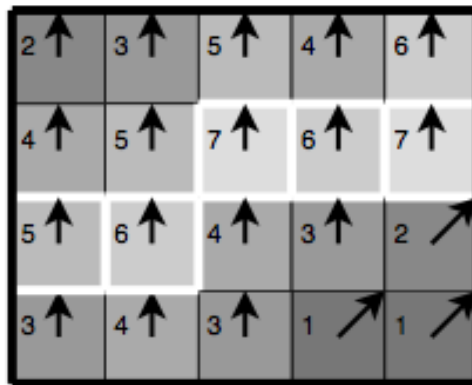


Figure 4. 14: Non-maximum suppression [107]

From this stage, a set of edge points that is in the form of a binary image is obtained.

- **Thresholding:**

The edge-pixels remaining after the non-maximum suppression step are still marked with their strength pixel-by-pixel. Many of these will probably be true edges in the image but some may be caused by noise or colour variations.

The simplest way to distinguish between these would be the use of a threshold.

The canny edge detection algorithm uses double thresholding, that is, edge pixels stronger than the high threshold are marked as strong; edge pixels weaker than the low threshold are suppressed and edge pixels between the two thresholds are marked as weak. When a different threshold is used for different regions in the image is also called adaptive thresholding [109].

In our work, the values for the low threshold, high threshold and the standard deviation (σ) are set empirically to be 0.01, 0.1 and 3 respectively.

- ***Edge tracking:***

Strong edges are immediately included in the final edge image. Weak edges are only included if they are connected to strong edges. The reason is that noise and other small variations are unlikely to result in strong edges, therefore, strong edges will most likely be true edges in the original image. The weak edges can either be true edges or noise/colour variations, which will probably be distributed independently of edges on the entire image and so only a small amount will be located adjacent to strong edges. Weak edges that are true edges are more likely to be connected directly to strong edges.

The image below presents sample binary gradient masks (from random experimental subjects), where (a), (b) and (c) show the forehead wrinkles, crow's feet and nasolabial furrow respectively:

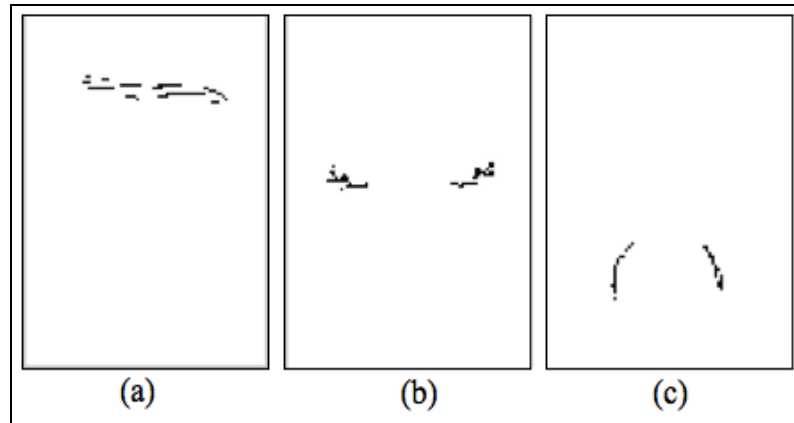


Figure 4. 15: Binary gradient masks

Up to this point, it is possible to generate full facial wrinkle maps in binary forms. These maps indicate the location of the wrinkles on human faces, while the intensities of those wrinkles are still not known. It is important to acquire such information for many reasons, in which one of them is when designing the 3D wrinkle formation system, we need to be able to predict which wrinkles appear first and which form later. For this reason, wrinkle intensity maps are generated in the next section.

4.4.5 Generating Two-Dimensional RGB Wrinkle Maps

The method for generating the colour maps is to approximate all wrinkles by collection of ellipses and calculate the minor-axis distance for each ellipse then arranges the minor-axis according to value.

For example, if a wrinkle is represented by the white pixels, then the ellipse will be like:



Figure 4. 16: An ellipse

Note that in the above example the wrinkle is represented by 4 pixels only but

realistically, wrinkles could have more than 100 pixels and are divided into 4 pixel length sections for ellipse fitting.

An ellipse is a smooth closed curve, which is symmetric about its major and minor axes. The distance between antipodal points on the ellipse, or pairs of points whose midpoint is at the center of the ellipse, is maximum along the major axis (2a), and a minimum along the perpendicular minor axis (2b).

An ellipse orientated along the axes is given by the following equation:

$$\left(\frac{x}{a}\right)^2 + \left(\frac{y}{b}\right)^2 = 1$$

Where a and b are the semi-major and semi-minor axes respectively.

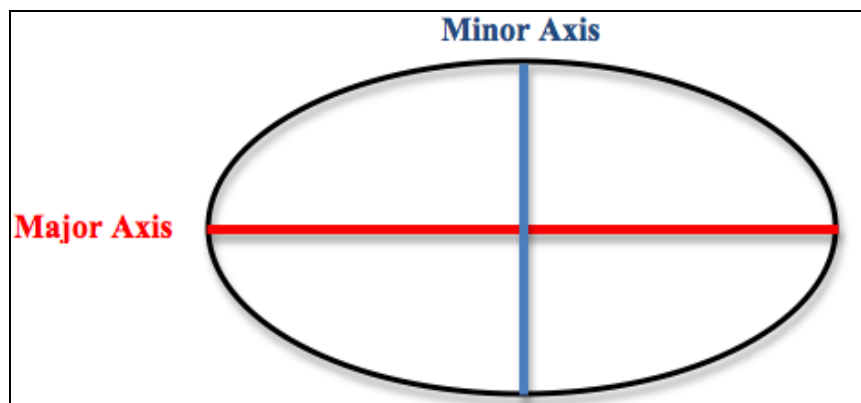


Figure 4. 17: An ellipse with its major and minor axes

More information on the ellipses can be found in [110].

Upon obtaining the values of the minor axes of the wrinkles, we then set a colour map that ranges from blue to red, where blue is the highest value (intensity) and red (4.16) is the minimum value.

An example illustrated in Figure 4.18 shows a coloured wrinkle map.

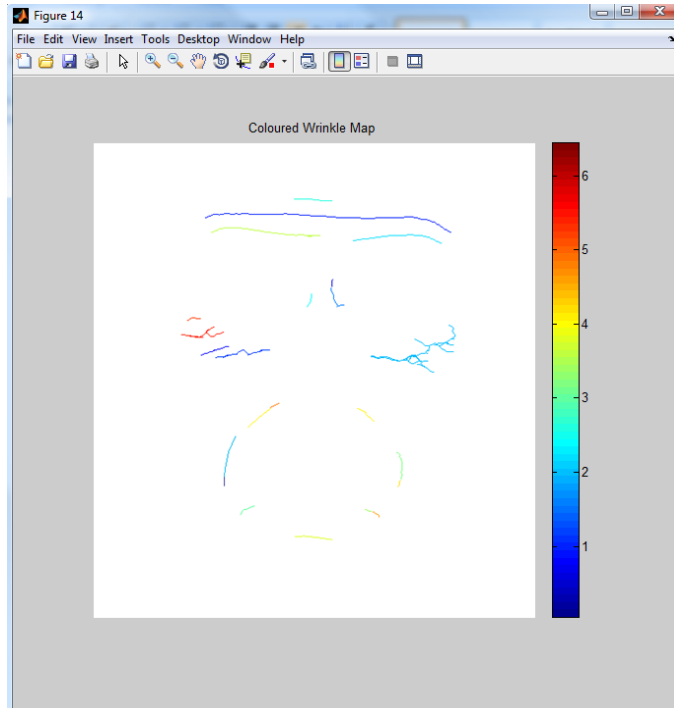


Figure 4. 18: A coloured wrinkle map with a side bar

4.5 Results

In this section, the results are presented for some selected individuals. For each individual, a binary and a colour map are presented as well as an outline of the wrinkle map on the face. All the generated results are automatically stored in image files.

The outlined wrinkles, in some cases, might not be completely aligned in position due to head orientations. This can be improved in the future by fixing the position of the head when capturing the six images of the face. Regarding the coloured maps, some wrinkles might not be clearly visible in the diagrams as those wrinkles are in the middle colour range; the colours in this range are generally faint, which makes the observation difficult on white backgrounds.

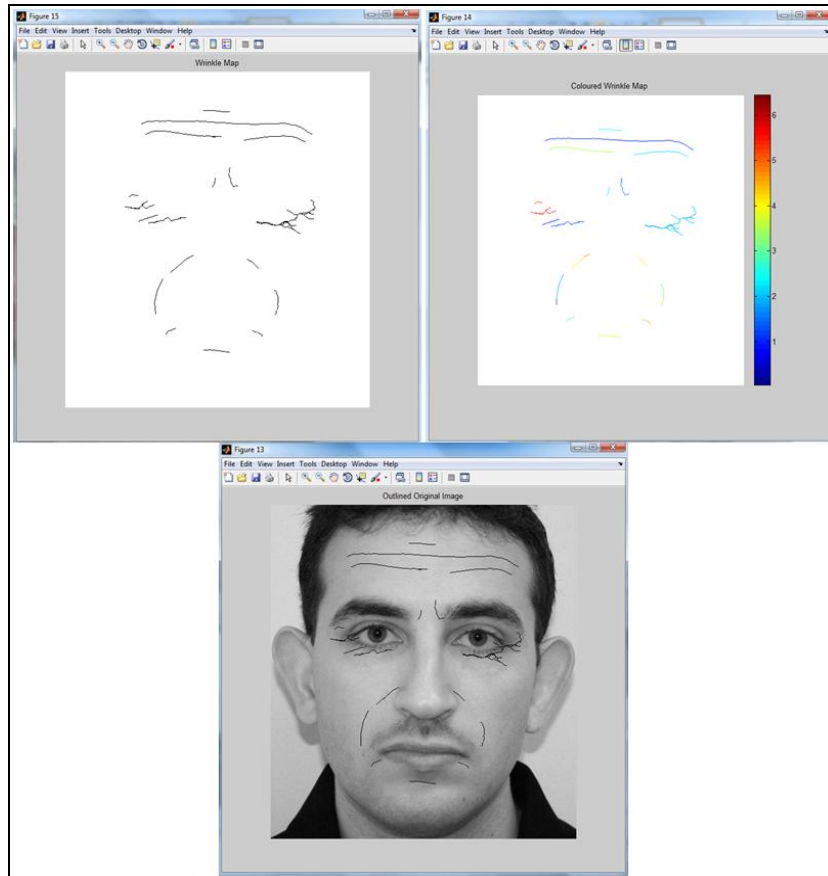


Figure 4. 19: Results for person A

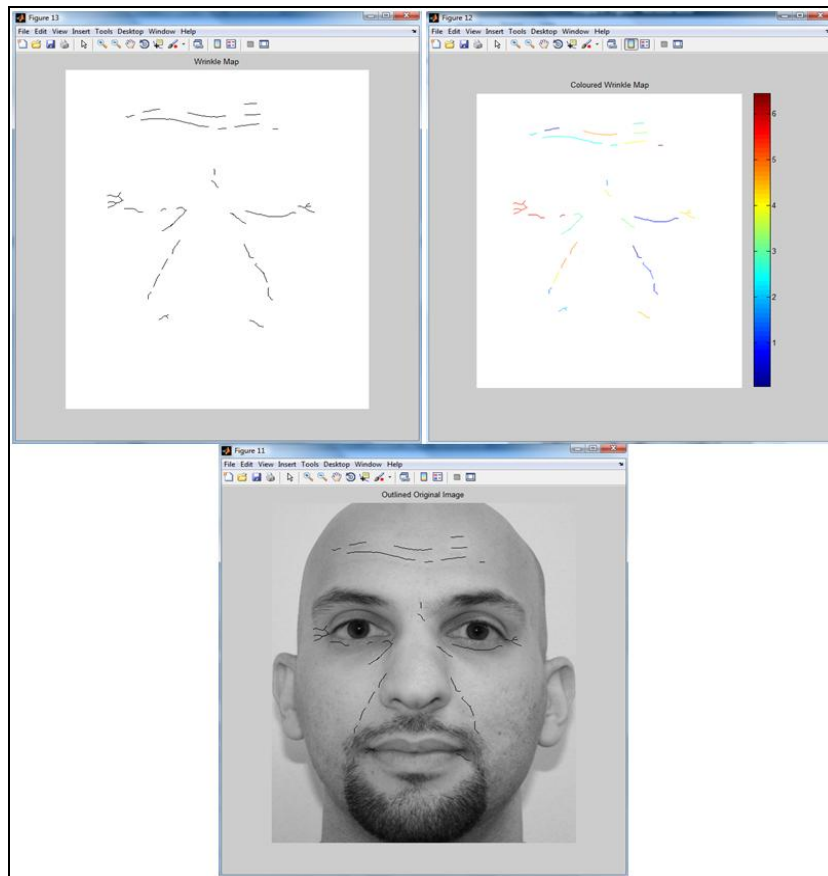


Figure 4. 20: Results for person B

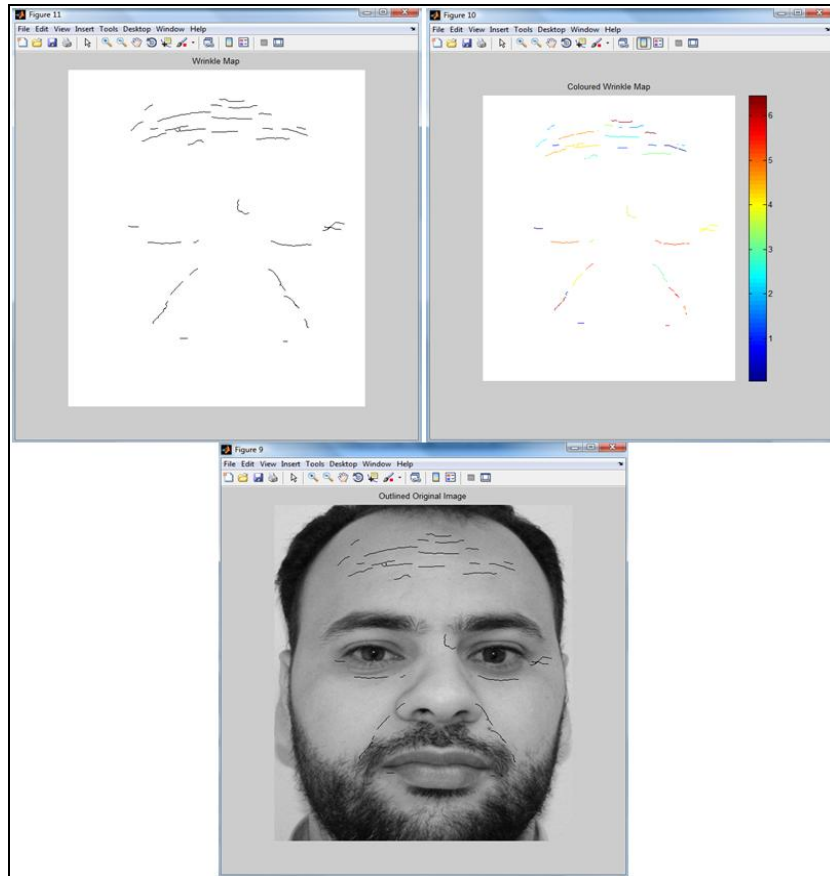


Figure 4. 21: Results for person C

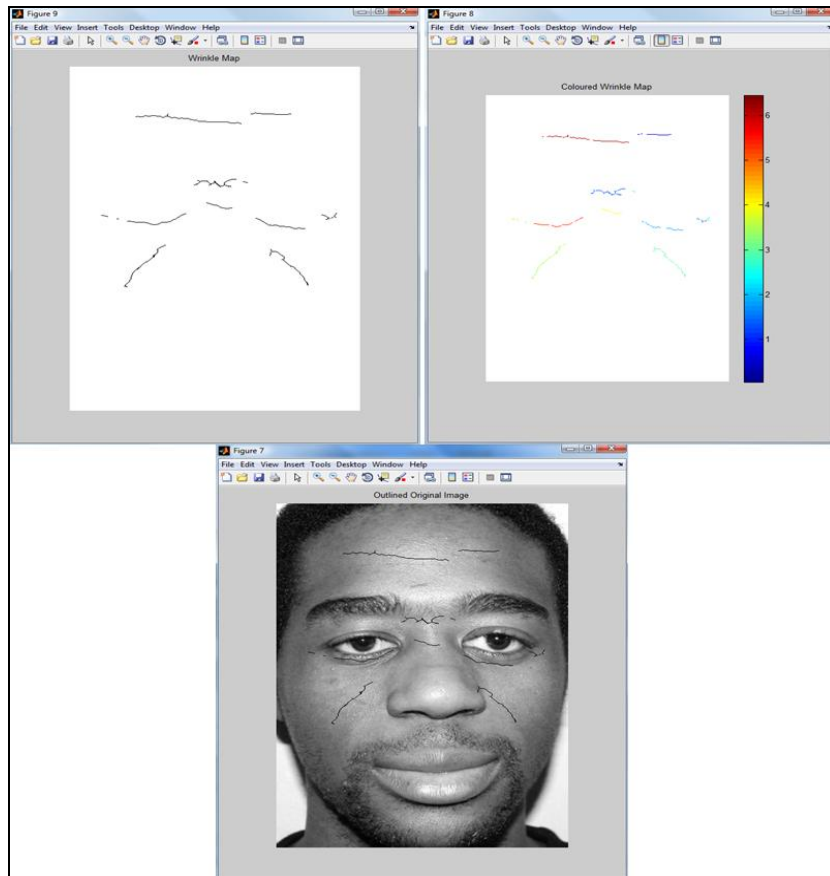


Figure 4. 22: Results for person D

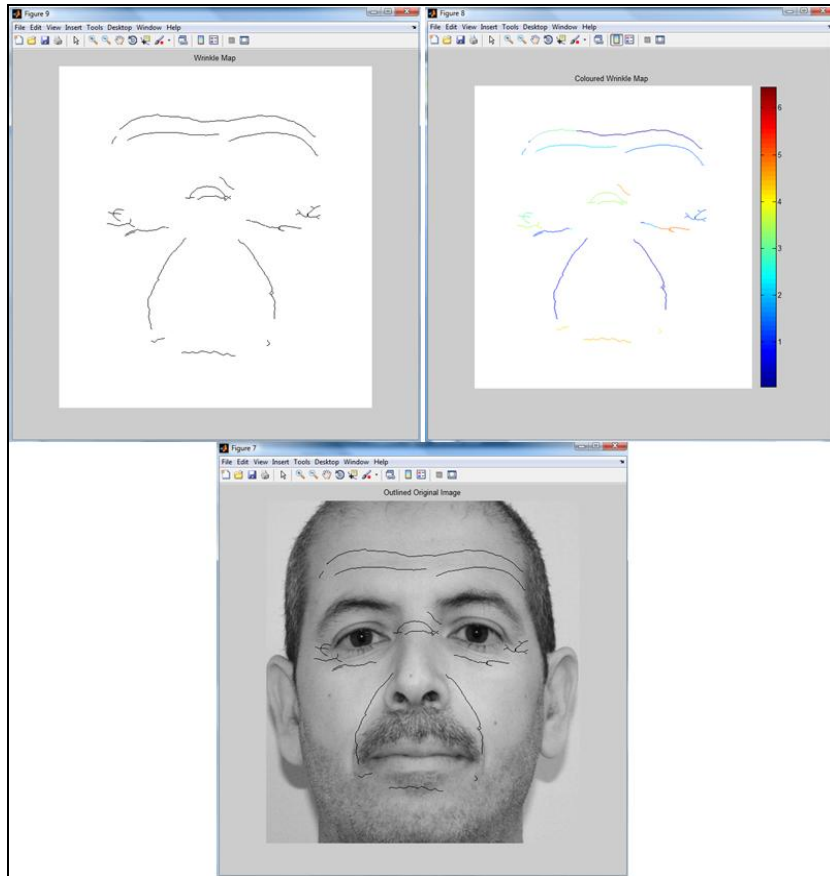


Figure 4. 23: Results for person E

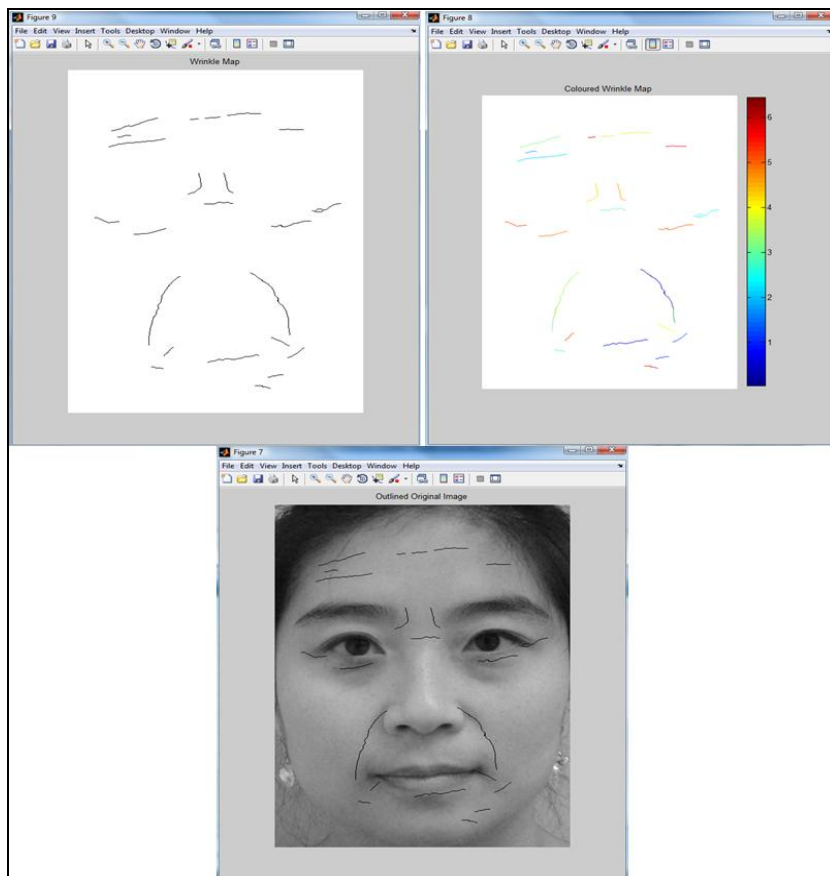


Figure 4. 24: Results for person F

4.6 Testing

The testing methodology is done by comparing the generated binary wrinkle map for every individual to the five original images with the expressions. This is performed in order to find out the number of wrinkles that have not been detected by the program, hence, discovering the level of error by calculating its percentage.

Any original wrinkle that has no indication on our generated wrinkle map will be classed as undetected, i.e. an error.

When only parts of a particular wrinkle have been detected, we class this wrinkle as a detected wrinkle, if the number of pixels of the detected wrinkle is half of the number of pixels of the original wrinkle.

The image below illustrates the comparison between the detected wrinkles (left hand side) and the original wrinkles (right hand side):

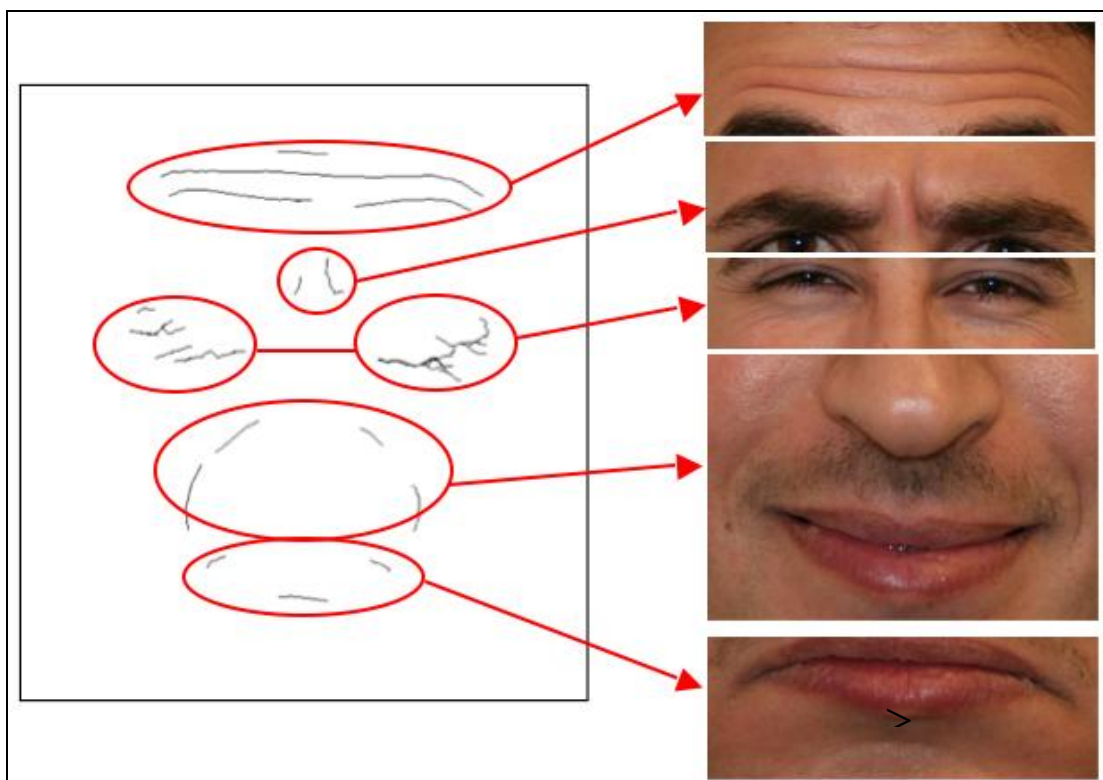


Figure 4. 25: Comparison between the original and the detected wrinkles

The percentage error is calculated as per Eq. (3.8) but this time, the ‘estimated value’ of that equation is substituted by the number of detected wrinkles.

So for Person A in the figure above, the percentage error (to the nearest decimal point) is calculated by the following:

$$|\%E| = \frac{19 - 23}{23} \times 100 = 17.4\%$$

Table 4.1 presents the error rates for all the experimental subjects; all values have been rounded up to the nearest decimal point.

Table 4. 1: Error rates for all experimental subjects

ID	%E
A	17.4
B	13.6
C	14.7
D	9.4
E	16.6
F	14.9
G	14.2
H	10.1
I	13.3
J	6.5
K	8.2
L	14.5
M	16.1
N	14.0
O	15.4

P	12.8
Q	15.8
R	16.7
S	14.8

Also by inspecting the generated results for 99 people, it is clear that the wrinkle map is unique for every person.

4.7 Discussion and Conclusion

In this chapter, image processing techniques were utilised to develop a novel computer system, which is the first of its type, that generates unique wrinkle maps for human faces. The two wrinkle maps that are generated will be used as prime factors to predict, for a given age of any individual, the change in the wrinkle appearance in three-dimensional manner. This will be explained further in the next chapter.

In addition to the above advantage of the usage of these wrinkle maps, the binary ones have the potential to be added as another element to the biometric applications for the reasons that they are common features and unique for every individual.

Signatures, handwriting, face images and fingerprints are biometrics, of long standing, used in the verification or authentication of documents. More recently, voices, gaits, handprints, 3D face information as well as retinas and iris scans, have

all been considered as biometric identifiers. Each of these has different merits, and applicability [111]. Our proposed application (Wrinkle Map WM) can fit and stands among the other applications as shown in Table 4.2.

Table 4. 2: WM strengths against other biometric applications

	Accuracy	Cost	Privacy	Integrity	Ease of use	Development	Faking identity
Iris	X		X				X
Retina	X		X				X
Hand					X	X	X
Signature					X	X	
Voice		X		X	X	X	
Gait			X				
2D face		X	X	X	X	X	
3D face	X		X	X	X	X	
WM	X	X	X	X	X	X	

Generally, the following issues are looked at when discussing the biometric applications: accuracy, cost, privacy, ease of use, ease of development, whether it allows integration with other systems and faking the identity.

- **Accuracy:**

From the test results, it was seen that the error rates were low, which indicate that most wrinkles were detected by the system. Statistically, the wrinkles around the eyes were the most difficult to detect and that is because these wrinkles are generally slender. Lighting effects in some images were also the reason for the discontinuity of some of those wrinkles. However, the error rates can be reduced by the use of high-resolution cameras (our experiment was conducted using 8 megapixel camera) and with the reduction of lighting effects.

- **Cost:**

The system requires basic equipments that include a camera, computer and the

software, which gives it the advantage to run at a low cost.

- **Privacy:**

Just like fingerprints, facial wrinkles are unique for every individual; this can be used as identification. The face is a vital part of the human body; this gives our system the advantage over the fingerprint technology.

- **Opportunity for development:**

The system can also be developed further to be able to generate three-dimensional wrinkle maps.

- **Integration:**

The system can certainly be integrated with other systems, for example, facial ageing simulation systems. Furthermore, our system can compete in the area of face detection, which itself can be integrated with other systems. The distinctive methods that were adopted in the development of the current system can also detect multiple faces in an image as shown in Figure 4.26. Our system overcomes the available face detection systems, such as [112, 113], due to its ability to detect wrinkles as an additional important feature.

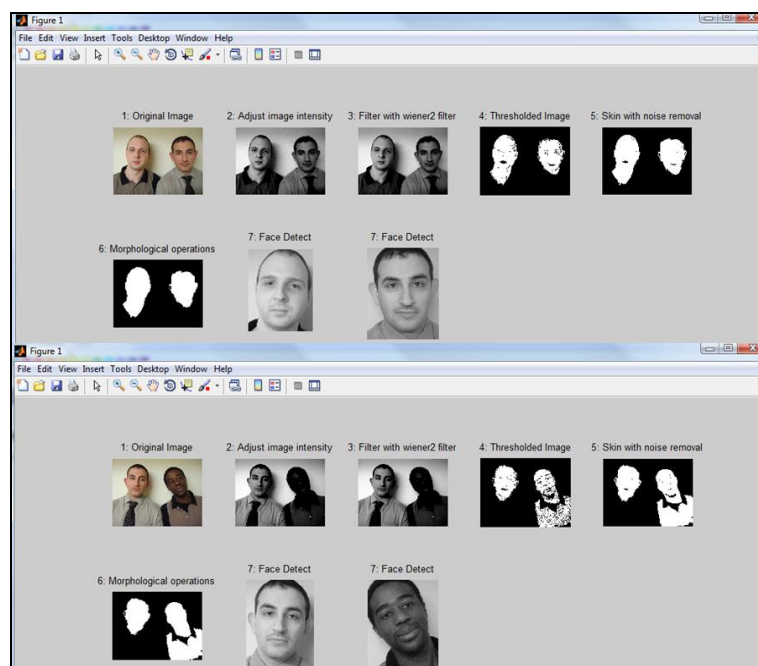


Figure 4. 26: Detecting multiple faces in images

- ***Identity Fraud:***

Faking the identity can be a drawback, especially with the use of plastic surgery.

In the next chapter, the generated wrinkle maps will be used further in a 3D wrinkle simulation system.

CHAPTER FIVE

5 3D Modelling, Simulation and Prediction of Facial Wrinkles

5.1 Introduction

In the previous chapter, a computer system was developed to generate two-dimensional wrinkle maps. In this chapter, these wrinkle maps will be used in the design of a three-dimensional system for the purpose of facial wrinkles simulation and prediction.

The available facial ageing simulation and prediction technologies lack in simulation accuracy, especially when simulating the appearance of wrinkles. This might be due to the fact that wrinkles appear in different locations on human faces and the amount of change in their development also differs. Failing to simulate the wrinkles can have a direct impact on the ageing prediction accuracy as wrinkles play a vital role as a major ageing feature.

One of the most popular 2D facial ageing simulation systems is the April Age Progression Software ‘age-me’ [114], which was developed by Aprilage Development Inc. On the other hand, FaceGen [115] is a widely know 3D face generator modelling software that includes an embedded ageing system. Both softwares are available for commercial purposes and share the disadvantage of generating wrinkles based on assumptions and no real data is considered.

Our findings will challenge both commercial softwares in the innovation of the techniques in setting solid grounds to generate 3D wrinkles (from real data) that can be used later for various reasons that may include security, 3D facial ageing simulation systems, facial animation, etc.

This work will commence by generating a 3D face model for any given individual, which for now are the test subjects from Figure 4.2. Their 2D binary wrinkles will be mapped on the corresponding 3D face models using the generated outlined images. NURBS curves will then be projected on those wrinkles to form a three-dimensional wrinkle map. The coloured wrinkle map, as well as some parameters, will be combined together in an algorithm to predict the appearance of the individual wrinkles in every age group that are divided into decades, starting from the age of 20. The simulation and prediction methods will take place under what are called neutral conditions, i.e. external and internal ageing factors will not be taken into consideration at this stage.

The flow chart in Figure 5.1 illustrates the stages of the work.

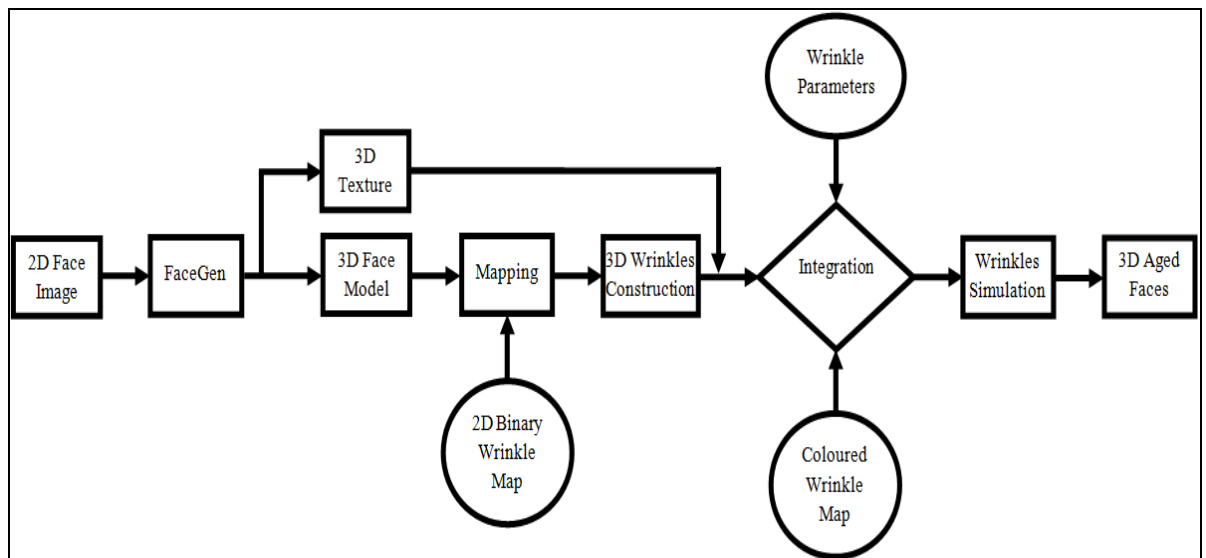


Figure 5. 1: Experimental procedures

The novelty of the adopted procedures in comparison to other available works, is the new elements that have been integrated and collaborated to boost accuracy and to generate a more realistic outcome.

The organisation of this work is as follows.

In section 5.2, the method will be shown, in which the 3D models are acquired. Section 5.3 explains the 3D face mesh and its further processing. Sections 5.4 and

5.5 talk about texture mapping and wrinkles construction respectively. The core work is represented by the wrinkle simulation and prediction, which is discussed in section 5.6. The results of the simulations and predictions are presented in section 5.7. The performance evaluation strategy will be discussed in section 5.8. Finally, section 5.9 will conclude the findings on the 3D modelling, simulation and prediction of facial wrinkles.

5.2 3D Face Creation

The construction of 3D face models using 2D face photographs, such as the work in [116], has become the focus of study on 3D face modelling, in which generated textures will affect directly the sense of reality of the generated 3D face models [117] and it is indeed one of the most difficult problems in the fields of computer graphics and computer vision.

On the other hand, 3D scanners are becoming widely employed for the task of 3D face generation and have been used by some researchers, such as Ansari et al. [118], in which an algorithm was developed for 3D face deformation and modelling using range data captured by a 3D scanner. The major limitation that can prevent the use of 3D scanners is their high cost.

However, in this work, the 3D face models are generated from the neutral face of any individual using FaceGen for its simplicity and relative low cost.

The 2D face image is marked (Figure 5.3) for feature point extraction then processed. The method is based on a 3D morphable face model that encodes shape and texture in terms of model parameters. In other words, the algorithm simulates the process of image formation in 3D face and it estimates 3D face and texture of faces from a single image to account for pose and illumination variations.

The stages of this process are shown in the figure below, where the 3D face model as well as the facemask (texture) are exported.

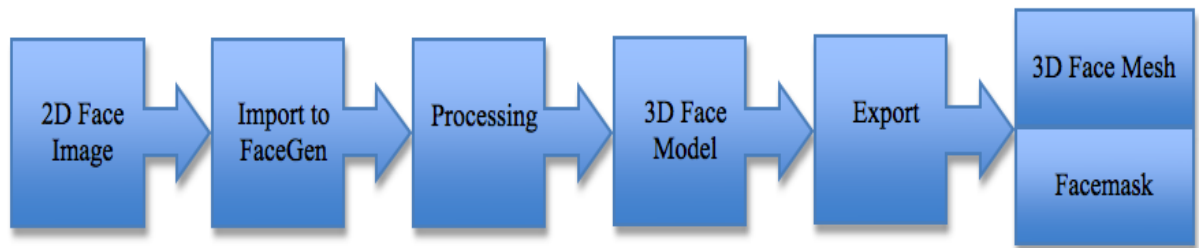


Figure 5. 2: The process of generating and exporting the 3D face model

The process of the image takes about 10 – 15 minutes depending on the speed of the system. The result of the 3D face model is displayed in Figure 5.4 while the exported materials are shown in Figure 5.5.

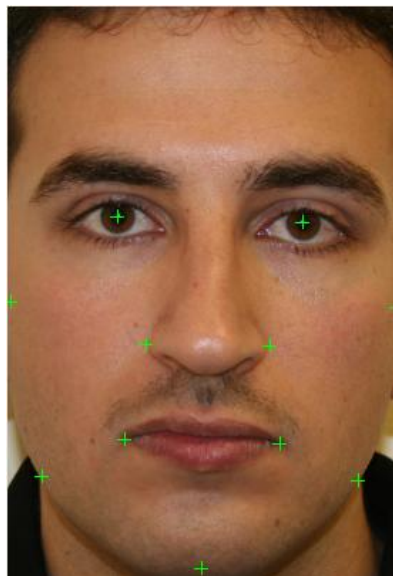


Figure 5. 3: Marked 2D face image



Figure 5. 4: The 3D face model

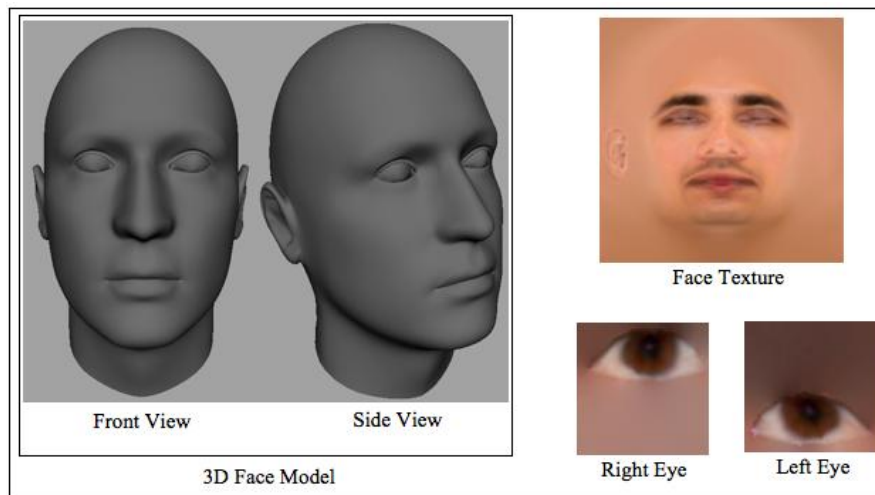


Figure 5. 5: Exported items

5.3 The 3D Face Mesh

The generated face models contain simple mesh (Figure 5.6); in the modelling process of wrinkles, we take into consideration the flow of the facial muscles, so that the edge loops are in the direction of the natural flow of the human muscles (as described in Figure 5.7).

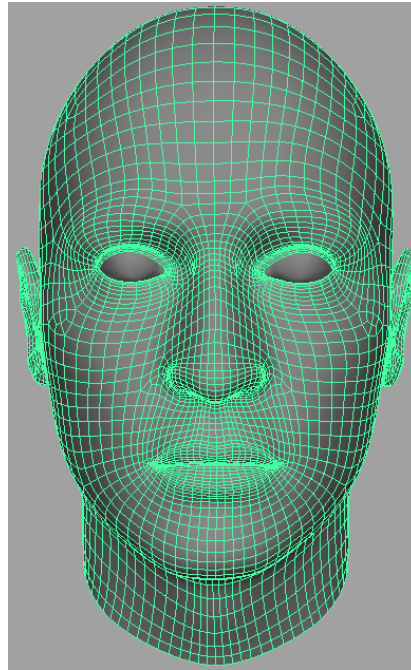


Figure 5. 6: 3D face mesh

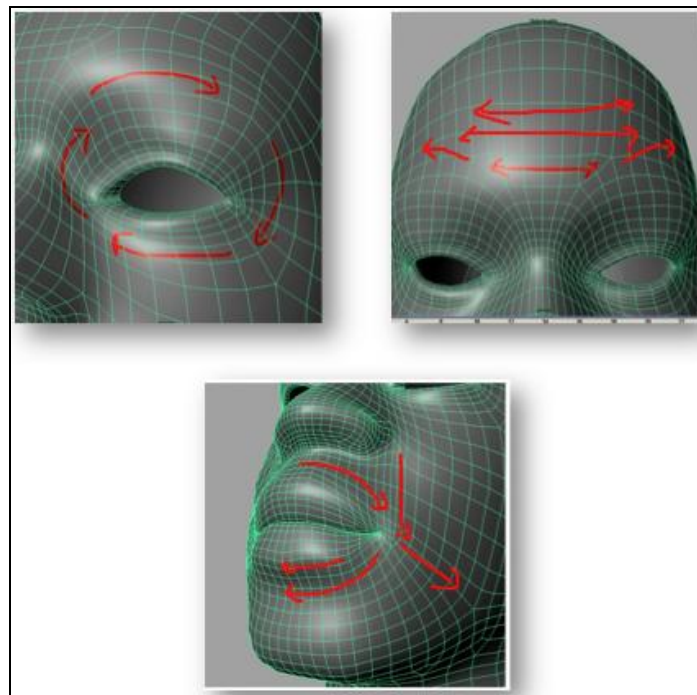


Figure 5. 7: Facial muscles flow

The 3D face has to be processed further for optimisation; this process involves increasing the mesh by adding edge loops in order to boost the smoothness of the wrinkles later in the simulation. The optimisation process is explained in the following example:

Imagine that we have a 5×5 face plane (Figure 5.8 (a)), the process searches for two edges and adds on a division, this process is repeated until a 10×10 plane is obtained (Figure 5.8 (e)). This progression will be applied on the whole face.

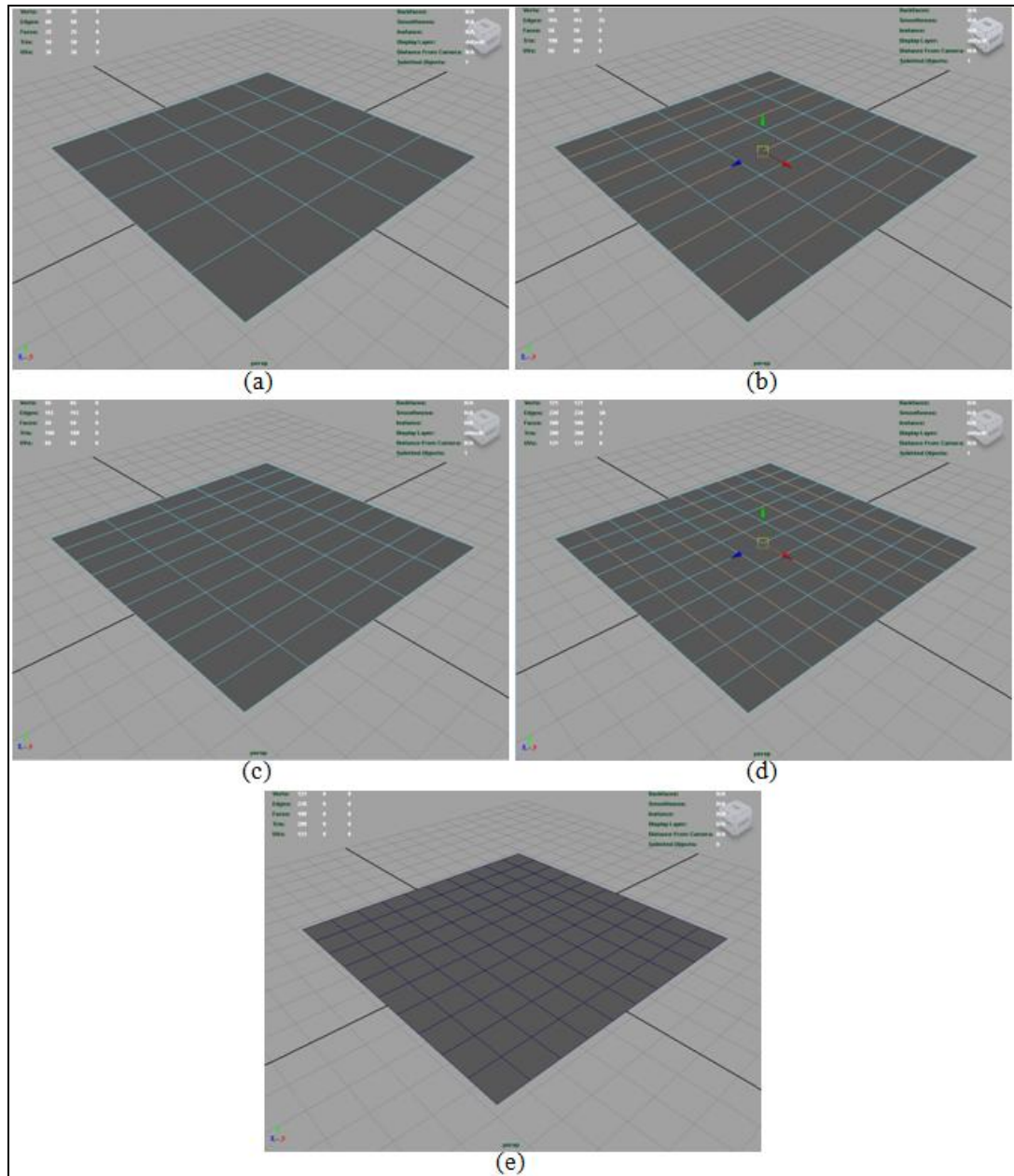


Figure 5. 8: Smoothing process

The resultant smoothed face (on the right) is displayed in the figure below in comparison with the original one (on the left).

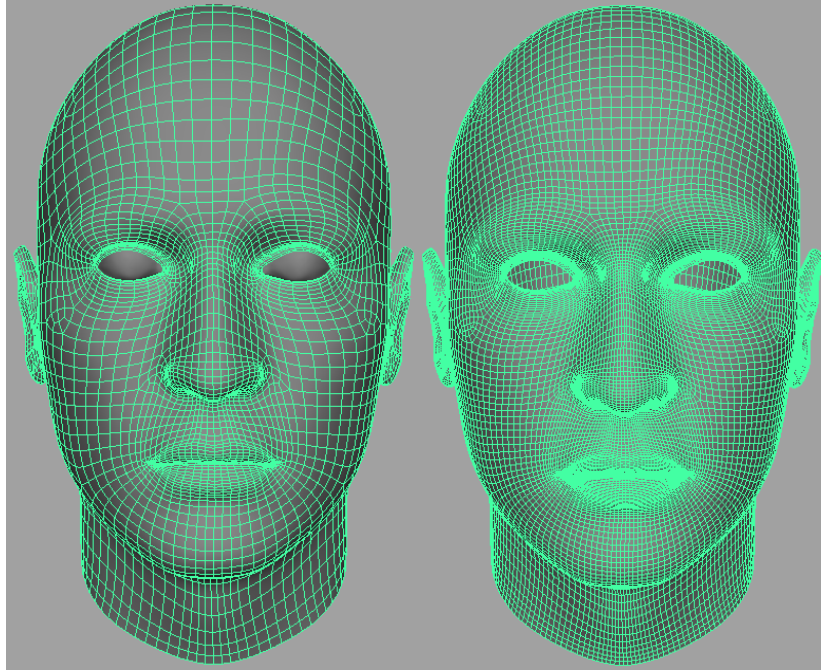


Figure 5. 9: The smoothed face in comparison with the original one

This method might cause the program to have a slow loading time due to the addition of more geometry to the model.

An alternative method to create wrinkles can be implemented by generating a so-called *normal map* [119, 120]. In 3D computer graphics, normal mapping is a technique used for faking the lighting of bumps and dents. It is used to add details without using more polygons, in other words, is a key technology to enhance the roughness and wrinkles of the surface with small amount of polygon data [121]. Normal maps were used in the work of Reis et al. [122] in the production of facial wrinkles, based on areas of influence.

The normal map consists of RGB information that tells the shader program, of any nature, how to react to the light.

We produced our own normal map (an example is shown in Figure 5.10); the depressions make the surface look deeper, which gives the illusion of wrinkles. In our work, accuracy and realism in terms of the wrinkle locations are top priorities; hence, using normal maps will be inadequate. For this reason, the higher resolution

3D face polygons will be used in this work despite the contingency of a slow loading time.



Figure 5. 10: Our generated normal map

5.4 Texture Mapping

Texture mapping is the method for adding detail or colour to a computer-generated graphics or 3D Models.

In this section, the texture that is generated in Figure 5.5 is considered using a UV space. The UV mapping is the process of texturing a 2D image on a 3D object. In contrast to X, Y and Z, which are the coordinates for the original 3D object in the modelling space, another set of coordinates is required to describe the surface of the mesh, so the letters U and V are used.

UV texturing allows polygons that signify a 3D object, to be coloured using an image, in which the image itself is called a UV texture map [123]. The UV mapping process involves assigning pixels in the image to surface mappings on the polygons,

usually done by repeatedly copying a triangle shaped piece of the image map and pasting it onto a triangle on the object [124].

The figure below shows an example of a 3D sphere that is opened up to be a UV map:

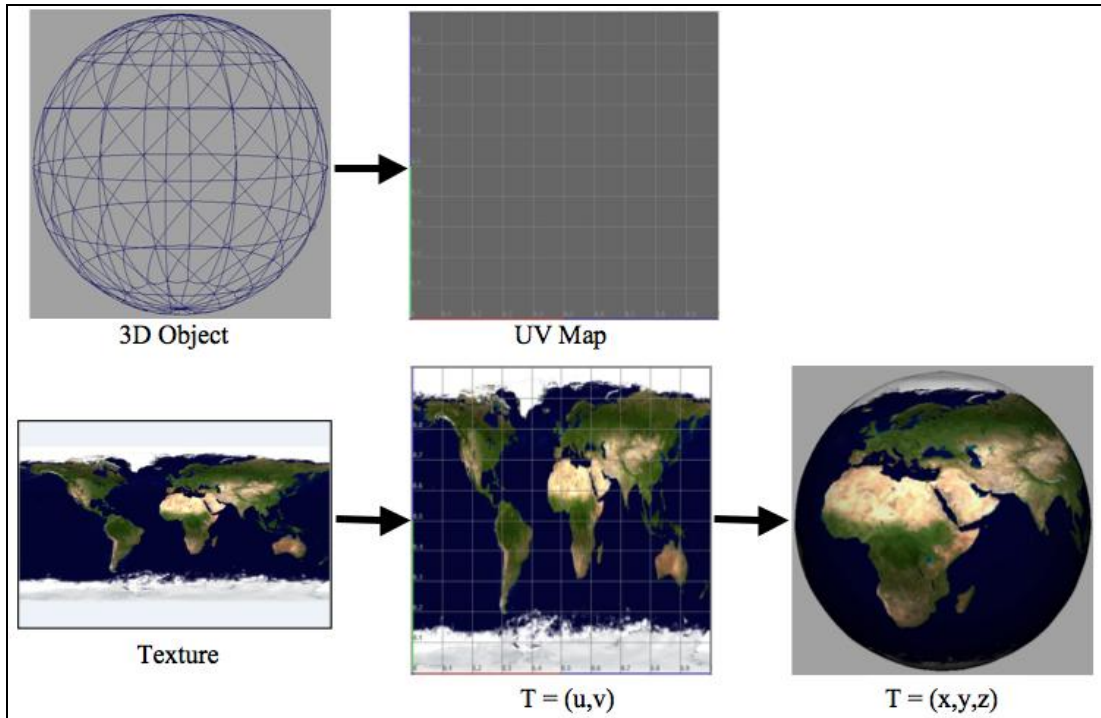


Figure 5. 11: A 3D sphere with its UV map

In our case:

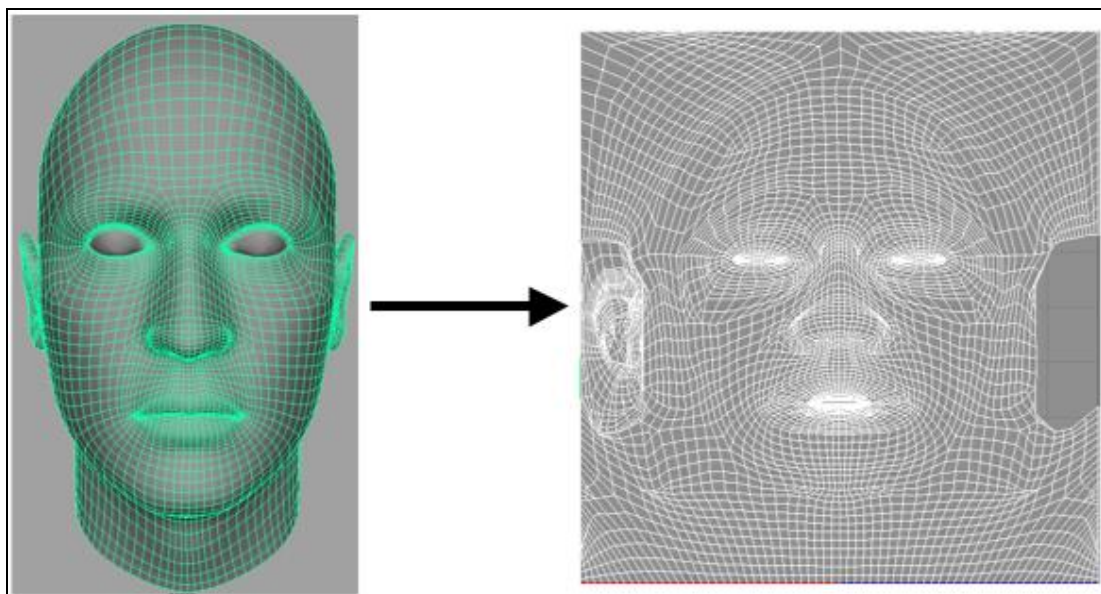


Figure 5. 12: Our 3D face and its UV map

The Texturing is done through this operation using MAYA:



Figure 5. 13: Texturing operation in MAYA

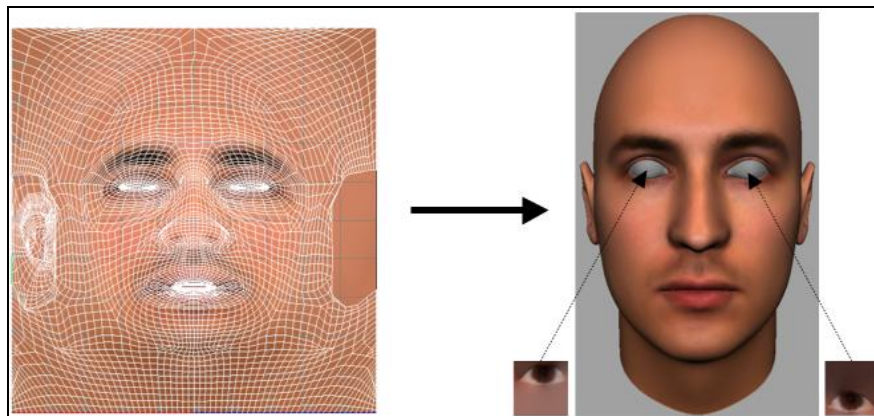


Figure 5. 14: Textured 3D head model

The eyes are textured in the same manner but on a smaller scale.

The final texturing result is presented in the figure below:



Figure 5. 15: Final texture

5.5 Wrinkles Construction

The generated binary wrinkle maps are mapped on their corresponding 3D face models; Figure 5.16 illustrates an example. Wrinkles are then constructed on the 3D models by the projection of the NURBS curves.



Figure 5. 16: The binary wrinkle map is textured on the 3D face model
Prior to the projection of the NURBS curves, the 3D model is made ‘Live’, which is a function in MAYA; when a 3D object is made ‘Live’, any projected 3D curve will adapt to the model’s shape. In other words, makes vertices snap to a surface (vertices are literally glued to the surface and can only move on it).

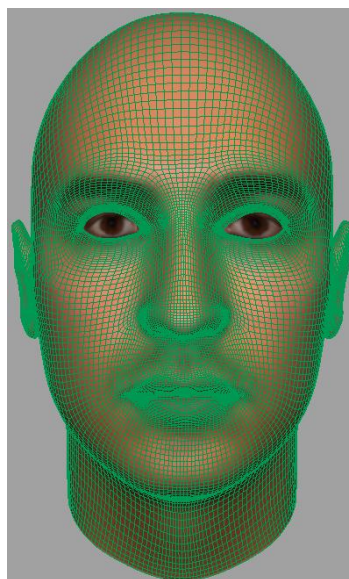


Figure 5. 17: ‘Live’ 3D object

Upon the projection of the NURBS curves; the curves are modelled to enhance the look of the 3D wrinkle maps. This is performed by observing the original images in order to add or fill gaps that might be present in the binary wrinkle maps due to detection failure for the reasons discussed in the previous chapter.



Figure 5. 18: An enhanced 3D wrinkle map

5.6 Wrinkles Simulation and Prediction

For the tasks of simulation and prediction, three elements (for any individual) are considered: the binary wrinkle map, the general development of the wrinkles over the decades (Table 1.1) and the coloured wrinkle map.

The binary map acts as a benchmark that displays the full facial wrinkles and their locations. Table 1.1 categorises those wrinkles into age groups that ascend from 20s to 70s, in other words, classifies them according to their likely appearance in any given age group. The coloured map will work within each age group, i.e. the wrinkles that have the highest intensity values will appear first and so on. For this stage, a threshold is set so that the numbers next to the colours bar (Figure 5.19) indicate the age in which the correspondent wrinkles are present. For example, when the simulation runs through the age group 30-39, any wrinkle that has the colour

below level 4 should appear; this must not contradict Table 1.1 (refer to this table for the order in which wrinkles are likely to appear on the different parts of the face). It is also important to know that ‘level 1’ on the colours bar does not resemble age 10 as our simulation starts to run from the age of 20, so therefore, the colours below level 2 are always present but again in accordance with Table 1.1.

Finally, the findings will be displayed in a form of a graph to study the behaviour of the wrinkles as age progresses. Figure 5.19 divulges the connections between the above elements.

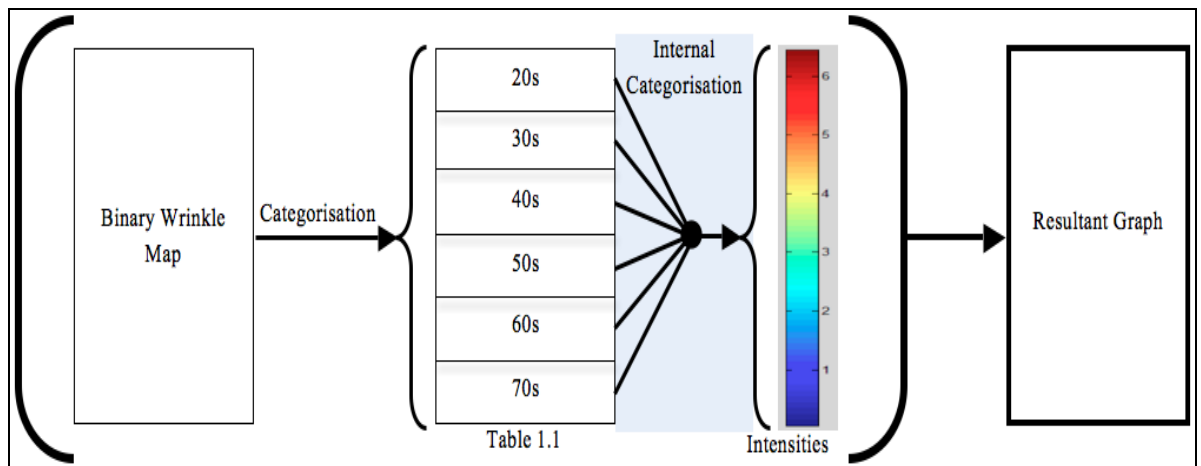


Figure 5. 19: Wrinkle elements and categorisations for age progression

Based on the outcome, each wrinkle in every age group is given a value between (0) and (-1). These values are understood by the MAYA program to be the degree of transformation in the z direction (depth), where (0) represents an inactive wrinkle and (-1) indicates a maximum transformation. For instance, in the 20s group (Figure 5.20), oromental grooves are given the values of (0) as inactive wrinkles at this age group. On the other hand, transverse frontal lines are given some negative values depending on their intensities.

An example is presented below, for Person A in the age range of 20 to 29, giving a further explanation for the categorisation process:

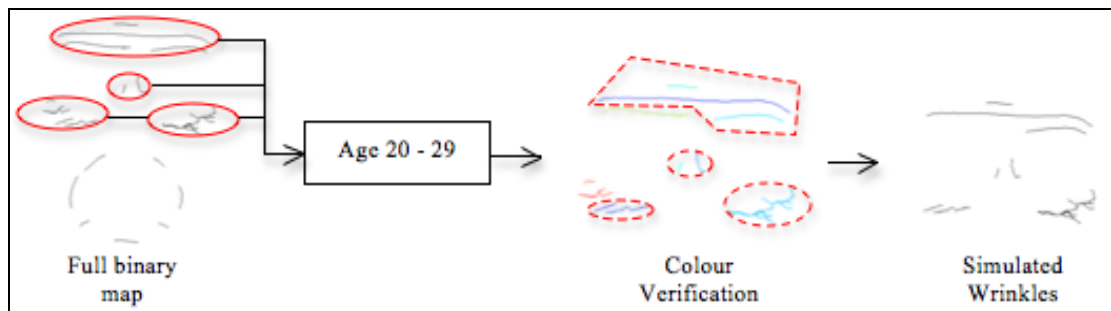


Figure 5. 20: A sample process for wrinkle categorisation

The adopted method is the most practical so far for this newly developed system that is the first of its type, especially, knowing that there is no quantitative information on the progression of facial wrinkles over the years, which might be due to the fact that every individual ages in a different manner under different conditions, as discussed in chapter one. However, in this work we are trying to find the best possible solutions based on qualitative analysis as well as our own findings from the previous chapter under unbiased conditions.

Carrying on from the example in the figure above, the whole face is considered in the diagram below indicating the number of wrinkles that must appear at every age group for Person A, where the total number of wrinkles for this person is 23.

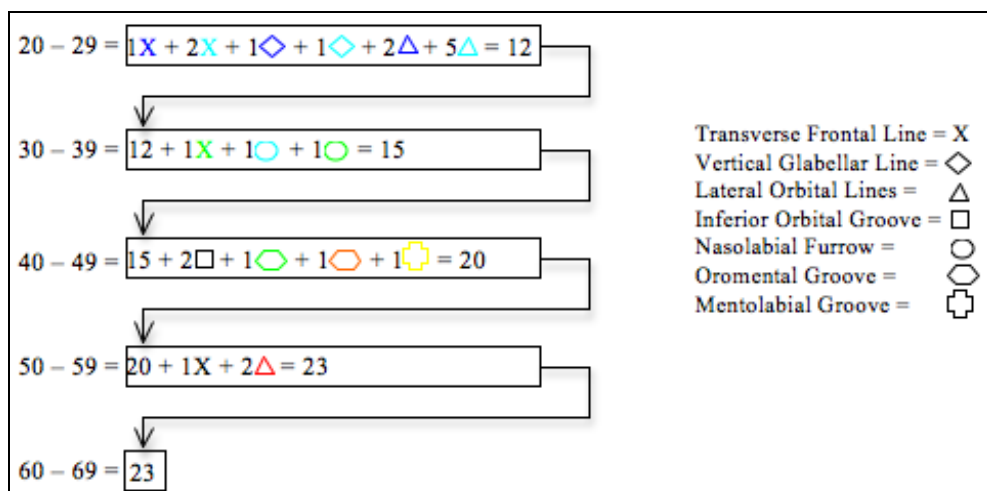


Figure 5. 21: The number of wrinkles that appear at every age group

Note that in the age groups 40-49 and 50-59, two inferior orbital grooves and one transverse frontal line have been added respectively. These wrinkles exist on the original image but failed to be detected by the wrinkle generator program, due to their very low intensities. The reason for adding them to the 3D model is to minimise the possible error occurrence.

The results, for every individual, are scattered on a graph in order to determine a pattern, thus, finding a relationship between the amount of change in the facial wrinkles in accordance to age progression. The determined relationship will be blended between the age groups and linked to a designed AGE bar.

The two axes of the graph will be denoted by the change in the facial wrinkles (as a percentage) being on the x-axis, while the age (in years) being placed on the y-axis. A sample graph is presented in Figure 5.22, for person A, which shows wrinkles progression against age.

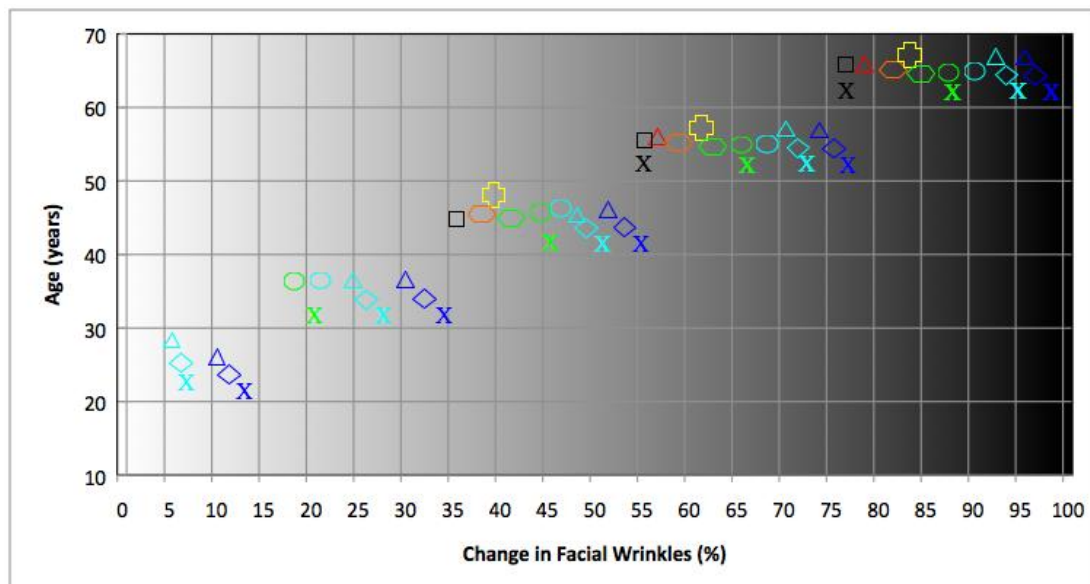


Figure 5. 22: A sample graph presenting the change in facial wrinkles against age

Because the values of the wrinkles are incremental, it is noted that a straight ‘best fit’ line can be drawn across the points (Figure 5.23). In mathematics, or more precisely,

in statistics, this whole operation is called Linear Regression Algorithm, and the ‘best fit’ line is called The Least Squares Regression Line [125].

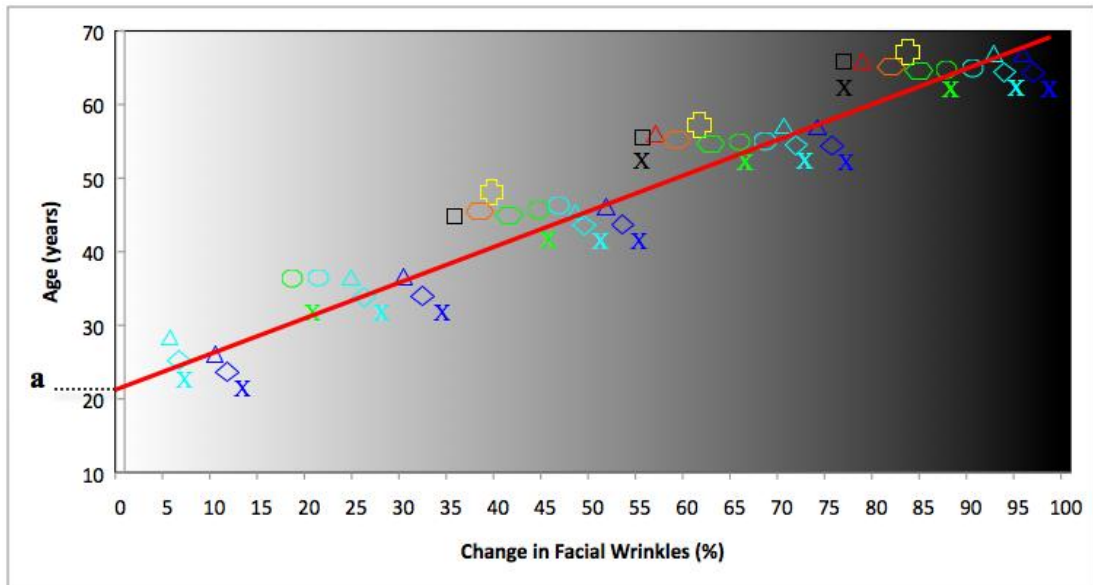


Figure 5. 23: A ‘best fit’ line is drawn across the points

‘a’ is the point where the line intercepts the y-axis.

5.6.1 Linear Regression Algorithm

In sciences, investigations or experiments are usually set up in attempts to find a relationship between two variables, in our case the change in facial wrinkles (x) against the age (y), where we use the information from x to estimate values of y . Since the x values are used to determine the facial look at a certain age, which are the y values, i.e. y values are dependent on the x values; for this, y values are called the response variables and x values are called the explanatory variables.

The equation of the straight-line is:

$$y = a + bx \quad (5.1)$$

Where a is the point of interception and b is the gradient of the line (Figure 5.24), and they can be found by the following:

$$a = \bar{y} - b\bar{x} \quad (5.2)$$

$$b = \frac{\sum (x - \bar{x})(y - \bar{y})}{\sum (x - \bar{x})^2} \quad (5.3)$$

If n is the number of the scattered points, Then:

$$\bar{x} = \frac{\sum x}{n} \quad (5.4)$$

$$\bar{y} = \frac{\sum y}{n} \quad (5.5)$$

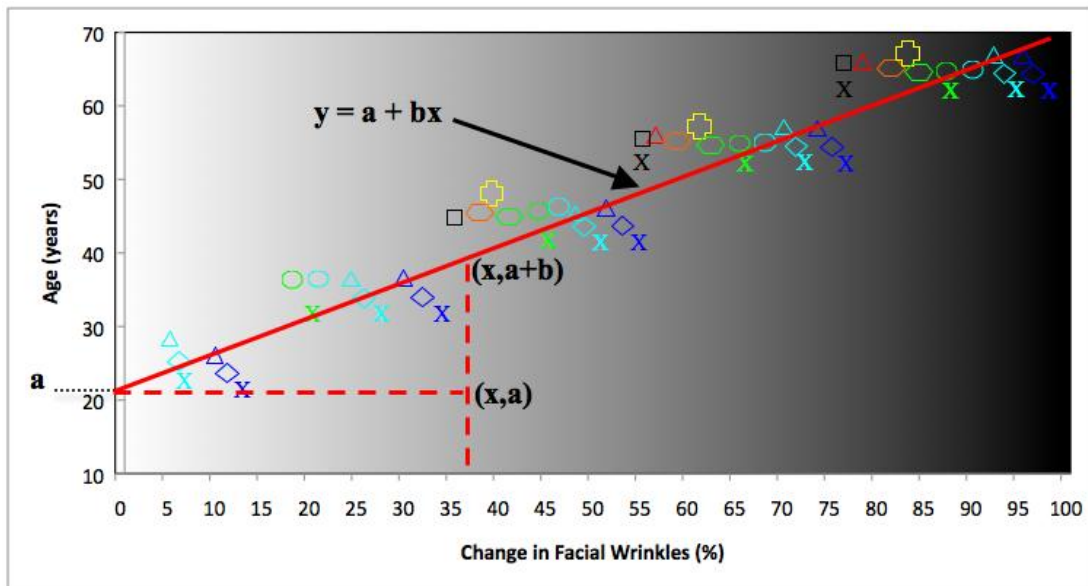


Figure 5. 24: A straight line with its variables

The linear regression algorithm was chosen over other regression algorithms for the reason that our wrinkles simulation runs under neutral conditions, i.e. no disrupting factors are involved. Generally, linear regression method has its value as a primary tool for modelling data because of its effectiveness and completeness. Practically speaking, it makes very efficient use of the data and good results can be obtained

with relatively small data sets. The theory associated with linear regression is well understood and allows for construction of different types of easily interpretable statistical intervals for predictions, calibrations and optimisations. These statistical intervals can then be used to give clear solutions to scientific problems. Linear regression method was also used in the task of facial ageing estimation by Ben et al. [126].

On the other hand, the use of nonlinear regression methods at this stage can be inadequate for the simple reason that more information is needed to perform the predictions in this manner.

5.7 Results

Some sample results are presented below and compared to the simulation results that are generated by the commercial software FaceGen. Our results are presented on the left hand side while FaceGen results are presented on the right hand side.



Figure 5. 25: Person A, 20-29



Figure 5. 26: Person A, 30-39



Figure 5. 27: Person A, 40-49



Figure 5. 28: Person A, 50-59



Figure 5. 29: Person A, 60-69



Figure 5. 30: Person D, 20-29



Figure 5. 31: Person D, 30-39



Figure 5. 32: Person D, 40-49



Figure 5. 33: Person D, 50-59



Figure 5. 34: Person D, 60-69



Figure 5. 35: Person P, 20-29



Figure 5. 36: Person P, 30-39



Figure 5. 37: Person P, 40-49



Figure 5. 38: Person P, 50-59



Figure 5. 39: Person P, 60-69



Figure 5. 40: Person R, 20-29



Figure 5. 41: Person R, 30-39



Figure 5. 42: Person R, 40-49



Figure 5. 43: Person R, 50-59



Figure 5. 44: Person R, 60-69

Our method is not limited to work on the standard head models that are taken from FaceGen only, but it accepts 3D face scans as well. The figures below are generated results using a 3D face scan for Person S and also compared to the generated results from FaceGen:



Figure 5. 45: Person S, 20-29



Figure 5. 46: Person S, 30-39



Figure 5. 47: Person S, 40-49



Figure 5. 48: Person S, 50-59



Figure 5. 49: Person S, 60-69

In addition to the above, the other commercial software that is called ‘age-me’ generated the following results for Person A and Person D:

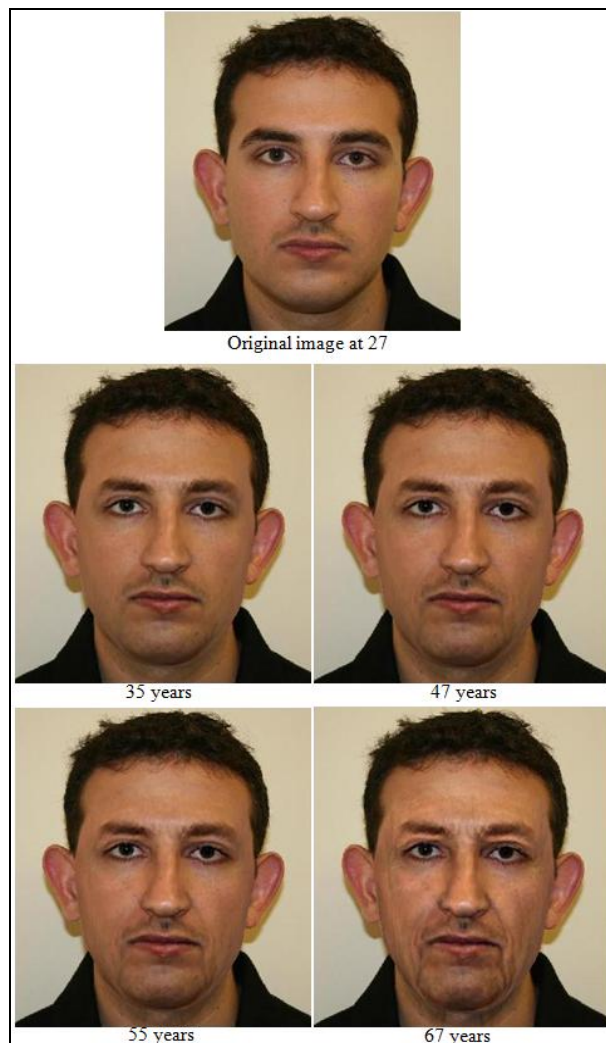


Figure 5. 50: Person A, 2D ageing simulation and prediction using age-me software



Figure 5. 51: Person D, 2D ageing simulation and prediction using age-me software
It is also noticed from Figure 5.51 that the appearance of the person does not change with age to any significant degree and this is another limitation of the age-me software.

5.8 Performance Evaluation Strategy

Theoretically, the performance of the system can be evaluated by acquiring real aged images of individuals at different ages (under controlled conditions). The simulation will then be run on a number of individuals and the generated results will be compared to the actual data in terms of the appearance of wrinkles. By performing the comparison, the performance of the system will be analysed to decide whether the performance is accepted or not.

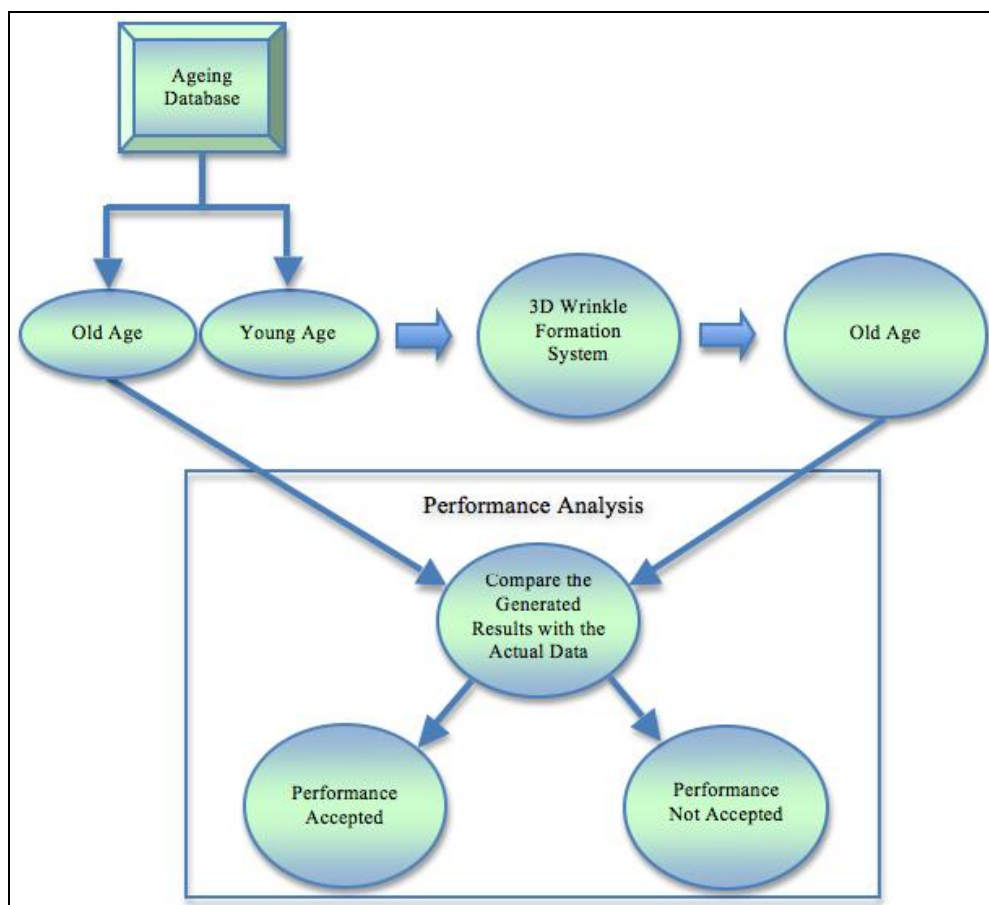


Figure 5. 52: Performance evaluation strategy

Practically, the above procedure cannot be performed at this stage due to the lack of available ageing databases with high quality images.

5.9 Discussion and Conclusion

In this chapter, novel techniques were used in the tasks of facial wrinkles simulation and prediction. Various parameters were utilised in order to develop this unique facial wrinkle pattern formation system, which include the generated wrinkle maps for any given individual along with published literature on the general development of the facial wrinkles over the years.

Details were also given in this chapter explaining the integration of these various elements in the development of this system that uses a linear function to predict the change of the facial wrinkles as age progresses. A clarification was also provided giving the reason of using linear function at this stage of this new system despite the fact that facial ageing in general progresses in a nonlinear manner under the influence of various factors.

Nevertheless, the system has the privilege of using real data that has high potential to boost the accuracy but on the other hand, testing the system is not practical at this stage for the difficulty in the data acquiring. However, the system was compared to other available popular technologies and proved competence. In comparison to FaceGen, it was seen from their results that their system could only display common facial wrinkles; for example, nasolabial furrow. It seems that a linear function is also used but it is applied to all input subjects in the same manner, while our linear function differs based on the information provided for every individual.

Better results than FaceGen were obtained by using the age-me software. This software uses 2D images and performs the age predictions using 2D approach. The generated wrinkles in this software do not match the actual wrinkle maps of the individuals, which shows that either some assumptions were made in the generation

of wrinkles based on data estimation or wrinkles were randomly produced. Though, both cases jeopardise the accuracy of wrinkles formation.

It is also worth mentioning that the developed system in this research has the distinctive advantage of its ability to accept standard (mean) 3D head models as well as 3D face scans. This can be beneficial, especially for future work, as will be explained in the concluding chapter (chapter six).

On the other hand, a limitation can be highlighted in our system that at this stage, factors affecting the development of wrinkles were not taken into consideration. This can be overcome by the use of history survey of each individual as will be discussed later in the future work.

In the next chapter, a broad conclusion will be drawn for the whole work underlining our findings and contributions. Proposals for future work will also be discussed, and in addition, theoretical plans for implementation will be provided.

CHAPTER SIX

6 Conclusion and Future Work

6.1 Conclusion

6.1.1 General Conclusion

Facial Ageing is indeed a challenging area of research as every human ages in a different manner under the influence of many biological and environmental factors. FA includes the progress that leads to the change of the skull, muscles, tissues, cells, etc as well as facial wrinkles.

For the fact that facial wrinkles are major developing elements associated with age progression, the aim of this work was to increase the accuracy in the tasks of facial ageing simulation and prediction by the utilisation of these wrinkles using novel approaches that overcome the current state-of-the-art technologies and will contribute in a variety of aspects, which include but not limited to:

- Global security departments: the change of the wrinkles appearance has a direct impact on the change of facial look of individuals. This reality can lead to a failure in matching faces of the same individuals over different time periods.
- Plastic surgery and cosmetics: with the increasing demands for the anti-ageing creams of a number of brands and the different treatments intending to reduce the visual impact of wrinkles on the face. The research of facial wrinkles can assist in the constant improvement of the various methods attempting to eliminate or reduce these wrinkles.

- The integration with facial ageing systems: the lack of accurate predictions in the current facial ageing systems due to the vagueness of real wrinkle information of individuals can be eliminated by the use of the developed techniques of this research.

The overall objectives were to extract the facial wrinkles of human faces in the form of maps then transfer the obtained data to be mapped on the corresponding face models in order to perform a series of simulations and predictions on their physical changes over time.

The system was developed in two parts:

- The first part was carried out by the employment of image processing tools to create a computer system that generates two-dimensional wrinkle maps from expressive faces. Facial expressions, as discussed before, reveal vital information regarding the shapes and positions of the wrinkles as well as their intensities. Likewise, the system can detect and extract wrinkles of faces with pronounced wrinkles without the need for expressions.

The use of 2D image-based algorithms in this research was due to the relatively low prices of equipment required for setting up such system in comparison to the cost factor of employing 3D scanners.

Although, the legacy of 2D image-based techniques are used at airports and by police, which have made 2D image applications widely available and popular at both academic and commercial levels but on the other hand, 2D data might suffer from pose variations and lighting conditions, etc. However, the experiment in this research was carried out under controlled conditions and proved validity by means of testing methodology.

- The second part of the system was to use the generated 2D wrinkle maps along with information regarding the gradual change of wrinkles over the decades to develop a three-dimensional system for wrinkles pattern formation. The use of the 3D system eliminates the limitations that are associated with 2D data.

The system simulates the wrinkles and predicts the change of facial appearance in term of wrinkles structure for any given age period (of 10-years), starting at the age of 20 and finishing at the age of 79.

6.1.2 Comprehensive Conclusion and Achievements

This section provides a detailed conclusion on the conducted experiments throughout this thesis. The achieved end systems are also discussed here, highlighting their strengths and weaknesses, while their opportunities of development are discussed in section 6.2.

- In chapter three, a new method was implemented for wrinkle length predictions by comparing different classifiers and applying linear functions. Although age progression behaves in a nonlinear way, the implemented approach showed that the linear process is valid, especially when dealing with small data periods. This assumption was backed up by the test results, in which small error rates were presented.

The experiments were carried out and tested on images of 80 individuals that were taken from two-dimensional facial ageing databases. The experiments were limited to the forehead areas as the images generally suffered from blurriness and poor quality. To overcome the limitations of the two-dimensional data, a three-dimensional facial ageing database has to be created. The problem with the later suggestion is the time factor, as it will take decades to build such a database.

The process initially started by cropping the forehead area of every individual then these 2D foreheads were mapped onto a 3D forehead model. NURBS curves were then projected to form a 3D representation of the wrinkle shapes in order to calculate their lengths in 3D space using geodesic distance. This adopted method reduces the possibility of error occurrence that might arise as a result of the issues accompanied with the 2D data.

For every experimental subject, the length of the wrinkles are calculated using the available data and the results were utilised with the involvement of linear interpolation and extrapolation algorithms to predict the length of the wrinkles for the missing data in the facial ageing sequence. The interpolation method estimates the value of an unknown data that lies in between two known variables, while the extrapolating technique works by learning a pattern from a series of data (minimum of two variables) and predicts a point beyond the actual data set. The later method was used to predict the length of the wrinkles of individuals at old ages. Generally, the extrapolation method is less reliable than the interpolation one as in the interpolation method the estimated data is quarantined between two known ones unlike the other method where the estimated value is not bounded by a maximum limit.

However, the two methods were tested on 30 individuals with the total of 85 wrinkles for each algorithm. The testing methodology involved the estimation and prediction of pre-known data and comparing the results to the original values. The highest generated error percentage for the interpolation and extrapolation algorithms were 13.1 and 18.7 respectively, which indicate low errors in the implemented techniques, thus, proved efficiency.

The experiments were limited to the forehead areas as the experimental data suffered from diverge light patches, different head orientations and so on. Nevertheless, the work was a setting off tool for further experiments to be conducted aiming to develop security measures by predicting the length of the wrinkles of individuals at different age spans, assuming that wrinkle lengths are unique for every person.

- The computer system described in chapter four was developed to detect and extract facial wrinkles from expressions. In the same chapter, a step-by-step explanation was given on the utilisation of various image processing techniques in the development of the system.

The system uses five expressive face images for any input individual. These images undergo a series of processes that result in a remarkable break-through that is represented by the generation of two wrinkle maps for any input entity. The input images were first converted to greyscale then filtered; these two steps are fundamental in image processing as they are performed for data and noise reductions. Face detection was carried out to eliminate the background as well as any unwanted objects. The advantage of the adopted face detection technique is its ability to detect faces of different shapes and colours in addition to the ability of detecting multiple faces in an image.

A type of filter that is known as gaussian filter was used to detect the wrinkles on the face. This type of filter is usually used to detect fine objects. The process resulted in the generation of the discussed wrinkle maps that are unique for every individual.

Having a system that generates facial wrinkle maps, does certainly serve many purposes, as mentioned earlier, in which one of them is the design of prediction

schemes on the change of facial wrinkles over time. In addition to that, wrinkles are unique for every individual, thus, can be used as a new biometric feature as discussed before.

The other advantage of the system is the expeditious computational time from the start of the operation until the results are generated.

- Chapter five presented the design of a 3D facial wrinkle formation system that uses real data for the simulation of wrinkles taking advantage of the wrinkle maps generator system. The general developments of wrinkles over the decades, which are known data, were also integrated in the design of the system to enhance the prediction of wrinkles appearance over age progression. In this system, the 3D approach eliminates the limitations that are associated with 2D systems.

For any target individual, wrinkle maps are generated using the system that was developed in chapter four; the binary map is then aligned on the same individual's 3D face model to enable the projection of the NURBS curves. Having done this procedure, 3D representation of the wrinkle locations is acquired.

With reference to the general change of wrinkle appearance over age, a threshold is set on the coloured map so that different intensity wrinkles appear at different stages of the age progression as explained earlier in chapter five.

The system uses a linear regression function for the wrinkle development over age progression as at this stage of the research, ageing operation is done under controlled conditions i.e. internal and external factors that have impact on the wrinkle development are not taken into consideration.

The results are 3D faces with embedded wrinkles that change in accordance to age progression.

In comparison to other available softwares such as FaceGen and age-me, the designed system proved its innovation and originality in the task of 3D wrinkle pattern formation.

6.1.3 Original Contributions

The main original contributions presented in this thesis can be summarised as follows:

- Developing new techniques to predict the shape of the wrinkles on the forehead area for 2D images of human faces in ageing sequences. This technique was tested on facial ageing databases.
- Creating a fully automated and robust method to detect facial wrinkles for digital images of frontal human faces. The method generates unique 2D binary wrinkle maps from facial expressions using various image processing techniques. These maps are used to display the location of the wrinkles.
- New tools are developed to generate 2D coloured wrinkle maps. The colours represent the depth of the wrinkles and can be used to determine the order in which wrinkles appear on the human face.
- A novel system was developed to generate 3D facial wrinkles from the wrinkle maps and predicts the change in wrinkle appearance over time based on qualitative analysis. The performance of the system was compared to other existing facial ageing systems.

6.1.4 Opportunity for Developments

Although this work presented novel techniques and outstanding results, however, there are still some limitations that are discussed below:

The new methods to predict the change in the wrinkle lengths were limited to the forehead areas. This limitation was due to the poor quality of the available databases as discussed before, which made the extraction of the wrinkles for the whole face difficult and would have produced inadequate results.

The developed computer system that generates full wrinkle maps for human faces from expressive facial images can have some drawbacks if the input images are taken under uncontrolled conditions.

However, the dataset that was used in the system was taken under controlled conditions but despite this, currently the system considers images of two-dimensional formats, and the limitations that are associated with 2D images were discussed earlier such as illumination and head orientation. Those limitations indeed affected the performance of the system in a way that some wrinkles or parts of wrinkles failed to be detected.

On the other hand, the depth of the wrinkles was measured based on the intensity of the wrinkles, which was defined by their edges; thus, no numerical values were produced.

For the 3D wrinkle formation system, a method was developed to predict the change in the facial wrinkles over time. This system relies on FaceGen as a tool to generate the 3D face models of individuals, which can be a disadvantage despite the simplicity of this method. FaceGen models might lack in accuracy with regards to the original images of the individuals, hence, it might be difficult to identify some

individuals due to textural differences between the original 2D face image and the generated 3D face model.

At this stage, the system carries out the simulations and predictions of wrinkles without taking into consideration any factor that affect the development of the wrinkles. This limitation forced the system to follow a linear pattern when processing the development of the wrinkles. But it is known that in real life wrinkles develop in a nonlinear manner, therefore, this limitation could prevent the system from reaching a better accuracy.

A strategy was drawn to evaluate the performance of the system, but no suitable data is currently available to implement the evaluation.

6.2 Suggestions for Future Work

- The length predictions that were limited to the forehead areas in this work can be extended to cover the entire face. This can be achieved if a better dataset is provided. With the integration of a life history survey for each individual, a subjective relationship can be discovered between certain activities and the increase in the length and number of facial wrinkles.
- Combining both systems from chapter four and chapter five into one by first, introducing a 3D scanner that will be used as an input device that scans faces with expressions. This method will reveal the 3D locations of the wrinkles instantly, thus, generating 3D wrinkle maps by extracting the control vertices of the wrinkles. The depth of the wrinkles on the other hand can be found as the following:

Inventing a 3D plane behind the face (Figure 6.1) and calculating the distance from the vertices of the wrinkles to the plane.

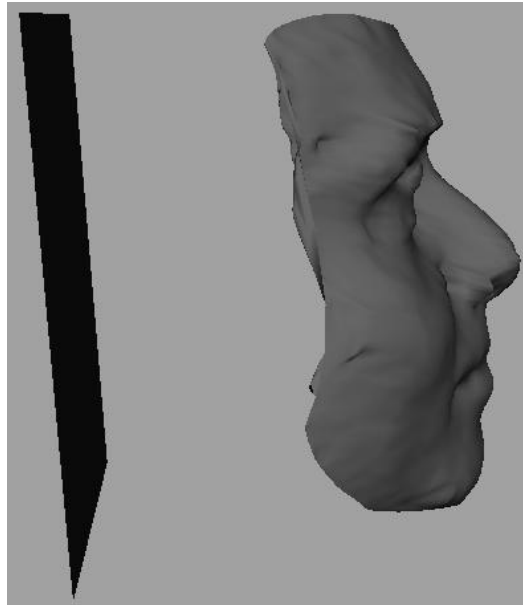


Figure 6. 1: A 3D plane is drawn behind a face

In addition to the above and for a further increase to the accuracy of the system, a quantitative study on the change of facial wrinkles should be carried out; this will assist in the following:

- A life history survey for every individual can be integrated in the system so then a nonlinear function will be used.
- The structural properties of the wrinkles can be investigated with regards to the ageing process.

References

1. Clement, J., and Marks, M., "*Computer Graphic Facial Reconstruction*". 2005, USA: Elsevier.
2. *TG Daily*. [cited 05/09/2007]; Available from: <http://www.tgdaily.com/content/view/33676/113/>.
3. Geng, X., Zhou, H., Zhang, Y., Li, G., and Dai, H. , "*Learning from facial aging patterns for automatic age estimation*", in *Proceedings of the 14th annual ACM international conference on Multimedia*. 2006: ACM New York, NY, USA., p. 307-316.
4. Bando, Y., Kuratate, T. and Nishita, T. , "*A Simple Method for Modeling Wrinkles on Human Skin*", in *the sixth international conference on Intelligent Systems Design and Applications*. 2002, IEEE: China. p. 225-230.
5. *Dermatology Texas*. [cited 06/04/2010]; Available from: <http://www.dermatologistdallas.com/JUveDERM.html>.
6. *You Are Beautiful*. [cited 06/04/2010]; Available from: <http://www.you-are-beautiful.co.uk/index-3.html>.
7. *American Society of Plastic Surgeons*. [cited 26/05/2010]; Available from: http://www.plasticsurgery.org/Patients_and_Consumers/Procedures/Procedure_Animations/Injectable_Fillers.html.
8. *Wrinkle Cream Guide*. [cited 07/04/2010]; Available from: <http://wrinklecreamguide.com/benefits-of-collagen-wrinkle-cream/>.
9. Albert, M., Ricanek, K., and Patterson, E., "*The Aging Adult Skull and Face: A Review of the Literature and Report on Factors and Processes of Change*". July 2004: University of North Carolina Wilmington, Wilmington, North Carolina.
10. Kitahara, T., Ichinose, M., and Nakasima, A., " *Quantitative evaluation of correlation of skull morphology in families in an attempt to predict growth change*". *European Journal of Orthodontics*, April 1996. **Vol. 18**(Issue 2): p. 181-191.
11. Ricanek, K., Patterson, E., and Albert, M., "*Age Related Morphological Changes: Effects on Facial Recognition Technologies*". 2004: University of North Carolina Wilmington, Wilmington, North Carolina.

12. *Photoaging*. [cited 10/01/2010]; Available from: <http://www.psychology.ecu.edu.au/photoaging/pages/whatis.html>.
13. *A2Z of Health, Beauty and Fitness*. [cited 05/05/2008]; Available from: http://health.learninginfo.org/smoking_skin.htm.
14. *Skin Care Counsel*. [cited 05/05/2008]; Available from: <http://www.skincarecounsel.com/the-effects-of-stress-on-your-skin>.
15. Lanitis, A., Draganova, C., and Christodoulou, C. , “*Comparing Different Classifiers for Automatic Age Estimation*”, in *IEEE Transactions on Systems, Man, and Cybernetics, Part B*. 2004. p. 621-628.
16. Geng, X., Zhou, Z., and Smith-Miles, K., "Automatic Age Estimation Based on Facial Aging Patterns". *Pattern Analysis and Machine Intelligence, IEEE Trans.*, 2007. **Vol. 29**(Issue 12): p. 2234-2240.
17. Phillips, P., Flynn, P., Scruggs, T., Bowyer, K., Chang, J., Hoffman, K., Marques, J., Min, J., and Worek, W., "Overview of the Face Recognition Grand Challenge", in *Conference on Computer Vision and Pattern Recognition*. 2005, IEEE.
18. Lu, X., and Jain, A., "Integrating Range and Texture Information for 3D Face Recognition", in *Seventh IEEE Workshops on Application of Computer Vision*. January 2007: Breckenridge, Colorado.
19. Wong, K., Lam, K., and Sui, W., "An Efficient Algorithm for Human Face Detection and Facial Feature Extraction under Different Conditions". *Pattern Recognition Society*. Published by Elsevier Science 2001. **Vol. 34**(Issue 10): p. 1993-2004.
20. Russ, T., Koch, M., and Little, C., "A 2D Range Hausdorff Approach for 3D Face Recognition", in *Computer Vision and Pattern Recognition*. June 2005, IEEE: San Diego, USA.
21. *Q&A on Face-Recognition*. [cited 09/10/2010]; Available from: <http://www.aclu.org/technology-and-liberty/qa-face-recognition>.
22. Bowyer, K., "Face Recognition Technology and the Security Versus Privacy Tradeoff". 2004, IEEE. p. 9-20.
23. *Face Recognition Vendor Test*. [cited 09/10/2010]; Available from: <http://face.nist.gov/frvt/frvt2006/frvt2006.htm>.
24. *News KaFe*. [cited 09/10/2010]; Available from: <http://newskf.com/british-schools-install-face-recognition-systems-for-students-not-to-be-late/11692/>.

25. Al-Qatawneh, S., "*3D Facial Feature Extraction and Recognition Using Machine Learning Techniques: An investigation of 3D Face Recognition including correction and normalisation of the data, extraction of facial features and Classification using machine learning techniques*". 2010, PhD Thesis. University of Bradford.
26. Patterson, E., Ricanek, K., Albert, A., and Boone, E., "*Automatic Representation of Adult Aging in Facial Images*", in *Proceedings of the Sixth IASTED International Conference on Visualization, Imaging, and Image Processing*. August 2006: Palma de Mallorca, Spain.
27. GILCHREST, B., SZABO, G., FLYNN, E., and GOLDWYN, R., "*Chronologic and Actinically Induced Aging in Human Facial Skin*". *The Journal of Investigative Dermatology*, June 1983. **Vol. 80**(Issue 1): p. 81s-85s.
28. *Oralift Facial Rejuvenation*. [cited 10/06/2010]; Available from: <http://www.oralift.com/>.
29. *L'OREAL*. [cited 10/10/2010]; Available from: http://www.loreal-paris.co.uk/en/gb/products/super-category.aspx?code=Skincare&cm_mmc=sem--google--Skincare%20Search--Age%20Control%20-%20Anti%20Aging%20Products.
30. Jain, A., Bolle, R., and Pankanti, S., "*Biometrics: Personal Identification is a Networked Society*". 1999, Norwell, Massachusetts, USA: Kluwer Academic.
31. *FG-NET database*. [cited 18/03/2008]; Available from: <http://www.fgnet.rsunit.com/>.
32. Ricanek, K., and Tesafaye, T., "*MORPH: A Longitudinal Image Database of Normal Adult Age-Progression*", in *IEEE 7th International Conference on Automatic Face and Gesture Recognition*. April 2006: Southampton, UK. p. 341-345.
33. Pittenger, J., and Shaw, R., "*Aging Faces as Viscol-Elastic Events: Implications for a Theory of Nonrigid Shape Perception*". *Experimental Psychology: Human Perception and Performance*, 1975. **Vol. 1**(Issue 4).

34. Pittenger, J., Shaw, R., and Mark, L., "*Perceptual Information for the Age Level of Faces as a Higher Order Invariant of Growth*". *Experimental Psychology: Human Perception and Performance*, August 1979. **Vol. 5**(Issue 3): p. 478-493.
35. Mark, L.a.T., J., "*The perception of growth in three dimensions*". *Perception and Psychophysics*, February 1983 **Vol. 33**(Issue 2): p. 193-196.
36. Bruce, V., Burton, M., Doyle, T., and Dench, N., "*Further Experiment on the Perception of Growth in Three Dimensions*". *Perception and Psychophysics*, 1989. **Vol. 46**(Issue 6): p. 528–536.
37. Lanitis, A., Taylor, C., and Cootes, T. , "*Towards Automatic Simulation of Aging Effects on Face Images*", in *IEEE Transactions on Pattern Analysis and Machine Intelligence*. 2002. p. 442-455.
38. Scandrett, C., Solomon, C., and Gibson, S, "*A person-specific, rigorous aging model of the human face*". *Pattern Recognition Letters*, November 2006. **Vol. 27**(Issue 15): p. 1776-1787.
39. Galton, F., "*Composite portraits made by combining those of many different persons into a single figure*". 1879. **Vol. 8**.
40. Thompson, D., "*On Growth and Form: The Complete Revised Edition*". 1992: Dover.
41. Burt, D., and Perrett, D., "*Perception of Age in Adult Caucasian Male Faces: Computer Graphic Manipulation of Shape and Colour Information*", in *Proceedings of Royal Society of London*. 1995. p. 137-143.
42. Ramanathan, N., and Chellappa, R., "*Modeling Age Progression in Young Faces*", in *Computer Vision and Pattern Recognition Conference*. 2006. p. 387-394.
43. Turk, M., and Pentland, A., "*Eigenfaces for Recognition*". *Cognitive Neuroscience*, 1991. **Vol. 3**(Issue 1): p. 71-86.
44. Kirby, M., and Sirovich, L. , "*Application of Karhunen-lo`eve Procedure for Characterization of Human Faces*". *Transactions on PAMI*, 1990. **Vol. 12**(Issue 1): p. 103-108.
45. Craw, I., and Cameron, P., "*Parameterising Images for Recognition and Reconstruction*", in *P. Mowforth (Ed.) Proceedings of the British Machine Vision Conference*. 1991: Berlin: Springer Verlag.

46. Rowland, D., and Perrett, D., "*Manipulating Facial Appearance Through Shape and Color*". IEEE Computer Graphics and Applications, 1995. **Vol. 15**(Issue 5): p. 70-76.
47. Sclaroff, S., and Isidoro, J. , "*Active blobs*", in *Sixth International Conference on Computer Vision*. 1998, IEEE. p. 1146.
48. Cootes, T., Edwards, G., and Taylor, C. "*Active Appearance Models*". in *Proceeding of the European Conference on Computer Vision*. 1998: Springer.
49. Blanz, V., and Vetter, T., "*A Morphable Model for the Synthesis of 3D Faces*", in *Proceedings of the 26th Annual Conference on Computer Graphics and Interactive Techniques*. 1999, ACM: New York, USA. p. 187-194.
50. Ramamoorthi, R., "*Analytic PCA Construction for Theoretical Analysis of Lighting Variability in Images of a Lambertian Object*". IEEE Transactions on Pattern Analysis and Machine Intelligence, October 2002. **Vol. 24**(Issue 10): p. 1322-1333.
51. Hutton, T., Buxton, B., Hammond, P., and Potts, H., "*Estimating Average Growth Trajectories in Shape-Space using Kernel Smoothing*". IEEE Transactions on Medical Imaging, 2003. **Vol. 22**(Issue 6): p. 747-753.
52. Scherbaum, K., Sunkel, M., Seidel, H., and Blanz, V., "*Prediction of Individual Non-Linear Aging Trajectories of Faces*", in *the European Association for Computer Graphics, 28th Annual Conference*. 2007: Prague, Czech Republic. p. 285-294.
53. Tong, Y., Park, U., and Jain, A., "*Face Recognition with Temporal Invariance: A 3D Aging Model*", in *the 8th IEEE International Conference on Automatic Face & Gesture Recognition*. September 2008: Amsterdam. p. 1-7.
54. Perrett, D., and Benson, P., "*Extracting Prototypical Facial Images from Exemplars*". 1993. p. 257-262.
55. Suo, J., Min, F., Zhu, S., Shan, S. and Chen, X., "*A Multi-Resolution Dynamic Model for Face Aging Simulation*", in *IEEE Conference on Computer Vision and Pattern Recognition*. June, 2007: USA. p. 1-8.
56. Xu, Z., Chen, H., and Zhu, S., "*A High Resolution Grammatical Model for Face Representation and Sketching*", in *Proceedings of the IEEE Computer Society Conference on Computer Vision and Pattern Recognition*. 2005: Washington DC, USA. p. 470-477.

57. Kwon, Y., and Lobo, N., "*Age Classification from Facial Images*". *Computer Vision and Image Understanding*, 1999. **Vol. 74**(Issue 1): p. 1-21.
58. Horng, W., Lee, C., and Chen, C., "*Classification of Age Groups based on Facial Features*". *Tamkang Journal of Science and Engineering*, 2001. **Vol. 4**(Issue 3): p. 183-192.
59. Kalamani, D., and Balasubramanie, P., "*Age Classification using Fuzzy Lattice Neural Network*", in *Proceedings of the Sixth International Conference on Intelligent Systems Design and Applications*. 2006, IEEE Computer Society: Washington DC, USA. p. 225-230.
60. Lanitis, A., Draganova, C., and Christodoulou, C. , "*Comparing Different Classifiers for Automatic Age Estimation*". *IEEE Transactions on Systems, Man, and Cybernetics, Part B*, February 2004. **Vol. 34**(Issue 1): p. 621-628.
61. Smola, A., and Olkopf, B., "*A Tutorial on Support Vector Regression*", in *Technical Report, Statistics and Computing*. 1998.
62. Gandhi, M., and Rajesh, G., "*A Method for Automatic synthesis of Aged Human Facial Images*". 2004, Masters thesis, McGill University.
63. Jobson, D., Rahman, Z., and Woodell, G., "*A Multiscale Retinex for Bridging the Gap Between Color Images and the Human Observation of Scenes*". *IEEE Transactions on Image Processing*, July 1997. **Vol. 6**(Issue 7): p. 965-976.
64. Tiddeman, B., Burt, M., and Perrett, D., "*Prototyping and Transforming Facial Textures for Perception Research*". *IEEE Computer Graphics and Applications*, 2001. **Vol. 21**(Issue 5): p. 42-50.
65. Tiddeman, B., Stirrat, M., and Perrett, D., "*Towards Realism in Facial Image Transformation: Results of a Wavelet MRF Method*". *Computer Graphics*, 2005. **Vol. 24**(Issue 3): p. 449-456.
66. Hussein, H., "*Towards Realistic Facial Modeling and Re-Rendering of Human Skin Aging Animation*", in *Proceedings of the Shape Modeling International Conference*. 2002, IEEE Computer Society: Washington DC, USA.
67. Liu, Z., Zhang, Z., and Shan, Y., "*Image-Based Surface Detail Transfer*". *IEEE Computer Graphics and Applications*, 2004. **Vol. 24**(Issue 3): p. 30-35.
68. Yin, L., and Basu, A., "*Generating Realistic Facial Expressions with Wrinkles for Model-Based Coding*". *Computer Vision and Image Understanding*, November 2001. **Vol. 84**(Issue 2): p. 201-240.

69. Yin, L., Royt, S., Yourst, M., and Basu, A., "*Recognizing Facial Expressions using Active Textures with Wrinkles*", in *Proceedings of the International Conference on ICME*. July 2003, IEEE. p. I - 177-80.
70. Zhang, Y., "*Muscle-Driven Modeling of Wrinkles for 3D Facial Expression*", in *IEEE international conference on multimedia and expo*. 2008, IEEE: Hannover. p. 957-960.
71. Tian, Y., Kanade, T. and Cohn, J. , "*Recognizing action units for facial expression analysis*", in *IEEE Transactions on Pattern Analysis and Machine Intelligence*. 2001, IEEE. p. 97-115.
72. Li, M., Yin, B., Kong, D. and Luo, X. , "*Modeling Expressive Wrinkles of Face For Animation*", in *Proc. of Fourth International Conference on Image and Graphics 2007*, IEEE. p. 874-879.
73. Antini, G., Berretti, S., Del Bimbo, A., and Pala, P., "*3D Face Identification Based on Arrangement of Salient Wrinkles*", in *IEEE International Conference on Multimedia and Expo*. July 2006: Toronto, Ont. p. 85-88.
74. Zhang, Y., and Ji, Q., "*Active and Dynamic Information Fusion for Facial Expression Understanding from Image Sequences*". *IEEE Transactions on Pattern Analysis and Machine Intelligence*, May 2005. **Vol. 27**(Issue 5): p. 699-714.
75. Ramamoorthi, R., "*Analytic PCA Construction for Theoretical Analysis of Lighting Variability in Images of a Lambertian Object*". *IEEE Trans. Pattern Anal. Mach. Intell.*, 2002. **Vol. 24**(Issue 10): p. 1322–1333.
76. Scandrett, C., Solomon, C. and Gibson, S., "*A Personspecific, Rigorous Aging Model of the Human Face*". *Pattern Recogn. Lett.*, 2006. **Vol. 27**(Issue 15): p. 1776-1787.
77. Ramanathan, N., Chellappa, R., and Biswas, S. "*Age progression in Human Faces : A Survey*". 2009 [cited 27/02/2010]; Available from: http://www.cfar.umd.edu/~soma/pdf/FacialAging_survey.pdf.
78. Giraldi, G., and Thomaz, C. "*Statistical Learning Models for Automatic Age Progression*". 2009 [cited 27/02/2010]; Available from: <http://arquivosweb.lncc.br/pdfs/age-progression.pdf>.

79. Suo, J., Chen, X., Shan, S., and Gao, W. "*Learning Long Term Face Aging Patterns from Partially Dense Aging Databases*". 2009 [cited 27/02/2010]; Available from: http://www.jdl.ac.cn/doc/2009/iccv09_Learning%20Long%20Term%20Face%20Aging%20Patterns%20from%20Partially%20Dense%20Aging%20Data%20bases.pdf.
80. Mehdi, A., Qahwaji, R., Ugail, H. and Mehdi, A., "*Construction of 3D Facial Wrinkles using Splines*", in *The 4th International Conference on Information Technology, Al-Zaytoonah University*. June 2009: Amman, Jordan.
81. Gould, D., "*Complete Maya Programming*". 2nd ed. 2005, USA: Elsevier Inc.
82. Maestri, G., "*Maya at a Glance*". 2005, USA: Sybex Inc.
83. Kimmel, R., and Sethian, J., "*Computing geodesic paths on manifolds*". 1998, Proc. Natl. Acad. Sci.: USA. p. 8431-8435.
84. Meijering, E., "*A chronology of interpolation: from ancient astronomy to modern signal and image processing*". Proceedings of the IEEE, 2002. **Vol. 90**(Issue 3): p. 319-342
85. Brezinski, C., and Redivo-Zaglia, M., "*Extrapolation Methods*". Applied Numerical Mathematics, September, 1994. **Vol. 15**(Issue 2): p. 123-131.
86. Autodesk. [cited 23/01/2010]; Available from: <http://usa.autodesk.com/adsk/servlet/pc/index?siteID=123112&id=13577897>.
87. Avatar. [cited 23/01/2010]; Available from: <http://www.avatarmovie.com/index.html>.
88. [cited 05/07/2008]; Available from: <http://devworld.apple.com/dev/techsupport/develop/issue25/schneider.html>.
89. Distance. [cited 03/03/2010]; Available from: <http://mathworld.wolfram.com/Distance.html>.
90. Euclidean Distance. [cited 03/03/2010]; Available from: <http://planetmath.org/encyclopedia/EuclideanDistance.html>.
91. Organic Chemistry. [cited 22/03/2010]; Available from: <http://www.yourformulasheet.com/index.php?/percent-error-formula.html>.
92. Percentage Error. [cited 22/03/2010]; Available from: <http://www.stecklesscience.org/Prologue/Percent%20error%20and%20how%20to%20find%20it.pdf>.

93. Ju, C., and Wang, Y., "*Automatic Age Estimation Based on Local Feature of Face Image and Regression*", in *Eighth International Conference on Machine Learning and Cybernetics*. July 2009, IEEE: Boading. p. 885-888.
94. Geng, X., and Smith-Miles, K., "*Facial Age Estimation by Multilinear Subspace Analysis*", in *International Conference on Acoustics, Speech and Signal Processing*. April 2009, IEEE: Taipei. p. 865-868.
95. Sethuram, A., Ricanek, K. and Patterson, E., "*A Hierarchical Approach to Facial Aging*", in *Computer Vision and Pattern Recognition Workshops* June 2010, IEEE: San Francisco, CA. p. 100-107.
96. González, R., and Woods, R., "*Digital Image Processing*". 2nd ed. 2002, Upper Saddle River, New Jersey: Prentice-Hall, Inc.
97. Yang, P., Liu, Q. and Metaxas, D., "*Boosting Coded Dynamic Features for Facial Action Units and Facial Expression Recognition*", in *Computer Vision and Pattern Recognition*. 2007, IEEE. p. 1-6.
98. Lim, S., "*Two-Dimensional Signal and Image Processing*". 1990, Englewood Cliffs, NJ: Prentice Hall.
99. Zarit, B., Super, B., Quek, F., "*Comparison of Five Color Models in Skin Pixel Classification*", in *Proceedings of the International Workshop on Recognition, Analysis, and Tracking of Faces and Gestures in Real-Time Systems*. 1999, IEEE: Corfu , Greece. p. 58-63.
100. *MathWorks*. [cited 10/03/2011]; Available from: <http://www.mathworks.com/help/toolbox/images/f8-20792.html>.
101. Sandeep, K.a.R., A., "*Human Face Detection in Cluttered Color images using skin color and Edge Information*", in *Indian Conference on Computer Vision, Graphics and Image Processing*. 2002. p. 1-6.
102. Otsu, N., "*A Threshold Selection Method from Gray-Level Histograms*". *IEEE Transactions on Systems, Man and Cybernetics*, 1979. **Vol. 9**(Issue 1): p. 62-66.
103. Goyani, M., Joshi, B., and Shikkenawis, G, "*Acceptance / Rejection Rule Based Algorithm for Multiple Face Detection in Color Images*". *International Journal of Engineering Science and Technology*, 2010. **Vol. 2**(Issue 6): p. 2148-2154.

104. Chandrappa, D., Ravishankar, M., and RameshBabu, D., "*Automated Detection and Recognition of Face in a Crowded Scene*". International Journal of Computer and Network Security, June 2010. **Vol. 2**(Issue 6): p. 65-70.
105. Rahman, M., Ren, J. and Kehtarnavaz, N., "*Real-Time Implementation of Robust Face Detection on Mobile Platforms*", in *IEEE International Conference on Acoustics, Speech and Signal Processing*. April 2009: Taipei. p. 1353 - 1356.
106. Canny, J., "*A Computational Approach To Edge Detection*". IEEE Transactions on Pattern Analysis and Machine Intelligence, 1986. **Vol. 8**(Issue 6): p. 679-698.
107. *Canny Edge Detection*. [cited 05/01/2011]; Available from: http://www.cvmt.dk/education/teaching/f09/VGIS8/AIP/canny_09gr820.pdf.
108. Geusebroek, J., Smeulders, A., and van de Weijer, J., "*Fast Anisotropic Gauss Filtering*". IEEE Transactions on Image Processing, August 2003. **Vol. 12**(Issue 8): p. 938-943.
109. Wellner, P., "*Adaptive Thresholding for the DigitalDesk*". 1993, EuroPARC Technical Report EPC-93-110.
110. Kong, J., Boyer, K., Saltz, J., and Huang, K., "*A New Model-Based Estimation of Ellipses for Object Representation*", in *IEEE Annual International Conference on Engineering in Medicine and Biology Society*. 2009: Minneapolis. p. 3637-3640.
111. Akarun, L., Gokberk, B. and Salah, A., "*3D Face Recognition for Biometric Applications*", in *Proc. European Signal Processing Conference*. 2005: Antalya.
112. Hsu, R., Abdel-Mottaleb, M., and Jain, A., "*Face Detection in Color Images*". IEEE Transactions on Pattern Analysis and Machine Intelligence, May 2002. **Vol. 24**(Issue 5).
113. Pai, Y., Ruan, S., Shie, M., and Liu, Y., "*A Simple and Accurate Color Face Detection Algorithm in Complex Background*", in *IEEE International Conference on Multimedia and Expo*. 2006: Toronto, Ont. p. 1545.
114. *April Age Progression Software*. [cited 17/01/2011]; Available from: <http://www.age-me.com/>.
115. *FaceGen*. [cited 31/03/2010]; Available from: <http://www.facegen.com/>.

116. Lin, W., Weijun, H., Rui, C., and Xiaoxi, W., "*Three-Dimensional Reconstruction of Face Model Based on Single Photo*", in *Proceedings of the International Conference on Computer Application and System Modeling 2010*, IEEE: Taiyuan. p. 674.
117. Wang, H., Zheng, Q., and Sun, Y., "*A Method of Generating Global View Texture Images in 3D Face Modeling*", in *The sencond International Conference on Information Science and Engineering (ICISE)*. December 2010, IEEE: Hangzhou, China. p. 3435.
118. Ansari, A., Abdel-Mottaleb, M., and Mahoor, M., "*3D Face Mesh Modeling from Range Images for 3D Face Recognition*", in *IEEE International Conference on Image Processing*. 2007: San Antonio, TX. p. 509-512.
119. Cohen, J., Olano, M., Manocha, D., "*Appearance-Preserving Simplification*", in *Proceedings of the 25th annual conference on Computer graphics and interactive techniques*. 1998, ACM: New York, USA.
120. Yang, B., Pan, Z., "*A Hybrid Adaptive Normal Map Texture Compression Algorithm*", in *Proceedings of the 16th International Conference on Artificial Reality and Telexistence--Workshops*. 2006, IEEE: Hangzhou.
121. Foley, J.a.D., A., "*Computer Graphics PRINCIPLES AND PRACTICE*". 2nd ed. 1996: Addison-Wesley Publishing Company.
122. Reis, C., De Martino, J., and Batagelo, H. "*Real-time Simulation of Wrinkles*". [cited 18/11/2010]; Available from: http://wscg.zcu.cz/wscg2008/papers_2008/short/b71-full.pdf.
123. Mullen, T., "*Mastering Blender*". 1st ed. 2009, Indianapolis, Indiana: Wiley Publishing, Inc.
124. Murdock, K., "*3ds Max 2009 Bible*". 1st ed. 2008, Indianapolis, Indiana: Wiley Publishing, Inc.
125. Attwood, G., Dyer, G., and Skipworth, G., "*Statistics 1*". New ed. 2000, Bath, UK: Heinemann Educational.
126. Ben, S., Chen, J., and Su, G., "*Piecewise Linear Aging Function for Facial Age Estimation*", in *Proceedings of the 16th IEEE International Conference on Image Processing*. 2009: Cairo, Egypt. p. 2753 - 2756.

Appendices

Appendix A: List of Publications

- A. Mehdi, S. Al-Qatawnah, R. Qahwaji, H. Ugail and A. Mehdi, “Position, Length and Number Estimation for Forehead Wrinkles”. Proceedings of the 3rd Mosharaka International Conference on Communications, Computer and Applications, October 2009, Amman, Jordan, pp. 38-43. ISBN: 9789957486075.
- A. Mehdi, R. Qahwaji, H. Ugail and A. Mehdi, “Construction of 3D Facial Wrinkles Using Splines”. Proceedings of the 4th International Conference on Information Technology, June 2009, Al-Zaytoonah University, Amman, Jordan.
- A. Mehdi, R. Qahwaji, H. Ugail and S. Ipson, “Facial Aging: Review and Analysis”. Proceedings of the Ninth Informatics Workshop, June 2008, Bradford, UK. ISBN: 9781851432516.